EPA-460/3-77-015
August 1977

CHARACTERIZATION AND RESEARCH INVESTIGATION OF METHANOL AND METHYL FUELS

U.S. ENVIRONMENTAL PROTECTION AGENCY
Office of Air and Waste Management
Office of Mobile Source Air Pollution Control
Emission Control Technology Division
Ann Arbor, Michigan 48105

This report is issued by the Environmental Protection Agency to report technical data of interest to a limited number of readers. Copies are available free of charge to Federal employees, current contractors and grantees, and nonprofit organizations - in limited quantities - from the Library Services Office (MD-35), Research Triangle Park, North Carolina 27711; or, for a fee, from the National Technical Information Service, 5285 Port Royal Road, Springfield, Virginia 22161.

This report was furnished to the Environmental Protection Agency by the University of Santa Clara, Department of Mechanical Engineering, Santa Clara, California 95053, in fulfillment of Grant No. R803548-01. The contents of this report are reproduced herein as received from the University of Santa Clara, Department of Mechanical Engineering. The opinions, findings, and conclusions expressed are those of the author and not necessarily those of the Environmental Protection Agency. Mention of company or product names is not to be considered as an endorsement by the Environmental Protection Agency.

Publication No. EPA-460/3-77-015

EPA-460/3-77-015

CHARACTERIZATION AND RESEARCH INVESTIGATION OF METHANOL AND METHYL FUELS

by

R.K. Pefley, L.H. Browning, W.E. Likos,
M.C. McCormack, and B. Pullman

Department of Mechanical Engineering
University of Santa Clara
Santa Clara, California 95053

EPA Grant No. R803548-01

EPA Project Officer: R.J. Garbe

Prepared for

ENVIRONMENTAL PROTECTION AGENCY
Office of Air and Waste Management
Office of Mobile Source Air Pollution Control
Emission Control Technology Division
Ann Arbor, Michigan 48105

August 1977

CHARACTERIZATION AND RESEARCH INVESTIGATION

OF METHANOL AND METHYL FUELS

FINAL REPORT

EPA Grant No. R803548-01

Project Officer - R. J. Garbe

R. K. Pefley

L. H. Browning

M. L. Hornberger

W. E. Likos

M. C. McCormack

B. Pullman

INDEX

		Page
	List of Figures	ii.
	List of Tables	iv.
	Abstract	v.
I.	Preface	1.
II.	Recapitulation of Work Objectives	2.
III.	Summary of Work and Projected Planning	6.
IV.	Discussion of Program Results	23.
	IV.1 Steady State Engine Performance and Exhaust Emissions Characterization - Methanol vs Indolene	23.
	IV.2 Alternate Fuel Induction Systems	54.
	IV.3 Methanol versus Indolene - A Comparison Based on Simulation of the Federal Emission Test Procedure and the Federal Highway Fuel Economy Test Procedure	67.
	IV.4 Thermochemical Engine Process Modeling	77.
	IV.5 Cold Starting and Lean Burning	91.
	IV.6 Engine Wear and Crank Case Blow by	99.
V.	Conclusions	105.
VI.	References	107.

LIST OF FIGURES

		Page
III.1:	NO_x Emissions - Methanol Vs. Jet Fuel in Gas Turbines	19
III.2:	CO Emissions - Methanol Vs. Jet Fuel in Gas Turbines	20
IV.1:	Test Engine - Dynamometer Configuration	25
IV.2:	Comparative WOT Indicated Power - Indolene (OEM) Vs. Methanol (OEM and Alternate Systems)	28
IV.3:	Comparative WOT Brake Power - Indolene (OEM) Vs. Methanol (OEM and Alternate Systems)	29
IV.4:	WOT Comparative Thermal Efficiency for OEM and Alternate Fuel-Air Induction Systems	30
IV.5:	14" Hg. Manifold Vacuum Comparative Thermal Efficiency for OEM and Alternate Fuel-Air Induction Systems	33
IV.6:	Exhaust Emissions Sampling System	35
IV.7:	CO_2, CO, and O_2 Vs. Cylinder Equivalence Ratio - Indolene Vs. Methanol	37
IV.8:	Comparative WOT Steady State NO_x Emissions - Indolene (OEM) Vs. Methanol (OEM and Alternate Systems)	39
IV.9:	Comparative 1/3 Brake Load Steady State NO_x Emissions - Indolene (OEM) Vs. Methanol (OEM and Alternate Systems)	40
IV.10:	Comparative WOT Steady State UBF Emissions - Indolene (OEM) Vs. Methanol (OEM and Alternate Ssytems)	42
IV.11:	Comparative 1/3 Brake Load Steady State UBF Emissions Indolene (OEM) Vs. Methanol (OEM and Alternate Systems)	43
IV.12:	Comparative Exhaust Aldehydes	45
IV.13:	Cylinder to Cylinder Variations in Equivalence Ratio - Methanol Vs. Indolene	47
IV.14:	Effects of Maldistribution on Spark Timing, Power, Air Flow Rate, and Fuel Flow Rate	49
IV.15:	Effects of Maldistribution on Power - Calculated Vs. Actual	50
IV.16:	Effects of Maldistribution on NO_x - Experimental Data	53
IV.17:	Calculated Maldistribution Effect on NO_x	53

Page

IV.18: Equivalence Ratio Vs. Percent of Wide Open Throttle - WHB Induction System 56
IV.19: Air Flow Rate Vs. Percent of Wide Open Throttle - WHB Induction System 58
IV.20: Electronic Fuel Injection System 59
IV.21: Effects of Injection Timing on Power, Thermal Efficiency and Emissions 61
IV.22a: Conceptualized Diagram of the Dresserator Induction System 64
IV.22b: Manifold Adapter Bracket 65
IV.23: Comparative Thermal Efficiency Across the Speed Range at Wide Open Throttle - Indolene Vs. Methanol 66
IV.24: Fuel Economy Vs. Equivalence Ratio for Alternate Fuel-Air Induction Systems on Methanol With the Indolene and Methanol OEM Results - Urban Driving 69
IV.25: Fuel Economy Vs. Equivalence Ratio for Alternate Fuel-Air Induction Systems on Methanol With the Indolene and Methanol OEM Results - Highway Driving 72
IV.26: Exhaust Emissions Vs. Equivalence Ratio for OEM and Alternate Fuel-Air Induction Systems for the Hot 1972 FTP Simulation 74
IV.27: Comparison of AC Coupled Data and Integrated Data 79
IV.28: Match of Computer Predicted Results to Actual Pressure Traces 80
IV.29: Comparison of Acutal Vs. Predicted Performance Data 83
IV.30: Comparisons Between Experimental and Predicted Dry Exhaust Emissions 84
IV.31: Computer Predicted Performance for 2000 RPM and 4000 RPM 86
IV.32: Computer Predicted Dry Emissions for 2000 RPM and 4000 RPM 87
IV.33: Computer Predicted MBT Compression Ratio Effect 88
IV.34: Computer Predicted Spark Retard Effects 89
IV.35: Prototype Methanol Cold Start System 93
IV.36: Effect of Fuel Type on Engine Wear 103

LIST OF TABLES

		Page
III.1	Energy Based Fuel Economy as a Percentage Improvement Over OEM Performance Using Indolene from Computer Simulation of FTP (Hot 1972 Procedure)	10
III.2	Vehicle Emissions Comparison from Computer Simulation of FTP (Hot 1972 Procedure)	10
IV.1	Base Line Test Matrix	26
IV.2	Exhaust Emission Measurement Technique	36
IV.3	Simulated Cases	68
IV.4	Simulated FTP Results	70
IV.5	Simulated HFETP Results	71
IV.6	Performance and Emissions Comparison at Match Point (WOT and 2000 rpm)	82
IV.7	History of Engine Events	102

ABSTRACT

The work reported herein deals with several aspects of using pure methanol as an alternate fuel.

A stock (OEM) Pinto engine mounted on a dynamometer has been used to compare methanol with Indolene* in terms of power, efficiency, and emissions for a variety of speeds and loads.

Although the engine was designed for use with gasoline, it was found that methanol was generally superior in power, thermal efficiency and reduced emissions with the exception of aldehydes.

Study of engine wear showed no serious consequences from the use of methanol. This is consistent with the evidence from our two road vehicles which have now been operating for more than 5 and 6 years respectively on pure methanol.

Measured maldistribution of the air-fuel mixtures among the cylinders of the test engine and variation of the mixture with speed and load reveal that these variations must be reduced for improved mileage and emissions from either gasoline or methanol. The problem is caused by the venturi carburetor and intake manifold.

Evaluation of alternates to the venturi carburetor and intake manifold.

Three different fuel metering systems were tested for a variety of speeds and loads using the dynamometer mounted engine. They were all found to provide superior steady state performance on methanol when compared with the OEM carburetor system with enlarged fuel jets for methanol.

One prototype (WHB)** fuel system solves the maldistribution problem among the cylinders and allows a 20-30% reduction in the idle speed. Forthcoming modifications are expected to tighten control of the air-fuel ratio as

---

*An unleaded gasoline of closely specified composition.

**The initials of the inventor, William H. Beekhuis.

functions of speed and load to a satisfactory degree at which time this system will be tested on a vehicle.

Mileage and emissions from a Pinto vehicle equipped with the various fuel metering systems have been computer predicted for the Federal emissions test procedure using laboratory engine measurements.

Again the alternate fuel preparation systems showed significantly superior performance on methanol in comparison with OEM-Indolene performance. The evidence indicates that lean-burning, methanol-fueled vehicles may meet statutory limits of emissions if tight control is maintained on the air-fuel ratio and spark advance. A Pinto vehicle has been acquired to provide actual evidence for comparisons with some of the computer predicted results.

A computer has been used to simulate the test engine's thermokinetic combustion events.

The computer model predicts power, fuel economy and emissions with air-fuel ratio, compression ratio, spark advance and speed as parameters. After matching the computer's prediction for a specific set of conditions, to the engine's performance, it was used to predict trends in power, fuel economy and NO_x emissions due to changes in air-fuel ratio, speed, and compression ratio. The trends were very similar to actual engine trends where they could be compared. The evidence clearly suggests use of higher compression ratios with methanol. While the trends are satisfactory, the model does not as yet satisfactorily deal with "squish" type combustion chamber effects nor quench zone effects. It will be modified to improve these modeling features.

Gas turbine converted to operate on methanol.

A small (60 hp) gas turbine has been converted to run on methanol. The conversion was easily accomplished but atomization of the fuel was found to be important in obtaining a reduction in CO and NO_x for methanol in comparison with jet engine fuel. The reduction in these pollutants was found to correlate with other experimental evidence and computer modeling studies upon using combustor inlet temperature as a basis for comparison.

Environmental factors of marine and aquatic methanol spills and photochemical smog are under study.

Preliminary experimentation relative to marine spills indicates that methanol is naturally present in that environment. It appears at this early stage of investigation that damage to the ecosystem from a major coastal spill may be localized and of short duration.

A photochemical smog chamber is being equipped with instrumentation to perform a comparative photochemical smog study between methanol and gasoline automotive exhaust. Results from this study will appear in subsequent reports.

I. PREFACE

This report is a continuation in a series of reports[1,2,3] evaluating methanol as an alternate liquid fuel with primary emphasis on automobile use. The work was started in 1968 and has progressed continuously since then. Over that time period the work has been partially funded by government agencies (EPA, ERDA, NASA and NAPCA), partially by the City of Santa Clara and the University. It has also been supported in part by donations from the Ford Motor Company, General Motors Corporation, Chrysler Corporation and Dresser Industries.

Although this report is being written primarily to fulfill contractual obligations with EPA and ERDA, it is also intended to comprehensively report on all aspects of our methanol program whether they have external sponsorship or not. The reasons for this are twofold. First, it serves as a total record of our activities. Second, it accentuates our belief that engineering developments associated with alternate energy planning must pay heed to a broad range of issues such as safety and environmental hazards while at the same time addressing specific issues such as engine performance and emissions.

This report relates the past year's efforts to the objectives established at the beginning of the year, to our prior work, and to our plans for follow-on programs.

We wish to acknowledge the contributions of our professional associates, Dr. M. A. Sweeney, Dr. P. D'Eliscu and our student associates: J. Nebolon, K. Overby, D. Rourk and J. Villemarie.

II. RECAPITULATION OF WORK OBJECTIVES

Is methanol a superior fuel to gasoline in terms of performance, emissions, economics, safety, and the environment if one or the other is to be made from coal and bio-mass energy resources in the coming years? This is the overall issue to which our following specific program objectives are related and which serves as the general basis for the subsequent discussion and analysis of our work.

II.1 Engine Performance and Emissions Characterization--Gasoline Versus Methanol: The objective here is to first establish a baseline of performance and emissions from a stock Pinto 2300 cc. engine using Indolene (a reference grade gasoline). Then, using the same test matrix, evaluate changes in performance and emissions when operating on methanol with low cost modifications to the stock air-fuel preparation system.

II.2 Alternative Fuel Induction Systems: Previous work has shown the maldistribution of the air-fuel mixture among the cylinders in a multicylinder engine to be a serious problem. Since some modifications to the fuel preparation system are mandatory in changing a gasoline fueled engine to methanol, the objective here is to explore alternates to the combination of venturi-carburetor and intake-manifold which appear attractive in alleviating the maldistribution problem while improving performance and emissions from methanol. The first phase of this exploration uses the same engine test set up and test matrix used for establishing baseline engine performance and emissions. The alternate fuel preparation systems selected for evaluation are:

a. Electronically controlled fuel injection system.
b. Dresserator multi-cylinder shockwave carburetor.
C. WHB individual cylinder shockwave carburetion system.

II.3 Simulation of Urban and Highway Driving in a Pinto: What is a meaningful way of efficiently comparing the extensive evidence accumulated from engine dynamometer tests of the various fuel

preparation systems? This objective question has led us to explore the use of experimental performance and emissions data in conjunction with a computer simulation of the Federal driving cycles for a Pinto vehicle. The composite evidence of efficiency and emissions from each fuel preparation system could then be easily contrasted, however, causes for the contrasts would require more detailed analysis of the data.

II.4 Thermo-chemical Engine Process Modeling: Computer simulation of the thermo-chemical events in an open cycle heat engine can be a valuable aid in predicting changes in performance and emissions which will result from use of an alternate fuel such as methanol. Our objective is to create such a computer model and tune it by use of specific engine parameters (those of the 2300 cc. Pinto) and performance test points. Then, use it to forecast changes in performance and emissions due to spark timing, compression ratio, equivalence ratio , speed, and load. Successful modeling, as attested to by comparison with experimental evidence can greatly reduce future test program time and cost in searching for the best engine modifications in accommodating methanol as a fuel.

II.5 Cold Starting and Lean Burning: Cold starting and lean burning are partially related issues for cold starting problems are often caused by the air fuel-vapor mixture being outside the flammability range. Methanol in pure form is not as suitable as gasoline for cold starting because of this. The objective here is to explore ways of improving the cold start ability of methanol. Improved fuel nebulization to prevent fuel droplets from separating from the air stream, catalytic partial dissociation into $CO + 2H_2$ to obtain a gaseous fuel with broad flamability limits, and intake manifold warming combustors are preferred avenues of exploration as they require no fuel modifications. Special starting fuels and fuel blending agents are considered as alternate possibilities.

Lean burning of methanol under automobile cruise operation has shown promise as a means of reducing NO_x emissions and increasing fuel economy. The generation of dissociated methanol ($CO + 2H_2$) by waste heat from the exhaust and use of this fuel to enhance this possibility has been of interest since the program's inception.[1] The objective here is to continue investigation of methods for satisfactory extension of lean burning as it relates to both cruise operation and cold starting.

II.6 Engine Wear Rate and Crankcase Blow-by: There may be changes in engine life expectancy due to shifts in friction and wear characteristics resulting from the use of alternate fuels such as methanol. The objective here is to track test engine wear rates by inspection for metals accumulation in the lubricating oil during the time the engines are being used for emissions and performance evaluations. Any evidence of concern would be cause for more focused investigations.

Analysis of the constituents in crankcase blow-by gases can also enhance understanding of wear rates. Our emissions test facility is being used to explore this evidence during the engine characterization studies.

II.7 Road Vehicles Performance: We have three vehicles operating on the road with methanol fuel. Two use pure methanol and one uses methanol-gasoline blends. The objective is to obtain real world experience with methanol fueled vehicles.

II.8 Supplementary Objectives: As our confidence in the suitability of methanol as an alternate fuel has grown, some important additional activities have sprouted which address the following questions:

a. What are the differences in photochemical reactivity between gasoline and methanol exhaust emissions?

b. What are the comparative biological hazards of methanol and petroleum marine spills?

c. Can small power gas turbines be easily modified to run on methanol and what effects does this fuel have on performance and emissions?

III. SUMMARY OF WORK AND PROJECTED PLANNING

Highlights of evidence resulting from our investigations are presented in this section of the report. It is also intended to provide a synoptic interpretation for guidance in follow-on program planning.

III.1 Engine Performance and Emissions Characterization--Gasoline* versus Methanol: The experimental phase of the program has focused on the steady state mapping of performance and exhaust emissions of a dynamometer mounted, 2300cc, Ford Pinto engine. A significant portion of this work was detailed in a previous report[3] and is augmented by the detailed discussion in Section IV.1. of this report.

The Indolene* and methanol baseline comparison with OEM** equipment indicated that gains in thermal efficiency and reduced exhaust emissions (with the exception of aldehydes) are obtained while operating on methanol at the same engine speed, load, and equivalence ratio (Φ)***. The following summary quantifies the important engine performance and exhaust emission comparisons.

A. Performance

a) The power from methanol ranges from 5% to 11% higher than that obtained from gasoline.

b) The indicated thermal efficiency from methanol is on the average 10% higher than from gasoline for the observed ranges of speed, load and (Φ).

B. Exhaust Emissions

a) NO_x emissions from methanol average a factor of 2 lower than gasoline NO_x emissions.

---

* Indolene was used as the reference gasoline in the majority of the work.

** OEM is used to identify original equipment of the manufacturer.

***Equivalence ratio (Φ) is defined as stoichiometric ÷ actual air-fuel ratio. Fuel system modifications are required to obtain this comparison.

b) The CO emissions in the lean region are about the same for methanol and gasoline, but lower for methanol in the rich region.

c) The hydrocarbon emissions, herein referred to as unburned fuel (UBF), show small but discernable advantage favoring methanol.

d) The aldehyde emissions are higher for methanol than for gasoline by a factor ranging from 1.2 to 10 depending on the equivalence ratio.

All of the observed comparative performance and emissions characteristics were subject to the inherent cylinder to cylinder variations in Φ of this particular 4-cylinder engine. In general, this maldistribution as we will call it, was worse when operating on methanol with variations in (Φ) approaching $\pm$ 40% in some of the worst cases. A maldistribution index (MI) was defined which allows estimation of these effects on the power output and thermal efficiency. Based on the observed maldistribution for both Indolene and methanol it appears that additional relative gains for methanol ranging from 2 to 5% in thermal efficiency (and power) are possible if the maldistribution is eliminated in the range $0.8 \leq \Phi \leq 1.0$.

The maldistribution of Φ creates widely scattered engine emissions evidence when the composites of all four cylinders are examined. This is particularly true of NO_x. As previously reported[3], the composite NO_x vs composite Φ almost has the appearance of having been produced by a random function generator.

Fortunately, the test program has also included individual exhaust cylinder measurements. From these measurements, the maldistribution effects on exhaust emissions of the NO_x, UBF and CO have been resolved.

III.2 <u>Alternative Fuel-Air Induction Systems for Methanol</u>: In addition to the baseline comparisons of Indolene and methanol in the OEM and slightly modified OEM equipment, three alternative fuel-air induction systems for methanol have been under investigation. They have been described previously[3] and identified as the WHB shock wave system, the Dresserator Inductor (Dresser Industries), and the electronic fuel injection (EFI) system. All three systems have been installed

and tested on the engine used in the baseline comparison. Their collective data indicates improvements in thermal efficiency, power, and exhaust emissions relative to both methanol and Indolene baselines. In addition, one system (WHB) has completely eliminated the maldistribution phenomena.

The WHB Shock Wave Carburetion System provides for individual cylinder metering of the fuel for each intake stroke by using the strength of the rarefaction wave generated by the intake process and attenuated by throttle setting. It clearly solves the maldistribution of fuel-air mixture among the cylinders. Typical variations are ± 2-3%. It also improves on full throttle OEM torque at higher engine speeds, because it provides less intake flow resistance. At lower speeds due to this lower intake flow resistance and excessive intake valve duration, some reversed flow of fuel and air occurs causing a reduction in torque as full throttle is approached. This system needs fuel orifice placement modifications to provide a more nearly constant air-fuel ratio over the speed and load range. Its performance in terms of simulated CVS testing is summarized in Table III.1.

The Dresserator Carburetor was found to provide very good thermal efficiency, particularly at part load conditions. This is attributed to improved air fuel mixing associated with the shock wave which is generated by the mixing nozzle. The carburetor was mounted on the intake manifold only after carefully testing for the best position from a maldistribution viewpoint. The maldistribution was still comparable with the OEM maldistribution and is obviously due to the intake manifold configuration. This carburetor also displayed serious fuel standoff problems at high-torque, low-speed conditions again confirming the evidence that the camshaft provides late intake valve closing for the lower engine speed range. This system needs improved air-fuel distribution to provide fully satisfactory performance. Its present performance which is incorporated in the CVS simulation is also shown in Table III.1.

Electronic Fuel Injection (EFI) was selected to provide ease of control of maldistribution and equivalence ratio. The system allows adjustment of the injection timing and adjustment of the amount of fuel injected for each cylinder. This flexibility is appealing. However, balancing air-fuel ratios among the cylinders for each speed and load required an iterative procedure between the EFI controller and the cylinder exhaust sample measurements. This proved too time consuming to be practical. Extensive performance emissions mappings with this system await resolution of this problem so CVS simulation of the data from this system is not as yet available. However, some steady state test results are presented in Section IV.

III.3 Simulation of Urban and Highway Driving in a Pinto The ultimate objective of comparisons among the alternate fuel systems is to identify the system or systems which will give best vehicle economy and emissions while maintaining drivability. With this in mind, the steady-state performance and emissions data generated for the various fuel-air induction systems operating on methanol have been used to predict fuel economy and exhaust emissions utilizing the Federal Emission Test Procedure (FTP) and Federal Highway Fuel Economy Test Procedure (HFETP). To perform this task, a computer program developed by the Jet Propulsion Laboratory was modified to include the HFETP and some additionally important factors. These program modifications are detailed in Section IV.3.

The Indolene baseline data was also utilized in the predictions and provided the basis for relative comparison with the alternate systems. Table III.1 summarizes the fuel economy results on an energy basis (miles traveled per million Btu of fuel used (mi/10^6 Btu)). It illustrates the advantages of methanol and the improvements derived from the alternate fuel-air induction systems for stoichimetric air to fuel ratio (Φ=1.0) and lean Φ where thermal efficiency is high.

TABLE III.1

Energy Based Fuel Economy as a Percentage Improvement Over OEM Performance Using Indolene* from Computer Simulation of FTP (Hot 1972 Procedure)

Equivalence Ratio Φ	1.0	0.9	0.8	0.7
Methanol - OEM system**	8	16	20	22
Methanol - Dresserator**	18	28	29	26
Methanol - WHB***	19			

*OEM result at Φ = 1.0 as predicted by the computer simulation, approximates the values for 1975 Pintos.

**A further improvement of 2 to 5% is to be expected upon elimination of the maldistribution of air-fuel mixture in the range $0.8 \leq \Phi \leq 1.0$.

***This system varied in Φ with a time averaged value of 0.98.

TABLE III.2

Vehicle Emissions Comparison from Computer Simulation of FTP (Hot 1972 Procedure)

Emissions (gms/mi)

Equivalence Ratio Φ	1.0			0.9			0.8			0.7		
	CO	UBF	NOX	CO	UBF	NOX	CO	UBF	NOX	CO	UBF	NOX
Indolene-OEM system	17.0	2.18	4.8	2.30	1.61	6.0	2.05	1.95	3.27			
Methanol-OEM system	13.10	1.13	1.91	2.03	1.14	3.18	1.78	1.92	1.49	2.0	3.34	.45
Methanol-Dresserator	11.9	1.53	1.79	1.83	1.72	3.19	1.64	3.14	1.61	1.90	5.93	.35
Methanol-WHB	24.02	2.16	2.59									

Exhaust emission comparisons are presented in Table III.2 for carbon monoxide (CO), unburned fuel (UBF), and oxides of nitrogen (NO_x) on a grams per mile (gms/mi) basis. These results represent the case of no maldistribution (MI = 0.0) since individual cylinder data was used as input for the simulation. An interesting result from the simulation predictions is near attainment of the Federal statutory NO_x standard of .40 gms/mi for the OEM system and the surpassing of the standard for the Dresserator Inductor operating on methanol at $\Phi = 0.7$. The methanol CO and UBF results are similar to those with Indolene with the CO emission standard of 3.4 gms/mi being easily met in the lean operating region for all systems including the Indolene baseline. At stoichometric Φ the OEM, Dresserator, and WHB systems on methanol all show 3/4 lower levels of UBF than Indolene shows on the OEM equipment. Note that the UBF results are mixed to some extent . Methanol typically shows rising values as $\Phi = 0.7$ is approached. In general, UBF and CO results need to be interpreted cautiously due to transient emissions behavior which is not taken into account by the steady state data used as input for the simulation.

In summary, it appears that two of the alternate systems show promise in increasing fuel economy and reducing exhaust emissions by operating at very lean values of Φ on methanol. Methanol's lean burning capabilities extend the operable range of Φ to 0.7 and possibly lower, thus making it an excellent candidate fuel for meeting the statutory NO_x standard.

Although these two alternate systems provide improvements in energy based fuel economy and emissions while operating on methanol, significant further improvement appears possible so that one more iteration on the design of each will be tested before they are placed on an automobile for road evaluation.

III.4 Thermochemical Engine Process Modeling: Thermochemical modeling of engine processes offers a low cost way of studying influences of compression ratio, spark advance and equivalence ratio on engine performance and emissions. Over the past two years, a computer model has been developed which uses thermodynamic and chemical kinetic equations along with engine parameters to predict mean effective pressure, spark advance for mean best torque, thermal efficiency, and engine exhaust emissions.

After finely tuning the model to the engine performance for a specific speed and load, the computer model was used to predict performance at other speeds. Subsequently, it was used to predict compression ratio effects on performance and emissions.

The results are very encouraging both from a modeling and engine performance point of view. The model predicted reasonable trends due to speed changes with the exception of spark advance for mean best torque. This discrepancy is believed to be due to the squish* type combustion chamber design of the 2300 cc engine which was not adequately simulated in the initial computer program.

More importantly, the model predicted a thermal efficiency and power increase of 14% when the compression ratio was raised from 8.44:1 to 14:1. The NO_x emissions increased 18% on a volumetric basis. However, when the spark was retarded 3° from MBT, the volumetric NO_x at 14:1 compression ratio fell to the level for 8.44:1 with MBT spark timing. This condition still provides a 13.7% increase in thermal efficiency and power and an attractive 12.4% reduction in $ISNO_x$** compared to the 8.44:1 CR.

Although the computer model predicts cylinder heat transfer, it does not currently model the wall quench zone relative to chemical reactions. Hence, it needs further development before it will correctly predict aldehydes and hydrocarbons. As previously mentioned, the squish chamber of the Pinto engine also needs to be more accurately modeled. With these improvements, there are opportunities for simulation studies relative to the control of hydrocarbon and aldehyde emissions and cold start phenomena. The computer can also be used to study performance effects due to the presence of water in the fuel whether it has been intentionally or unintentionally added as well as the effects of other blending agents or impurities.

---

*The cylinder head has a valve recessment zone and a flat faced zone in close proximity to the piston at top dead center.
**$ISNO_x$ is NO_x on the basis of grams per indicated horsepower hour.

III.5. Cold Starting and Lean Burning: Pure methanol has a vapor pressure temperature relationship combined with a high heat of vaporization which causes cold starting difficulties when the ambient temperature drops into the range of 32-41° F (0-5° C).

Equilibrium thermodynamic studies indicate the potential for generating a cold start gaseous fuel by decomposing methanol. This gaseous fuel which is primarily $2H_2$+CO has wide flammability limits and offers the possibility of serving as a pilot fuel for cold starting and lean burning if it is concentrated in the vicinity of the spark plug. For cold starting, it is estimated that a flow rate range of 0.1 to 0.6 gram/sec would be desirable. Higher flow rates are desired, after the engine is running, for continued lean burn pilot fuel. However, the generation of this gaseous fuel under cold start conditions is seen as the more difficult problem and is receiving our primary attention.

Bench type experiments using battery power to heat a small bore, stainless steel decomposition tube have resulted in decomposition percentages as high as 50-60% at flow rates of approximately 0.5 grams/sec. This is in the desirable range. The hardware required to achieve this result appears to be reasonably adaptable to automotive use. However, the power and energy requirements from the battery appear excessive--being in the range of a kilowatt for 1-5 seconds. These bench experiments are discussed in detail in Section IV.5.

An engine experiment has been devised for determining the least amount of pilot gaseous fuel necessary for cold starting. A cold chamber is available which allows engine cold soaking and start up. Hollow electrode spark plugs have been made available.* Dissociated methanol ($2H_2$ + CO) will be supplied through the hollow electrode to create a rich gaseous mixture near the spark plug during the engine cranking process.

---

*Donated by Mr. E. Leshner of Fuel Injection Development Corporation

Future plans include conducting the engine cold start experiments and making an assessment as to the feasability of dissociating methanol using battery energy for cold starting. If the results are favorable, the hollow electrode spark plugs will also be studied as a means of introducing dissociated methanol as a pilot fuel for lean burn control during normal engine operation.

III.6. Engine Wear Rate and Crankcase Blow by: Conflicting evidence is found in the literature as to engine wear rates using methanol as a fuel in comparison with gasoline.

Oil samples from our test engine have been monitored for accumulation of metals since the test program's inception two years ago. Atomic absorbtion spectrophotometry has been used for the metals detection. The engine has experienced repeated speed and load cycling on both methanol and gasoline fuels.

The evidence to date is summarized as follows:

(a) The influence of the variations of speed and load on the wear rates of iron, chromium, and lead were strong enough to mask any variations in wear rates due to use of different fuels.

(b) In the case of copper, it appears that methanol causes somewhat higher wear rates. However, because the differences are small (see Section IV.6), it will require specific wear rate tests to fully establish the degree of difference, if any.

It is intended that the wear rates will continue to be monitored throughout the ensuing test program.

The composition of the blowby gas which escapes from the combustion chamber into the crankcase of an engine is of importance in engine wear. These gas constituents come into intimate contact with the lubrication oil and the strong oxidizing

constituents such as nitrogen dioxide can be particularly harmful. As an element of our comparative study of methanol and gasoline, an effort is being made to analyze the blowby gases from our test engines.

To date, data has only been taken on the methanol fueled engine. However, there is data in the literature for gasoline fueled engines which allows a rough comparison. This qualitative evidence indicates that the NO_2 concentrations in the blowby gases from our methanol fueled engine are about the same as those from gasoline. This is an interesting piece of evidence because the oxides of nitrogen in the exhaust of a methanol fueled engine are well below those from gasoline. Further study is necessary to fully confirm this evidence and to provide an adequate explanation if it is found to be correct.

III.7 Vehicle Performance: Three street vehicles, which have been described in some detail elsewhere[4], have been operated on methanol for extended periods of time. A 1970 American Motors Gremlin is now in its 7th year of operation on pure methanol. It has operated throughout that time period without any failures in major engine or fuel system components. One car in a pool of cars operated by meter readers in the City of Santa Clara has been using pure methanol as a fuel since its purchase over five years ago. It is a 1972 Valiant. It too has operated with no failures of major fuel system or engine components throughout its operational life. A third car operated by the City of Santa Clara is in its third year of operation on methanol gasoline blends. The blends have varied from 0 to 20% by volume. Typically it operates on a 10% blend. It too has experienced no major fuel system or engine component failures. This car is also 1972 Plymouth Valiant.

The vehicles operating on pure methanol have received modifications to the carburetor jetting to correct for the shift in air-fuel ratio requirements due to the fuel change. More heat has also been supplied

to the intake manifold because of the high heat of vaporization requirement for methanol. The vehicle operating on blends has not been altered.

During the past year, an interesting problem has appeared. A supply of surplus methanol from one of the ERDA laboratories was donated to our project. The methanol has been stored for approximately seven years in 55 gallon steel drums. Upon inspection, the methanol appeared to have a slight discoloration and was known to contain some water. To avoid phase separation, this methanol was not used in the vehicle operating on blends, but it was used in the two vehicles operating on neat methanol. One of these vehicles experienced stoppage on the road. Inspection revealed a gelatanous mass collected ahead of the 3 micron porosity fuel filter.

Analysis leads us to the conclusion that a compound, hydrousferric oxide, is the cause of the trouble. Characteristically, this compound first formed as very small particles which apparently passed through the filter in the supply line used for fueling the vehicle. Heat and agitation associated with vehicle road operation accelerated coagulation such that the precipitated material would not pass through the fuel line filter and the vehicle starved for fuel. By filtering this contaminated methanol through activated charcoal, it is being restored as a fuel suitable for our vehicle use.

The vehicles will be continued in operation and will be the subjects of mechanical inspection and further CVS testing during the ensuing 12 months.

III.8.a. Photochemical Reactivity Studies: The photochemical reactivity of the emissions from methanol fueled combustion processes has not been adequately investigated. Toward that end, an investigation is being initiated using a smog chamber made available by the ERDA, Bartlesville Energy Research Center. This chamber is being equipped with appropriate instrumentation and is expected to be operational within this calendar year.

The objective of the tests now being planned is to compare the photochemical reactivity of exhaust gases from three fuels: methanol, Indolene, and Chevron unleaded gasoline with and without catalysts for each fuel. The reactivity index will be a composite based on smog chamber measurements of hydrocarbon consumption rate, NO consumption rate, NO_2 peaking time, and ozone formation. Exhaust samples will be taken from a single vehicle run on the Federal driving cycle.

III.8.b. Biological Hazards of Methanol Spills: During the past year Dr. P. D'Eliscu of the Biology Department with University funds has investigated four aspects of methanol toxicity relating to marine or estuarine species:

(a) Acute toxicity to substrate-forming invertebrates, algae, free-living vertebrates and surface water plankters.
(b) Chronic exposure to methanol of selected invertebrates and subsequent reproductive changes.
(c) Chronic exposure of various crustacean and subsequent molting ratio changes.
(d) Comparison of gasoline versus methanol toxicity under varying conditions.

As a sample of early results, a concentration of about one percent methanol in sea water proved to be toxic to many common components of rocky intertidal, mud flat, and estuarine ecosystems if heavy metals were eliminated from methylation. Lower levels of methanol proved toxic if metal contamination is considered.

Preliminary assessment of methanol toxicity to small marine and estuarine organisms is encouraging to environmentalists. The effects of immediate spills or leaks would probably be minimal except in a very proximal area where concentrations reach one percent. Since methanol is quite miscible, volatile and degradable,

gross environmental impact from moderate spills is unlikely. Individual rare species may be more significantly affected, however.

Continuing studies include a comparison of gasoline and methanol as coastal marine pollutants, the effects of tidal period, and aeration recovery of organisms from short term exposure.

III.8.c. Conversion of a Small (60 hp) Gas Turbine to Methanol: A computer modeling study of a gas turbine combustor contrasting emissions of NO_x and CO from methanol fuel with simulated jet fuel has previously been reported.[5] This model predicts an 80% reduction in NO_x and a 45% reduction in CO for homogeneous and stoichiometric conditions in the primary zone of the combustor which served as a model. For that study, air entered the combustor at a pressure of 15 atmospheres and at a temperature of 800° F.

During the past year a 60 horsepower Solar T-45M-13 gas turbine engine which powers a water pump has been modified to operate on methanol fuel. The conversion was accomplished by doubling the orifice area of the sleeve metering valve within the fuel regulator. Exhaust concentrations of NO_x, NO, CO, hydrocarbons, CO_2 and oxygen were measured during turbine operation on Jet A fuel and on methanol. Fuel injection pressure (and subsequent droplet size) was varied by changing simplex fuel nozzles during the experiments. An air-assist atomizing nozzle was also tested in an effort to obtain the smallest possible droplets.

The following two bar graphs (Figures III.1 and .2) summarize combustor/turbine emissions from this and five other experiments and contrast them with the computer predictions. In each graph is plotted the relative amount of pollutant emissions for methanol as compared to distillate fuel. The relative emissions are plotted against combustor inlet temperature (CIT). Two effects can be seen in the graph of relative NO_x emissions. The smallest droplets, produced by air-aided atomizing nozzles, reduced relative NO_x levels by 60%-80% for methanol for all combustor inlet temperatures shown. The larger

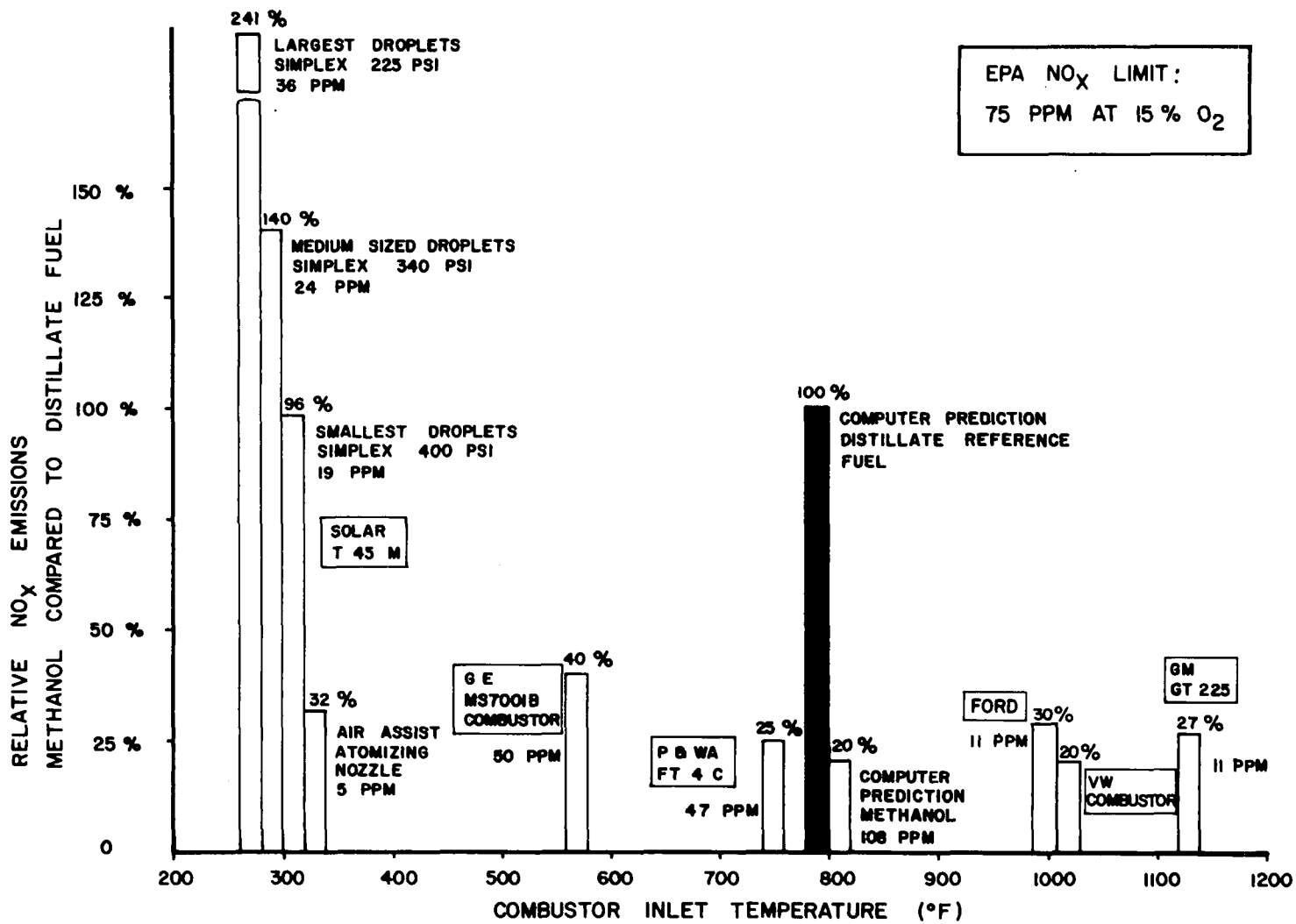

FIGURE III.1 : NO_X EMISSIONS — METHANOL VS JET FUEL IN GAS TURBINES

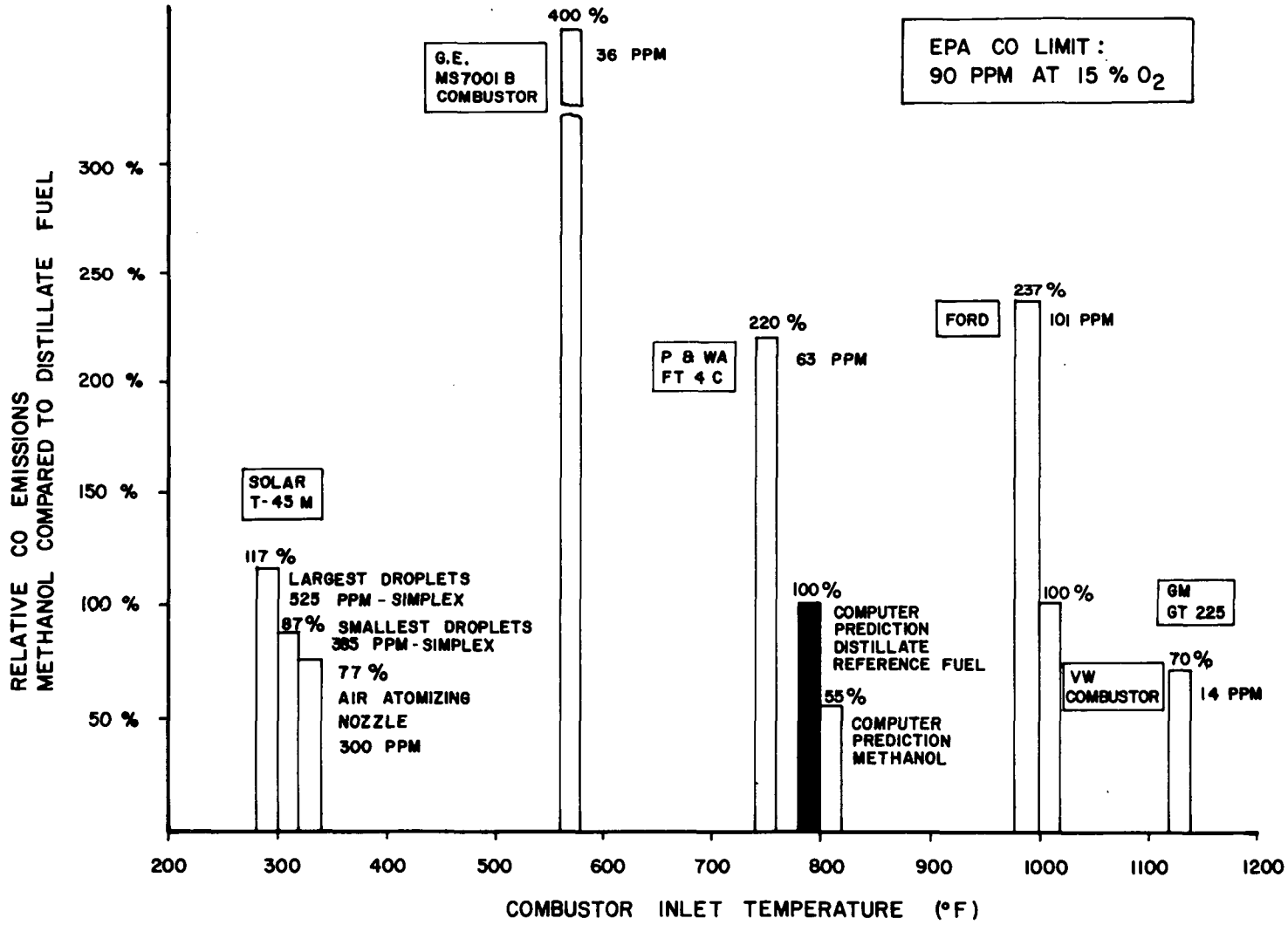

FIGURE III.2: CO EMISSIONS - METHANOL VS JET FUEL IN GAS TURBINES

droplets, produced by simplex-fuel pressure atomizing nozzles, produced NO_x emissions from methanol in the range from 96% to 241% of distillate fuel NO_x emissions. Therefore, at low CIT the initial droplet size is very important for actually achieving the low NO_x potential of methanol combustion that has been predicted by computer study and produced by turbines at higher CIT values.

A detailed study of the droplet burning contrasts between methanol and jet fuel would be necessary to accurately explain the contrasts seen in this evidence. However, it is believed to be strongly related to the relatively high heat of vaporization of methanol (506 Btu/lbm vs 110 Btu/lbm for distillate fuel) and the doubling of the fuel flow rate for methanol to achieve the same energy release rate. The combination of these two factors indicates that for equal droplet sizes the methanol drops will take longer to evaporate compared to distillate fuel droplets. The proportionately larger amount of burning in the form of droplet combustion, which occurs near stoichiometric, high temperature conditions, results in the excess NO_x production for methanol with large initial droplet sizes. It is thought that the Delavan Swirl-Air nozzle produced very small droplets (<20μM) which overcame the droplet evaporation limitation of the simplex nozzles and reduced the percentage of droplet burning and hence NO_x production.

The relative carbon monoxide emissions were also decreased with smaller droplets in the present experiment. However, it is evident from the experiments shown in Figure III.2. that the relative CO emissions are strongly dependent on CIT. This trend is clearly evident for all experiments using the more efficient air-aided atomizing nozzles.

The high absolute levels of CO at low CIT values are caused by the flame quenching effects of the cool secondary air mixing with the combustion products. This quenching effect is greatly aggravated in the T-45M-13 by asymmetric airflow into an elbow type combustor. As the CIT values rise, among the more modern and symmetrical combustors reported in the literature, the quenching effects are strongly reduced and relative CO values correspondingly decrease. Methanol's predicted lower CO

emissions were achieved at very low and at very high CIT, as the graph indicates. The absolute values of NO_x and CO are well below the EPA standards of 75 PPM NO_x and 90 PPM CO for all of the engines with air-aided atomizing nozzles.

Engine power output was achieved at consistently lower (40° F) exhaust temperatures with methanol. This resulted from the increased cooling of incoming combustor air caused by methanol's high latent heat of vaporization and by increased mass flow through the turbine with methanol. The practical consequence is that power output may be increased in a turbine which is limited in allowable sustained turbine inlet temperature. Alternatively, at the same power output the maintenance interval may be significantly increased due to lower temperatures at the turbine inlet.

In conclusion, the NO_x emissions of a small gas turbine with low CIT were reduced by as much as 68% with methanol fuel and careful fuel atomization. The carbon monoxide emissions were also reduced 23%. There is general agreement in trend between this evidence and the experimental and computer simulation evidence found for turbines operating at higher CIT values. Either engine power or maintenance intervals may be increased due to reduced turbine inlet temperatures with methanol. Droplet burning studies should be conducted to fully understand the best burning technique for liquid fed methanol flames so that its excellent burning characteristics can be fully exploited.

IV. DISCUSSION OF PROGRAM RESULTS

The purpose of this section of the report is to provide a more detailed explanation of the component elements of our program, the methods of procedure in the investigations, and interpretations of the evidence derived from the various phases of the program to date.

IV.1. Steady State Engine Performance and Exhaust Emissions Characterization - Methanol vs Indolene

An experimental parametric evaluation of a Pinto 4-cylinder 2300 cc engine operating on Indolene and methanol is presented in this section. In section IV.1.1 comparative engine performance and exhaust emissions are contrasted for the "as supplied" or OEM equipment operating on Indolene, and the modified (enlarged carburetor jets and increased manifold heating) OEM equipment operating on methanol. Additional comparative data for three alternate fuel-air induction systems operating on methanol is also presented. The maldistribution of the fuel-air mixture among cylinders in conventionally manifolded multicylinder engines is one problem that was eliminated with two of the three alternate systems. To properly treat the experimental data of the system with maldistribution, it became necessary to define a maldistribution index. This topic is covered in section IV.1.3. Operational and design aspects of each of the three alternative systems are discussed in section IV.2.

IV.1.1. Comparative Steady State Performance and Exhaust Emissions: The objective of the comparative mappings of performance and emissions is to draw contrasts between gasoline and methanol. These contrasts are drawn in terms of engine power, thermal efficiency, lean burn capability, and the pollutant exhaust emissions of carbon monoxide (CO), unburned fuel (UBF), oxides of nitrogen (NO_x) and aldehydes (HCHO). This objective is approached from two directions which can be summarized in question form: a) With minimal modifications, can a conventional gasoline engine yield equivalent or better operation while operating on methanol? b) Can additional improvements on

methanol be attained through the use of alternate practical fuel-air induction systems?

IV.1.1.1. Experimental Procedure: A 1975 California Ford Pinto 2300 cc engine was used to drive a laboratory electric dynamometer and instrumented for the measurement of engine control and output variables and exhaust emissions. A schematic which shows this equipment and the points of measurement and control for the steady state testing of the OEM equipment is shown in Fig. IV.1. The intake manifold and heater were removed for tests with two of three alternative systems, and exhaust "headers" replaced the OEM exhaust for two of the three alternate systems.

Five different configurations of air-fuel preparation systems were investigated. These are summarized below:

1) The stock OEM equipment operating on a reference gasoline (Indolene), however, without EGR.
2) The stock OEM equipment with enlarged carburetor jets to permit double the fuel flow rate for operation with methanol as a fuel, and externally controlled intake manifold heating.
3) The stock intake manifold with the Dresserator Inductor instead of the stock carburetor with methanol as a fuel and externally controlled manifold heating.
4) An electronic fuel injection (EFI) system with its own intake manifold operating on methanol.
5) The WHB individual cylinder induction system (no intake manifold) operating on methanol.

The Dresserator and WHB systems utilized a header type exhaust system during portions of the testing. The first four configurations were mapped for engine performance and exhaust emissions according to the steady state test matrix shown in Table IV.1.

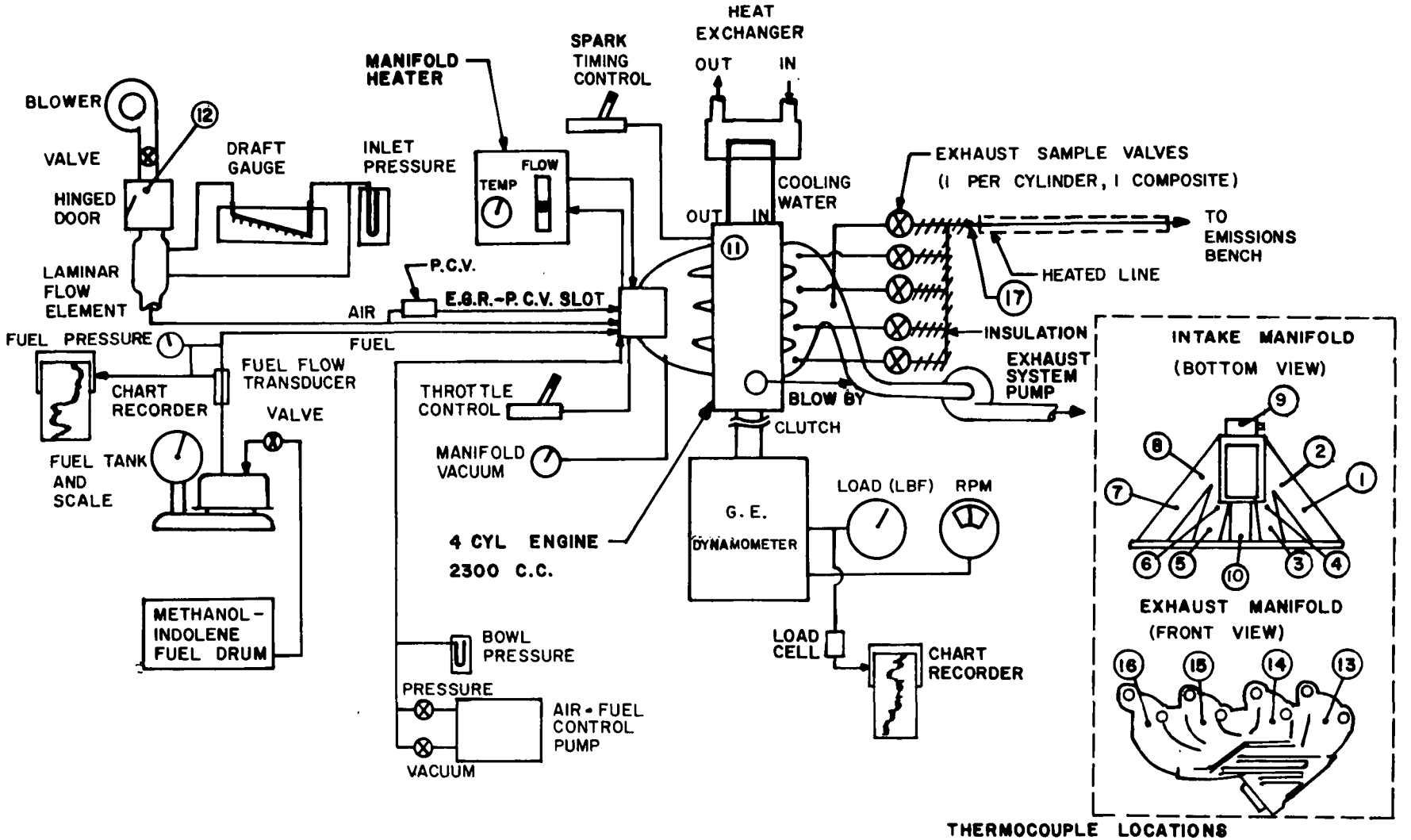

THERMOCOUPLE LOCATIONS

1. CYL 1-HEAD
2. CYL 1-PLENUM
3. CYL 2-HEAD
4. CYL 2-PLENUM
5. CYL 3-HEAD
6. CYL 3-PLENUM
7. CYL 4-HEAD
8. CYL 4-PLENUM
9. WATER TEMP-PLENUM
10. WATER TEMP-HEAD
11. OIL TEMP
12. L.F.E. AIR TEMP
13. CYL 1 EXHAUST
14. CYL 2 EXHAUST
15. CYL 3 EXHAUST
16. CYL 4 EXHAUST
17. EXHAUST EMISSIONS SAMPLE

FIGURE IV-1: TEST ENGINE-DYNAMOMETER CONFIGURATION

TABLE IV.1.

BASE LINE TEST MATRIX

Engine Speed (RPM)	Φ(1)	Load (Fraction)(2)	Spark Setting (°BTDC)	Ambient Temperature (°F)
Idle	0.6(5)	1/4	MBT(3)	70
1000	0.7(5)	1/3	Other(4)	Other(4)
1500	0.8	2/3		
2000	0.9	Full		
2500	1.0			
3000	1.1			
3500(4)	1.2			
4000(4)				

Notes: (1) Equivalence ratio, i.e., stoichiometric ÷ actual A/F.

(2) Fraction load is designated by intake manifold vacuum: Full = 0" hg vac; 2/3 = 7"; 1/3 = 14", 1/4 = 18"

(3) Minimum spark advance for best torque

(4) Implies less than a full complement of speed, equivalence ratio, and load settings will be used for these conditions.

(5) Methanol only

The prinicpal independent variable in this testing was the fuel-air equivalence ratio (Φ). With the exception of the WHB system, techniques were utilized which permitted a wide range of Φ values for each configuration. While operating on methanol, the different configurations were tested in the range of Φ = 0.6 and Φ = 0.7 to explore methanol's lean burning capabilities.

The range of Φ for the WHB system was fixed by the geometry of the fuel metering hardware, and thus Φ could not be the primary independent variable for tests with this system. By changing the fuel metering hardware, nominally rich and lean test points (relative to a standard sets of jets) were obtained.

The test matrix also emphasized part load (high manifold vacuum) and low speeds since the combination of these two is the normal engine operating mode for everyday urban driving. The steady state maps generated from this testing were then used as input to a computer program which predicted fuel economy and emissions for the Federal Test Procedure (FTP) and the Highway Fuel Economy Test Procedure (HFETP). The results are detailed in Section IV.3.

IV.1.1.2. Power, Thermal Efficiency and the Lean Misfire Limit: Figures IV.2. and IV.3. display, for wide open throttle (WOT), indicated and brake horsepower. Figure IV.4. presents indicated thermal efficiency. These are shown as functions of Φ for the five fuel-air induction systems previously cited. Here Φ is the composite or average Φ value of the four cylinders. A new variable termed the maldistribution index (MI) appears with each system curve. This index is defined out of necessity to quantify effects on power, thermal efficiency, and emissions of the inherent maldistribution of the fuel-air mixture among the cylinders.

The value of MI accompanying each curve is defined as the mean deviation (across the range of Φ values) for the two most deviant Φ cylinder values. A more complete definition of maldistribution can be found in Section IV.1.3. For now it is sufficient to note that increasing values of MI mean greater maldistribution, and the effect on power and thermal efficiency can be estimated fairly accurately.

Power and the Lean Misfire Limit: Figure IV.2. indicates that at WOT methanol yields an increase in indicated power ranging from 6% (OEM-methanol @ Φ = 0.8) to 11% (WHB @ Φ = 1.0) over the OEM-Indolene results. All the alternate systems yield higher power than either OEM-Indolene or OEM-methanol systems.

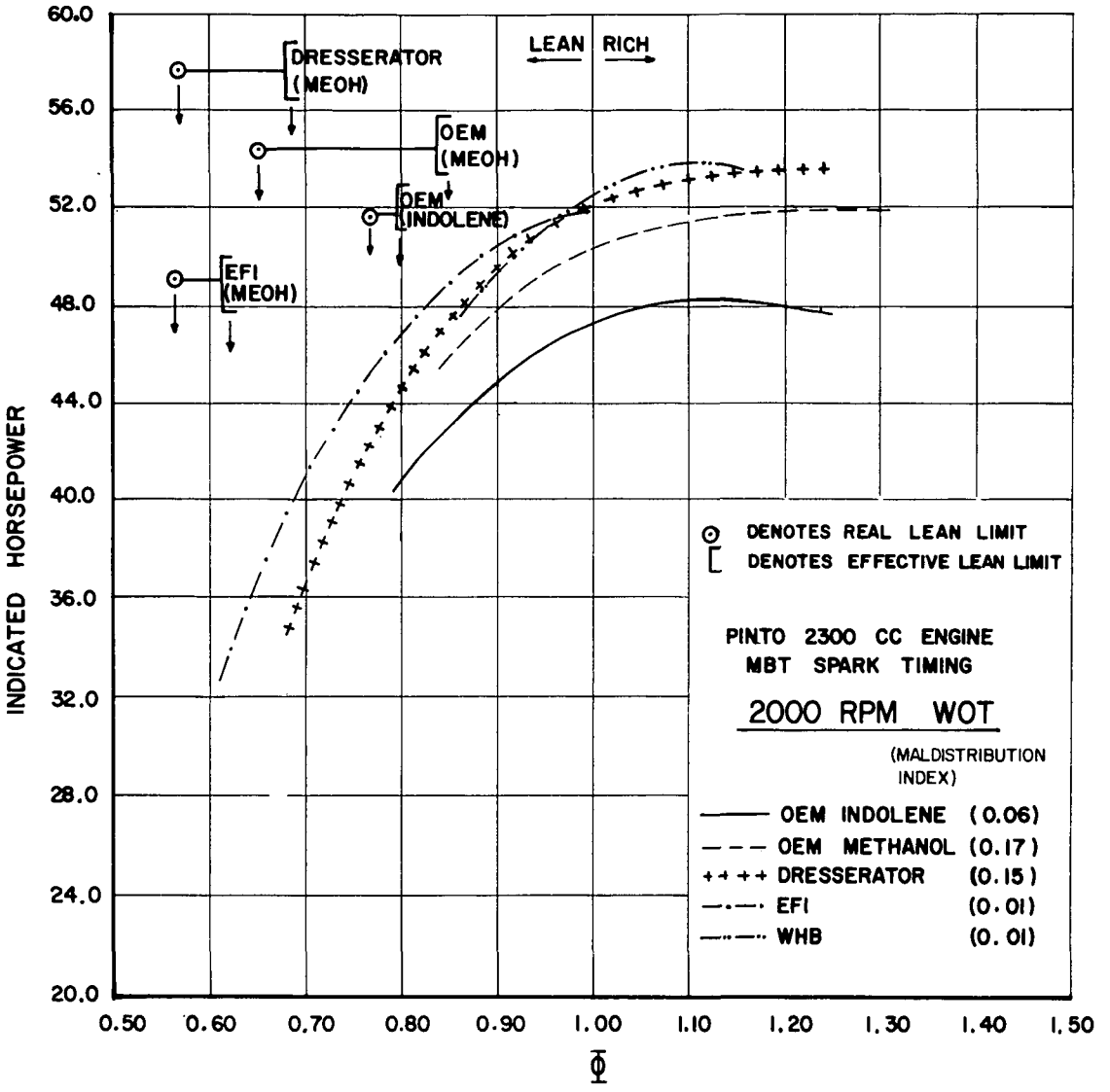

FIGURE IV.2 COMPARATIVE WOT INDICATED POWER – INDOLENE (OEM) VS METHANOL (OEM AND ALTERNATE SYSTEMS)

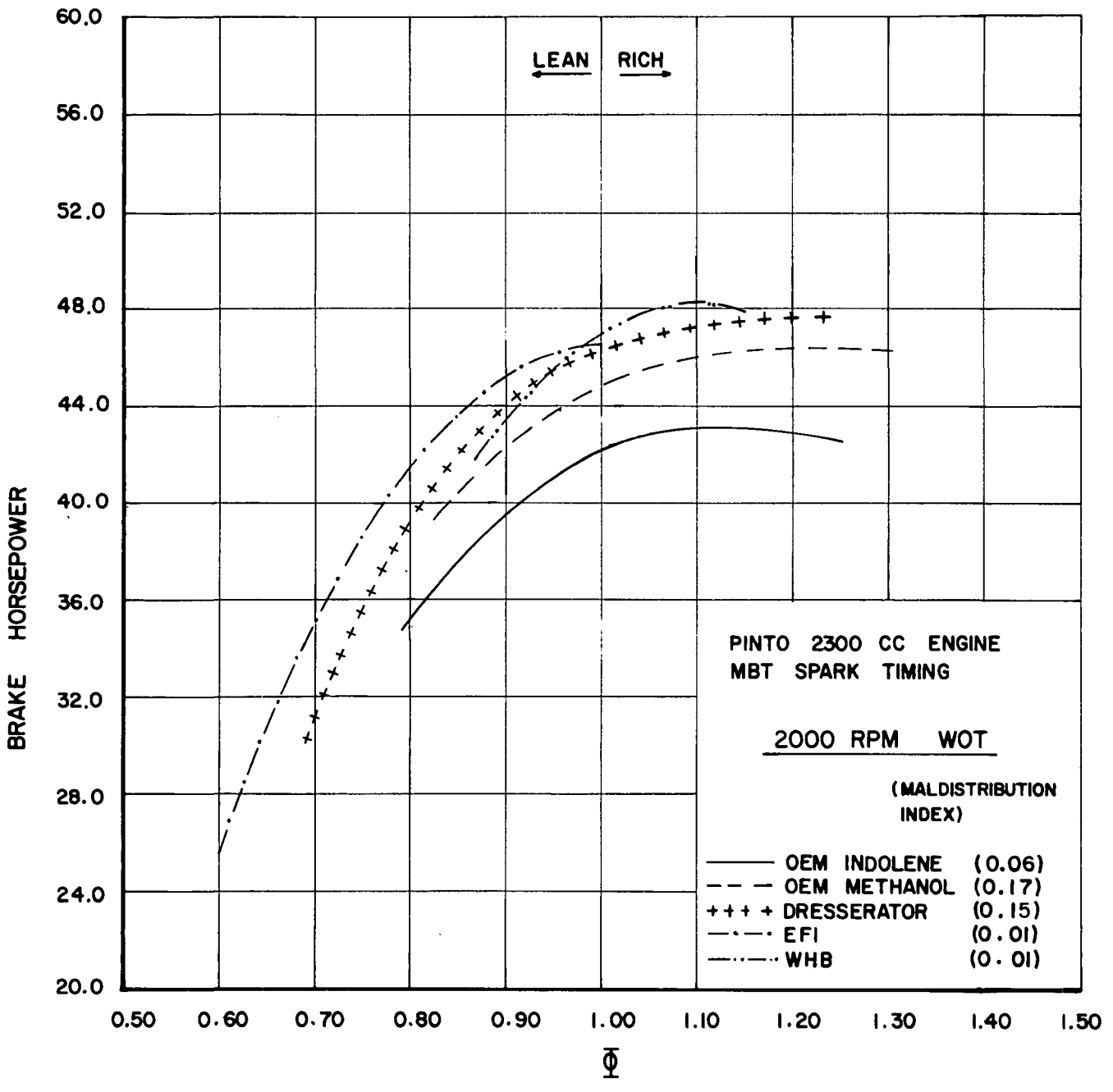

FIGURE IV.3: COMPARATIVE WOT BRAKE HORSEPOWER – INDOLENE (OEM) VS METHANOL (OEM AND ALTERNATE SYSTEMS)

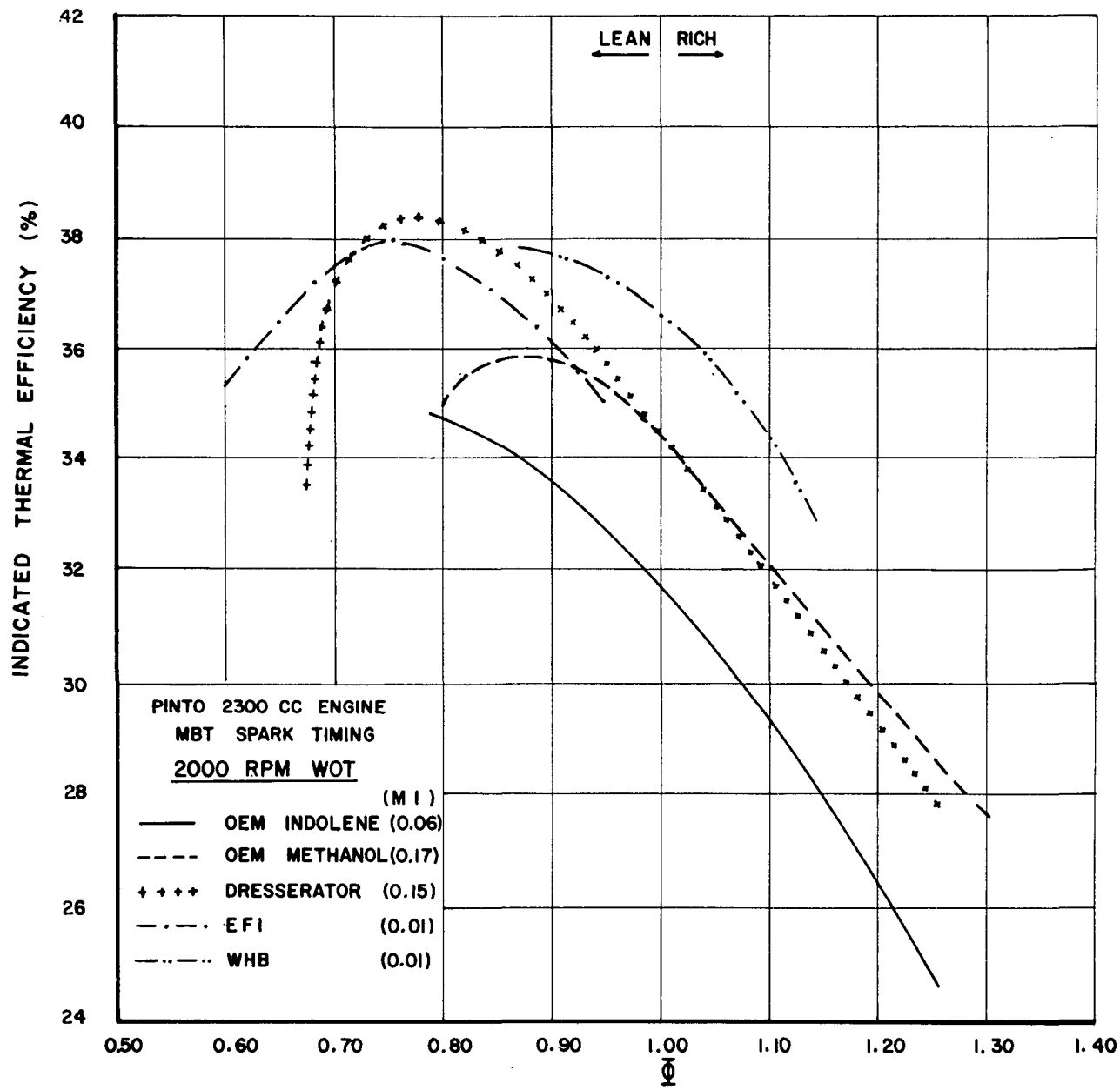

FIGURE IV-4: WOT COMPARATIVE THERMAL EFFICIENCY FOR OEM AND ALTERNATE FUEL-AIR INDUCTION SYSTEMS

The graphical evidence is typical I.C. engine behavior. As Φ becomes lean, there is a fall-off in power. For the systems with significant maldistribution, the apparent or effective lean misfire limit occurs at higher equivalence ratios as is indicated in the top left hand portion of the curve. The value of Φ for the cylinder approaching lean misfire is also indicated. The EFI system was capable of operating at the leanest Φ since each injector could be set to eliminate maldistribution. The WHB system lean limit does not appear since jet geometry did not permit Φ values much leaner than $\Phi = 0.9$. Note that methanol's true lean limit was found to be close to $\Phi = 0.58$ for both the EFI and Dresserator data, while the OEM-gasoline data indicates its characteristic lean limit near $\Phi = 0.77$. The MI values of 0.15 for the Dresserator and 0.17 for the OEM-methanol indicate that in the lean region gains in power of 6 to 10% are possible if maldistribution is eliminated. This would also extend the lean operating limit of both systems and simultaneously raise the thermal efficiency. The implications of this effect are important since it is in the lean region where peak thermal efficiency occurs. The brake power results at WOT in Figure IV.3 show trends similar to the indicated power. The WHB system shows slightly higher values because the pumping losses at WOT are somewhat less than those of the other systems.

Thermal efficiency (Fuel economy on an energy basis): The indicated thermal efficiencies* in Figure IV.4 correspond to the power curves of Figure IV.1. All of the alternate systems and the OEM-methanol configuration show significant improvements in thermal efficiency over the OEM-Indolene results (15% for WHB at $\Phi = 1.0$, 10% for Dresserator at $\Phi = 0.9$ and $\Phi = 0.8$, and 9% for the OEM-methanol at $\Phi = 1.0$). Location of the peak efficiency depends on the system used and its MI value, but all occur in the lean region as expected. For this engine speed of 2000 RPM the EFI shows the leanest peak of

---

*Based on a lower heating value of 19,032 btu/lbm for Indolene and 8570 btu/lbm for methanol.

all the systems at $\Phi = 0.75$. The Dresserator yields the highest thermal efficiency (38.5%), but because of the maldistribution, the fall off at leaner Φ values is very abrupt. The maldistribution index of 0.17 for the Dresserator indicates that if the maldistribution were eliminated, an additional gain in thermal efficiency in the range of 5 - 10% is possible. The WHB system shows the highest thermal efficiency at stoichiometric Φ of all the systems and thus makes it a very attractive system. The exhaust headers were responsible for a 6% increase in thermal efficiency at this speed and throttle setting. The Dresserator on the other hand also utilized the headers but showed no benefit in thermal efficiency over the stock exhaust system. If maldistribution was eliminated from the OEM-methanol and the Dresserator-methanol configurations, it is possible that these two would match the WHB the thermal efficiency at $\Phi = 1.0$.

Indicated thermal efficiency evidence, for 1/3 load, from all the systems at 2000 RPM is seen in Figure IV.5. The trends are similar to the WOT results with a few exceptions. In general, all the alternate systems and the OEM-methanol configuration show significant gains over the OEM-Indolene baseline results. Dresserator and WHB systems yield a 15% gain in thermal efficiency at $\Phi = 1.0$. The MI values at the 1/3 load setting are lower for the systems with inherent maldistribution (OEM-Indolene, OEM-methanol, and Dresserator). As expected, the effective lean misfire limit occurs at higher values of Φ than the WOT conditions for both methanol and Indolene with the exception of the OEM-methanol results. This exception is a result of maldistribution at the WOT condition which masks the true lean limit. The Dresserator and WHB systems show the highest thermal efficiencies (38% @ $\Phi = 0.75$ and 37% @ $\Phi = 0.87$, respectively) but the fall off at leaner values of Φ is more dramatic than the WOT cases. Unlike the WOT results for the EFI, the part load results show a thermal efficiency lower than the OEM-methanol which approaches the OEM-Indolene results in the very rich region. Also, unlike the WOT results, the WHB system shows results similar to the Dresserator. Test data with the OEM exhaust system indicated that neither the Dresserator nor the WHB system gained thermal efficiency at part load when the exhaust headers were installed.

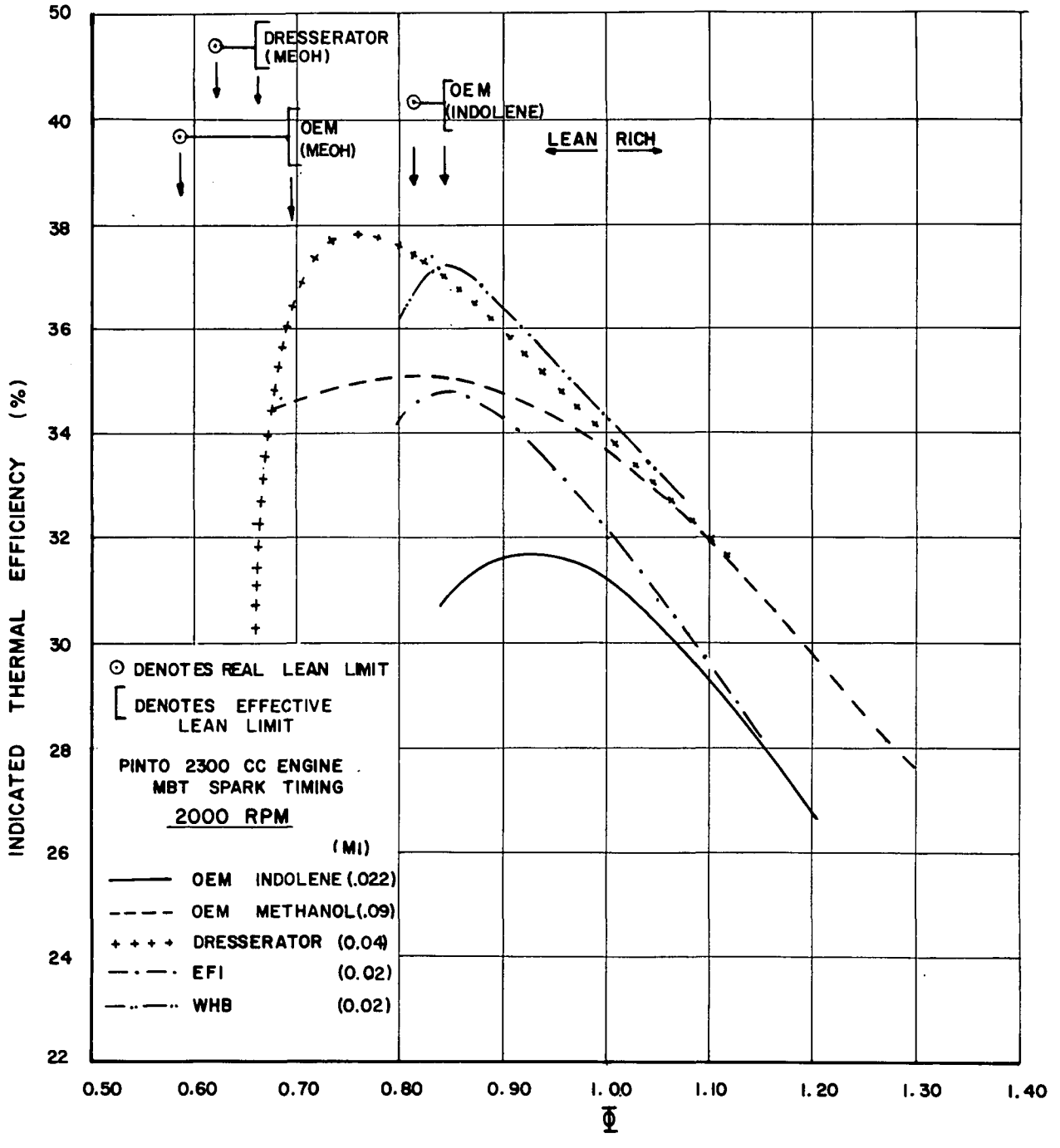

FIGURE IV.5 14" HG MANIFOLD VACUUM COMPARATIVE THERMAL EFFICIENCY FOR OEM AND ALTERNATE FUEL - AIR INDUCTION SYSTEMS

The Dresserator again shows a high thermal efficiency at very lean Φ and a characteristic abrupt drop off in thermal efficiency past that peak. Dresserator data at all speeds and loads shows this severe drop off in thermal efficiency. The OEM-methanol and EFI results do not display this type of behavior. It is claimed that the Dresserator produces a highly atomized and homogeneous air-fuel mixture. Whether or not this is indirectly confirmed by the thermal efficiency results pends further analysis of the data since differences in maldistribution and MBT spark setting cloud this issue. The drop off is due to a substantial power decrease, yet, no misfire occurred. Further analysis is under way to explain why the Dresserator unit shows this characteristic hump in thermal efficiency at all speeds and loads while the OEM-methanol and EFI systems do not.

In summary, these power and thermal efficiency results are typical of the results seen at other speeds. In general, the alternative systems yield improvements in fuel economy (energy basis) of from 5 to 18 percent over the OEM-Indolene baseline at like values of Φ across the speed and load range. The WOT power from methanol ranges from 2 to 10% higher than from Indolene. The lean flammability characteristics of methanol permit very lean steady state operation that is well beyond the limit of gasoline.

IV.1.2. Comparative Exhaust Emissions: Like the power and thermal efficiency of the four-cylinder engine test results, exhaust emissions were highly influenced by the variations in Φ among the cylinders for the steady state test points. This maldistribution can effectively randomize the composite (average of the four cylinders) emissions measured during steady state testing when plotted against the averaged value of Φ. To preclude this kind of result, emission measurements were taken for each of the individual cylinders. The results are presented on a grams per indicated horsepower-hour (gms/ihp-hr) basis as functions of each cylinder's value of Φ. The measured emissions include the principal combustion species CO_2, O_2, and H_2O (deduced) and the pollutant species CO, NO, NO_x, UBF, and aldehydes (HCHO). Figure IV.6. is a schematic of the exhaust sampling system and Table IV.2. indicates the method of detection and equipment used in these measurements.

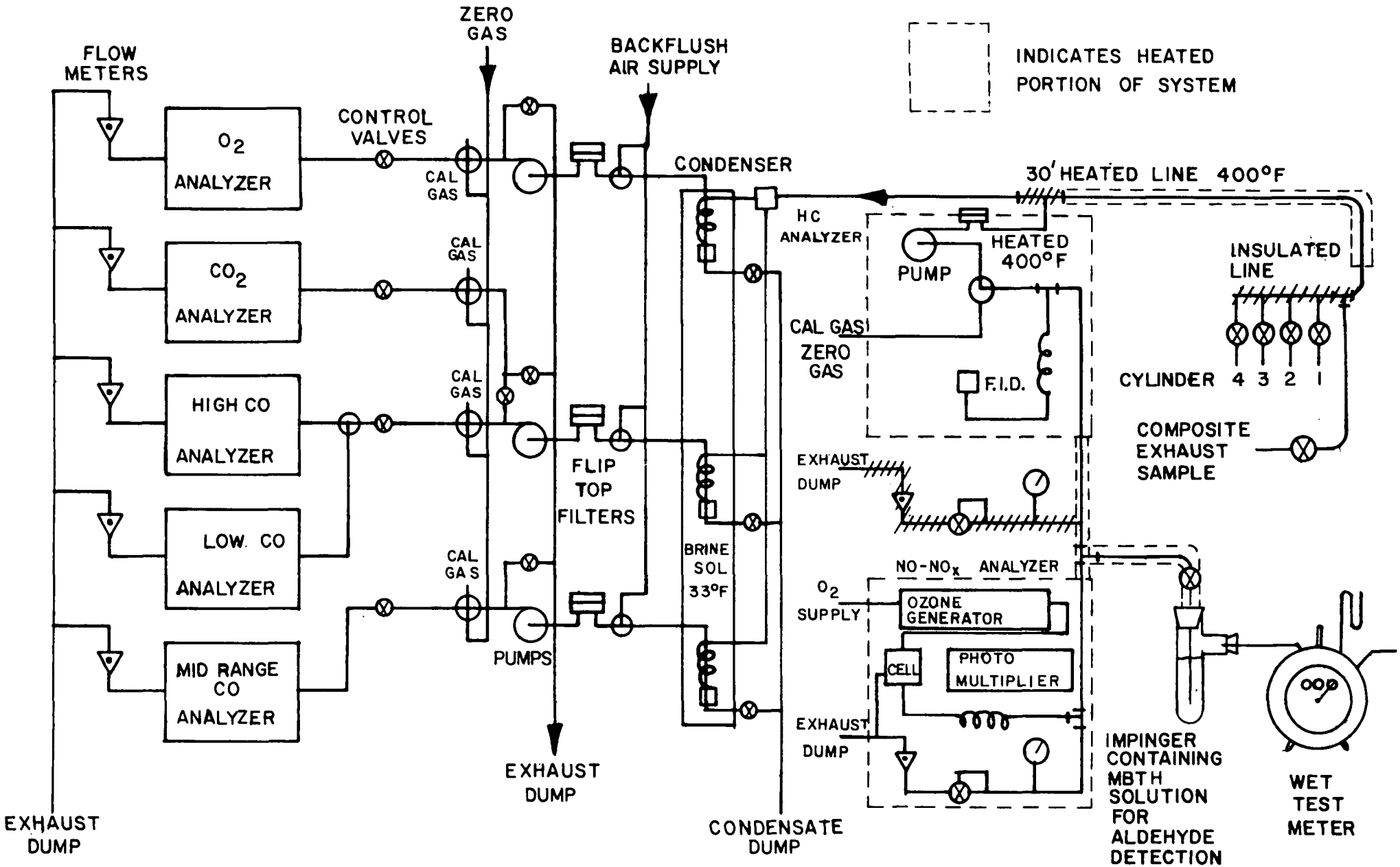

FIGURE IV.6 : EXHAUST EMISSIONS SAMPLING SYSTEM

TABLE IV.2

Exhaust Emission Measurement Technique

Species	Method	Continuous Monitoring	Manufacturer and Model
CO_2	NDIR*	yes	Beckman-315B
CO	NDIR	yes	Beckman 315B
O_2	polarographic	yes	Beckman-OM-11
UBF	heated FID**	yes	Beckman-402
NO/NO_x	chemiluminescent	yes	Beckman-951H
aldehydes	MBTH*** (wet chemistry)	no	B & L Spectronic 20

*NDIR-nondispersive infrared

**FID-flame ionization detector (measured response factor of 0.85 for CH_3OH)

***MBTH-3-methyl-2 benzothiazolone hydrazone (total aldehydes as HCHO)

Comparative CO_2, CO, and O_2: The exhaust emission species of CO_2, CO, and O_2 are three of the combustion species which follow fairly predictable behavior. Figure IV.7 indicates that their "dry" mole percentages are usually functions of Φ only. The results are curve fits of individual cylinder measurements for all the data from all the fuel-air induction systems investigated. The methanol results show slight differences from the Indolene. The different systems on methanol produced virtually invariant results. Characteristic of all the systems is the scatter of data around stoichiometric Φ. The Dresserator CO_2 points which are circled illustrate the trend. It is believed that this scatter is indicative of the nonhomogeneity of the inducted charge. If this is true, then both lean and rich burning occurs within any cylinder. Thus, the CO_2 results take on values lower than the peak value of CO_2 that would be attained with a homogeneous charge at $\Phi = 1.0$. Further study is needed to determine whether or not the experimental evidence can be used to yield a quantitative statement about the degree of stratification.

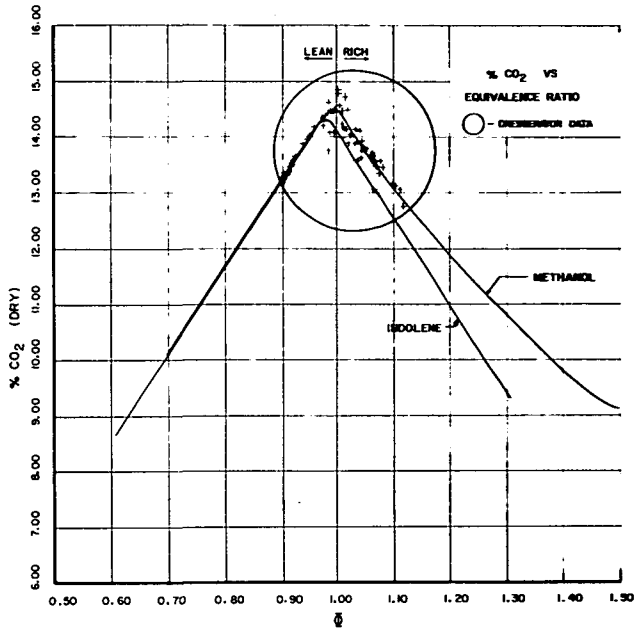

PINTO 2300 CC ENGINE.
METHANOL CURVE INCLUDES DATA FROM OEM, DRESSERATOR, WHB, AND EFI SYSTEMS.
MALDISTRIBUTION INDEX = 0.0

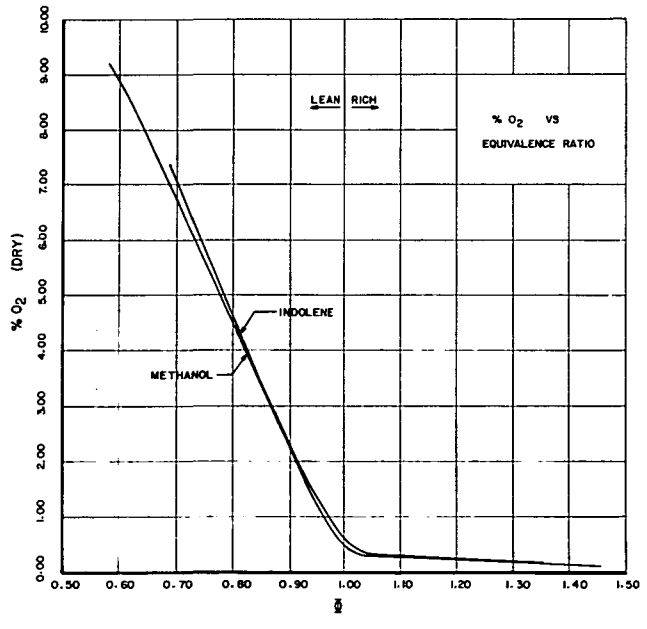

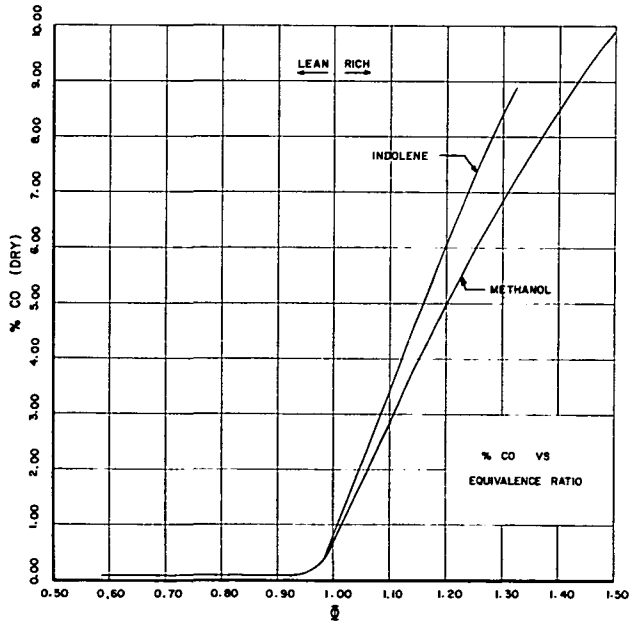

FIGURE IV.7: CO_2, CO, AND O_2 VERSUS CYLINDER EQUIVALENCE RATIO. INDOLENE VERSUS METHANOL.

Comparative NO_x: Through sampling of the individual cylinders of the Pinto engine and curve fitting the MBT data points, comparative MI = 0.0 (no maldistribution) curves of NO_x emissions for the various systems were plotted as a function of the cylinder Φ value. In Figure IV.8, the WOT results at 2000 RPM show that methanol yields lower values of NO_x than the OEM-Indolene data. The WHB system shows the lowest peak values which are about one-half the magnitude of Indolene results. The EFI (and perhaps the WHB system) show the lowest NO_x at stoichiometric Φ. Note that the maldistribution index has not been indicated since cylinder data was used to construct the curves. The close agreement in results for the methanol systems indicates that mixture preparation may be comparable for OEM-methanol, EFI and Dresserator systems or that mixture preparation doesn't dramatically effect in-cylinder NO_x formation. The WHB results near Φ = 0.9 may indicate a difference in fuel-air preparation in comparison to the others, since spark advance was nearly the same (32.5 to 34°BTDC) for all the systems at this Φ.

The 1/3 brake load results in Figure IV.9. at 2000 RPM show behavior quite different than is demonstrated at WOT. The EFI system yields the lowest values of NO_x of all the methanol systems. Its peak value is about 5 times lower than the OEM-Indolene peak. Whether or not the EFI exhibits this behavior at the other speeds remains to be verified since only 2000 RPM data was obtained. Unlike the WOT results, the WHB system shows comparable NO_x when compared with the other methanol systems. This is surprising in that the WHB system at this load had a MBT spark advance of 30°BTDC which is roughly 10 degrees retarded relative to the EFI, Dresserator, and OEM methanol spark timings at Φ = 0.85. (The corresponding MBT spark timings were 44, 44.5 and 41.5 degrees BTDC, respectively.) Mixture homogeniety may be a key to explain the results, but further analysis is required to verify this. In general, though,

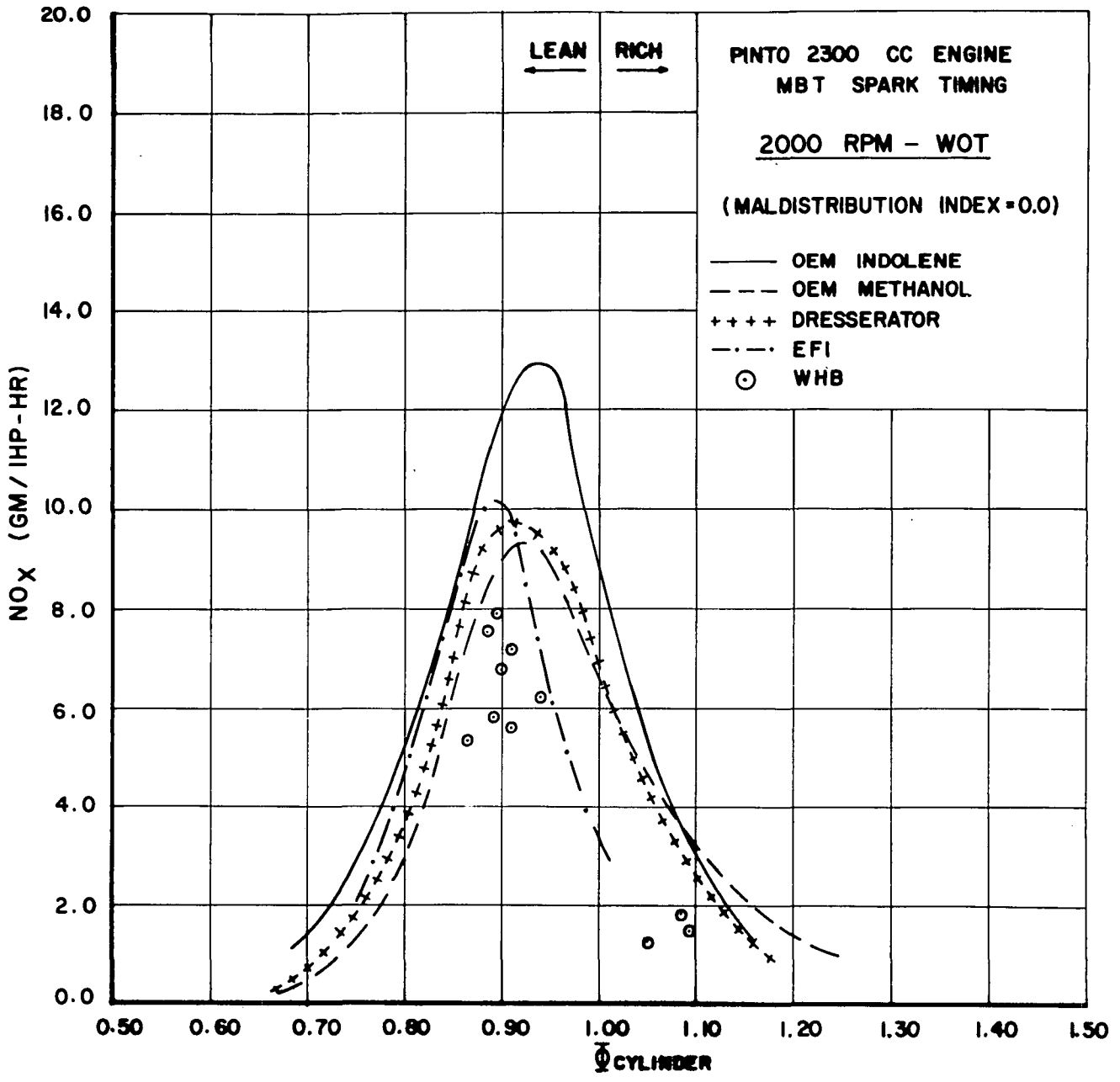

FIGURE IV-8: COMPARATIVE WOT STEADY STATE NO_X EMISSIONS - INDOLENE (OEM) VS METHANOL (OEM AND ALTERNATE SYSTEMS)

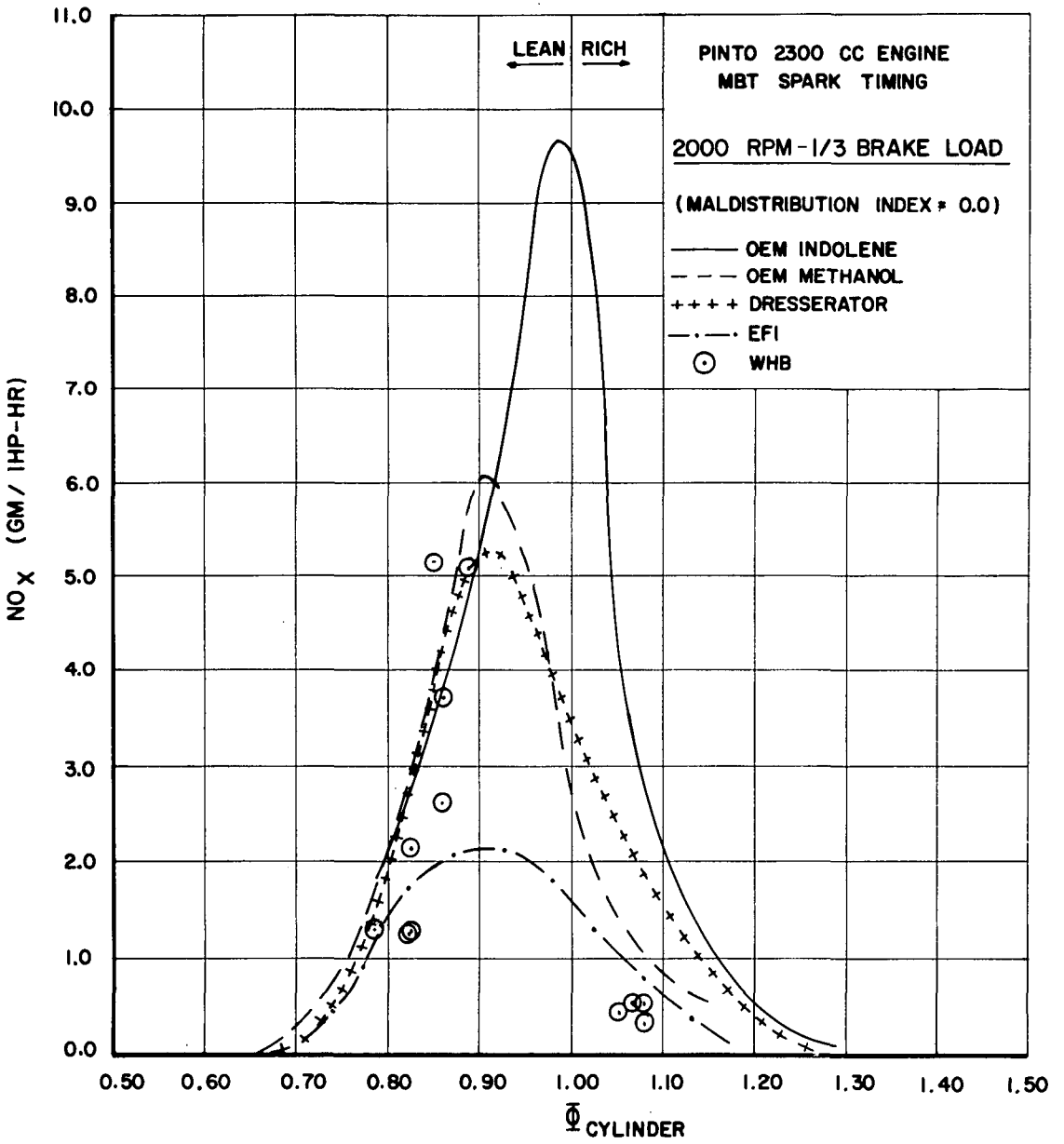

IGURE IV.9 COMPARATIVE 1/3 BRAKE LOAD STEADY STATE NO_X EMISSIONS – INDOLENE (OEM) VS METHANOL (OEM AND ALTERNATE SYSTEMS)

all the methanol systems show lower peak values of NO_x at the part load settings. In the very lean region (Φ = 0.7) the NO_x is under 0.5 gms/ihp-hr. This low value along with the corresponding WOT value of approximately 1.0 gm/ihp-hr provides the incentive for operating the engine at this equivalence ratio to meet the Federal NO_x statutory standard of .40 gms/mi. The FTP simulation results (Section IV.3) indicate that Dresserator and the OEM-methanol configurations can better and nearly meet respectively the standard at this equivalence ratio.

Comparative UBF: Unburned fuel comparisons at WOT and 1/3 brake load for 2000 rpm appear in Figures IV. 10. and IV.11. Indolene is reported as $CH_{1.85}$ and methanol as CH_3OH on a grams per indicated horsepower-hour basis. Again, individual cylinder data has been curve fit and displayed as a function of the cylinder Φ value. The systems operating on methanol show lower values of UBF when compared with the OEM-Indolene. The benefit is small but discernible. The WHB results are not shown at WOT because exhaust headers were also used with this fuel system. The headers, in conjunction with the cam which supplies significant valve overlap, aspirated fuel from the intake to the exhaust. However, in moving to the part load condition (Figure IV.11) the results from the WHB system were comparable with the other alternative systems on methanol. Again, all the other methanol systems showed a slight benefit over the OEM-Indolene and were comparable among themselves. Characteristic of lean operation on liquid fuels is the increasing nature of UBF emissions as the lean mixture limit is approached. At Φ = 0.7 the engine is not seeing any misfire on methanol, yet UBF is quite high.

In interpreting these results, it should be mentioned again that the exhaust gases were sampled near the exhaust valve on the downstream centerline of the exhaust port (1" from the valve). This implies that although the results show correct comparative

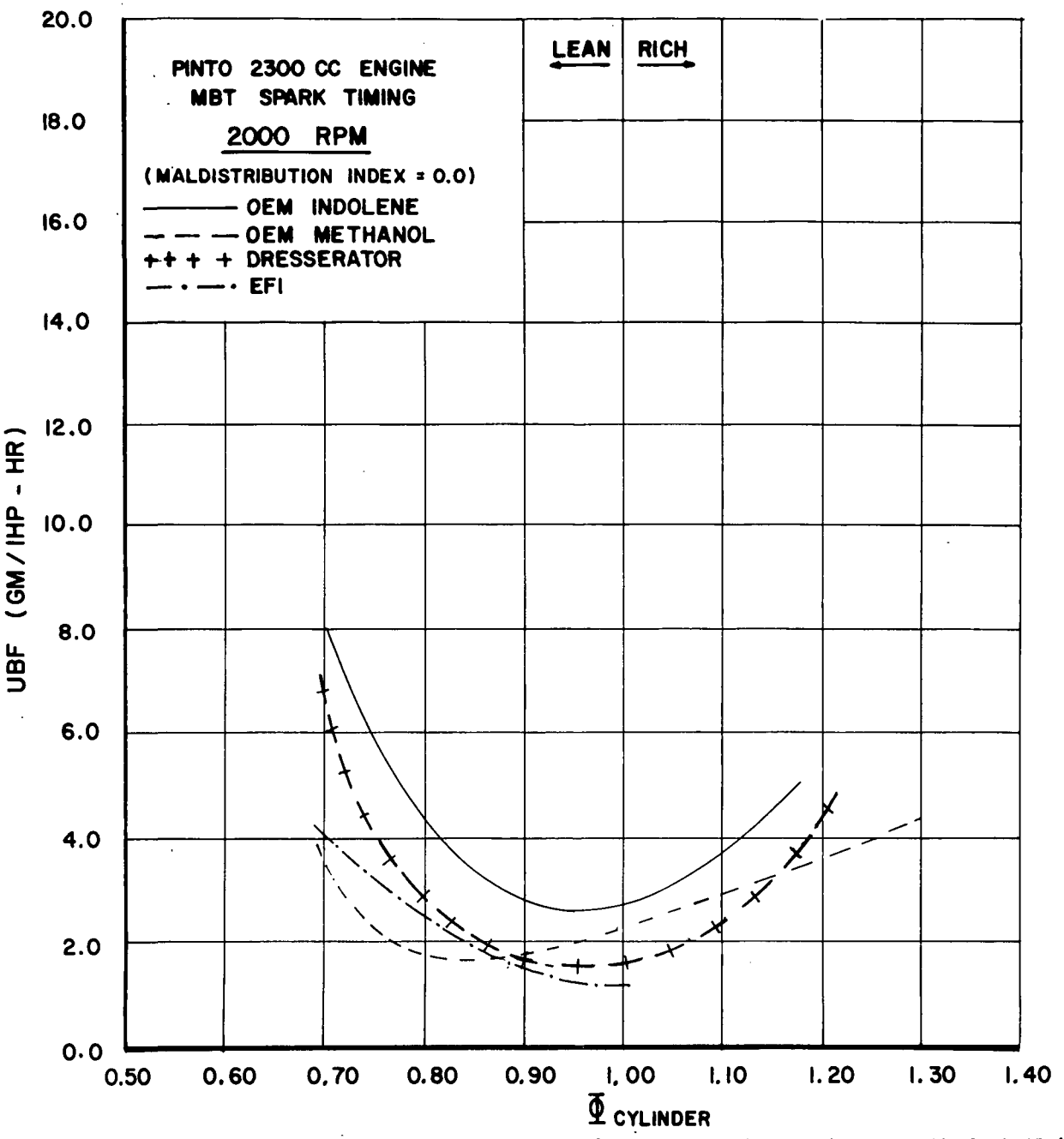

FIGURE IV. 10: COMPARATIVE WOT STEADY STATE UBF EMISSIONS INDOLENE (OEM) VS METHANOL (OEM AND ALTERNATE SYSTEMS)

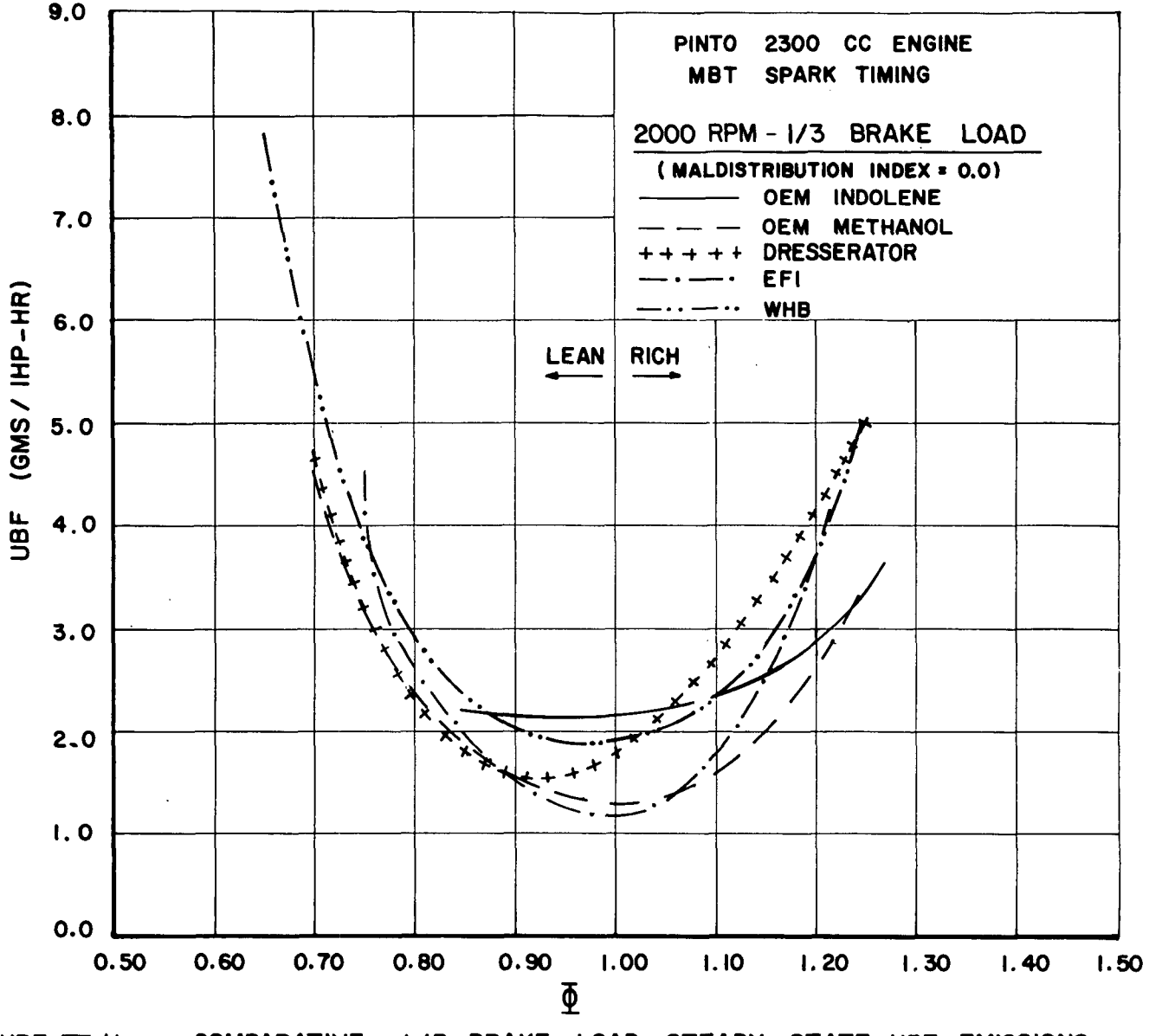

FIGURE IV.11: COMPARATIVE 1/3 BRAKE LOAD STEADY STATE UBF EMISSIONS INDOLENE (OEM) VS METHANOL (OEM AND ALTERNATE SYSTEMS)

evidence, they include a systematic bias that is introduced by two effects. First, there is stratification of UBF in the exhaust gases due to the manner in which exhaust gases are expelled from the cylinder on the exhaust stroke. Secondly, oxidation of UBF takes place in the exhaust system in the presence of excess oxygen, with the effect being more pronounced at the higher loads. Measurements of the composite exhaust sample downstream indicate that these reported results are at least two times higher than results that would be measured at the tailpipe of an automobile which didn't have an oxidation catalyst.

Comparative Exhaust Aldehydes: Figure IV.12. is a plot of exhaust aldehydes (as formaldehyde) as a function of the composite or average Φ for the four cylinders across the speed and load range. The bar with each system curve represents the range of the data. Few individual cylinder measurements were made due to the time involved in performing the wet chemical technique (MBTH*) necessary to determine total exhaust aldehydes. As a result, the maldistribution of fuel and air plays a role in obscuring the comparative evidence for the systems with significant MI. In general, the aldehyde results for methanol fueled systems show values of aldehydes ranging from two to ten times greater than the aldehydes associated with the OEM system operating on Indolene. The WHB system shows the highest aldehydes which is in agreement with UBF findings. In contrast to Indolene results, all the systems operating on methanol show increasing aldehydes at rich values of Φ. Though not shown, the EFI system produced aldehyde results as high as 4 gms/ihp-hr at $\Phi = 0.9$ when the injection timing was close to top dead center. Injection timing could also be manipulated in the WHB system by selecting the proper main jet geometry. For the range of jets observed, the aldehydes did not vary significantly.

---

*2 Methyl-3-Benzothiazolone-Hydrazone

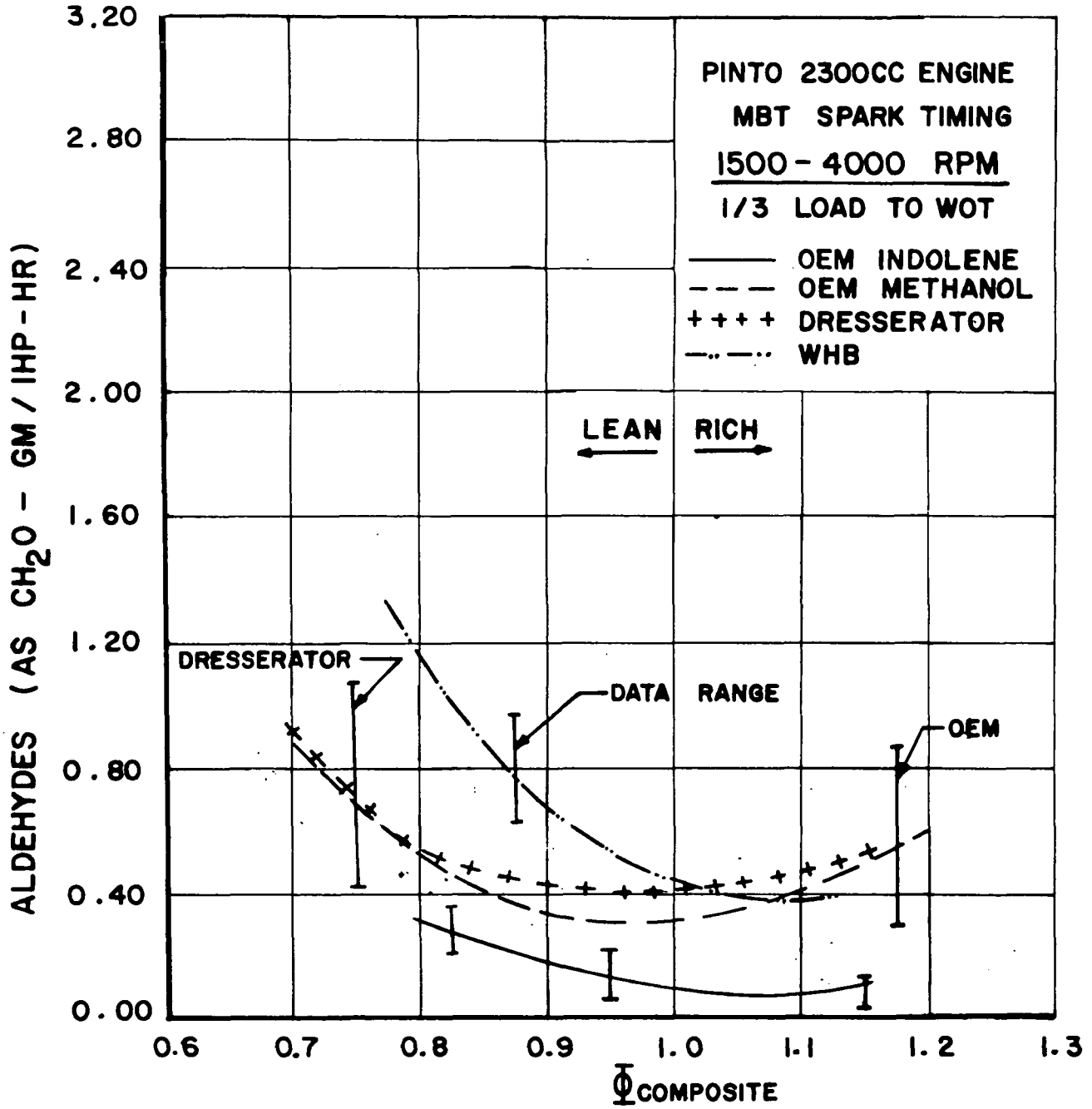

FIGURE IV.12: COMPARATIVE EXHAUST ALDEHYDES VS EQUIVALENCE RATIO

Though aldehyde emissions are higher with methanol, their magnitudes are small in comparison to other exhaust species. Nonetheless photochemical smog consequences with increased aldehydes is not known and thus methods for reducing this one pollutant from methanol fueled engines is being studied.

IV.1.3. Definition of a Maldistribution Index (MI): Maldistribution or variations in equivalence ratio (Φ) among the individual cylinders of multicylinder engines is characteristic of practically all production SI engines which have an intake manifold with a venturi type carburetor. Poor nebulization or atomization of the fuel droplets combined with inadequate mixing with the air stream leads to this phenomena. The 4-cylinder Pinto engine used in generating the steady state maps of performance and emissions is no exception to this rule. Figures IV.13 shows the variations as a function of manifold vacuum at two engine speeds for the OEM baseline tests on Indolene and the OEM baseline tests on methanol, respectively. The average Φ of the four cylinders is used as a normalizing parameter (Φ cyl/Φ average). Characteristically, both Indolene and methanol fuels show increasing maldistribution as the full load condition (0.0 in Hg) is reached. This maldistribution can be bounded in terms of the leanest and richest cylinder which gives rise to a definition. The maldistribution index (MI) is defined as:

$$MI \equiv \frac{\Phi\,(\text{richest cylinder}) - \Phi\,(\text{leanest cylinder})}{2\,\Phi\,(\text{average})}$$

This simple definition of maldistribution can't represent all possible arrangements of Φ values among four cylinders; however, it does appear to be an adequate index to quantify changes resulting from maldistribution in engine power and thermal efficiency. In describing exhaust emissions, the index appears to be inadequate, especially with respect to the NO_x. These two observations are explained in the following paragraphs.

SPEED	MAN VAC (IN HG)	MALDISTRIBUTION INDEX INDOLENE	METHANOL
2000 RPM	0"	0.08	0.17
	7"	0.05	0.05
	14"	0.025	0.09
3000 RPM	0"	0.06	0.11
	7"	0.065	0.09
	14"	0.03	0.05

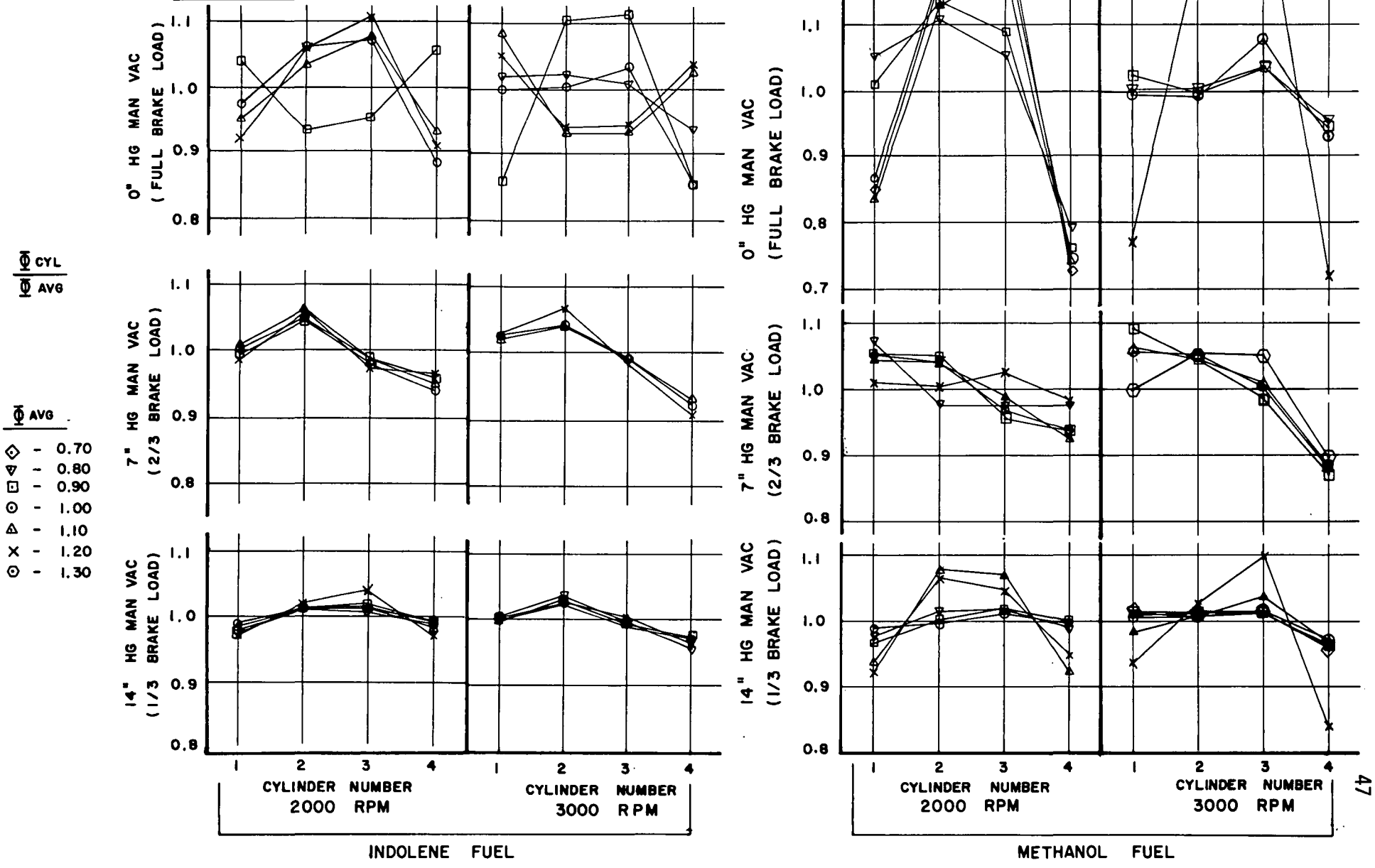

FIGURE IV.13 : CYLINDER TO CYLINDER VARIATIONS IN EQUIVALENCE RATIO - METHANOL VERSUS INDOLENE

Effect on Power and Thermal Efficiency: In Figure IV.13 the average MI for the Φ range at each speed and load corresponding to the graphical evidence appears in tabulated form for both fuels. The values of MI indicate that at the same speed and load methanol is showing a higher degree of maldistribution in the OEM intake manifold/carburetor combination. Figure IV.14 illustrates the effects that this maldistribution has on engine operating variables and outputs. Here, ignition timing, indicated power, fuel flow rate, air flow rate, and the maldistribution appear as functions of Φ (average). The maldistribution, which appears at the bottom of the figure, has been plotted on a vertical axis instead of a horizontal axis. The cylinder numbers appear by each point. In this particular set of seven steady state data points, four of the points show severe maldistribution (MI = 0.20 to 0.30). With severe maldistribution, the MBT spark timing appears overadvanced, and the power is decreased dramatically relative to the points of little maldistribution. Power is down by 11% at Φ = 0.9 and 9% at Φ = 1.0. Since the fuel flow rate is not effected by the maldistribution, the power drop can be translated directly into a thermal efficiency decrease of 11% and 9% respectively. This decrease in power (and thermal efficiency) at a given average Φ can be attributed to the cylinders that are operating lean combined with non-MBT spark timing that exists for all four cylinders. The contributions from these two factors are illustrated in Figure IV.15. In this figure, engine power for a no maldistribution case is plotted as a function of Φ (highest curve). Assuming that MBT conditions are maintained for each cylinder, maldistribution effects can be calculated by assuming some form of maldistribution among the cylinders. Two cases are plotted which represent MI = 0.10 and MI = 0.20. It is assumed that the values of Φ for each cylinder deviate linearly from Φ average. For the assumed symmetrical maldistribution, the calculated percentage decrease in power (MBT-each cylinder) is tabulated along with the observed percentage decrease in power (non MBT-each cylinder). The differences between calculated and observed values indicates that the additional deficit due to non-MBT conditions more than doubles the deficit due to

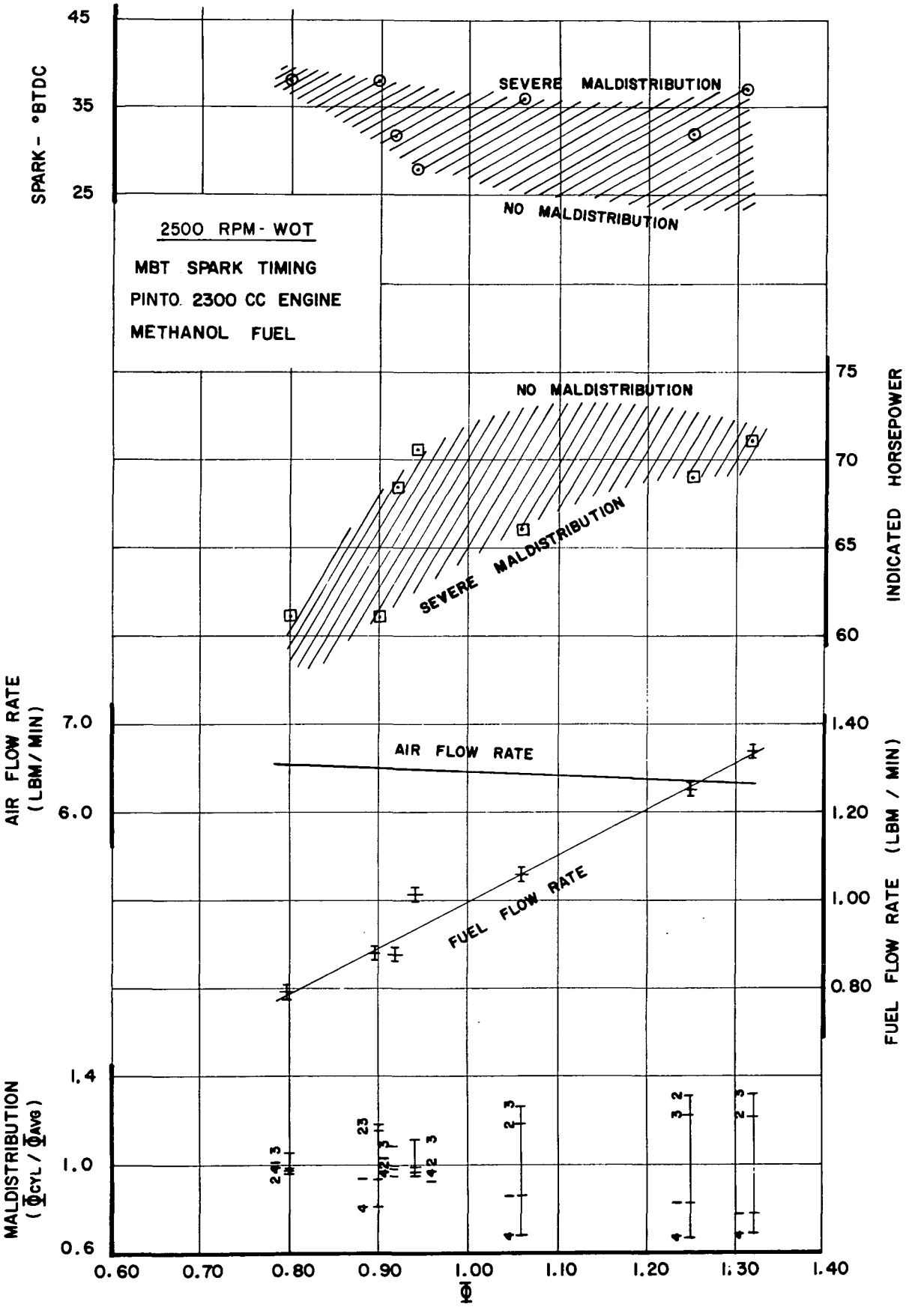

FIGURE IV.14: EFFECTS OF MALDISTRIBUTION ON SPARK TIMING, POWER, AIR FLOW RATE, AND FUEL FLOW RATE

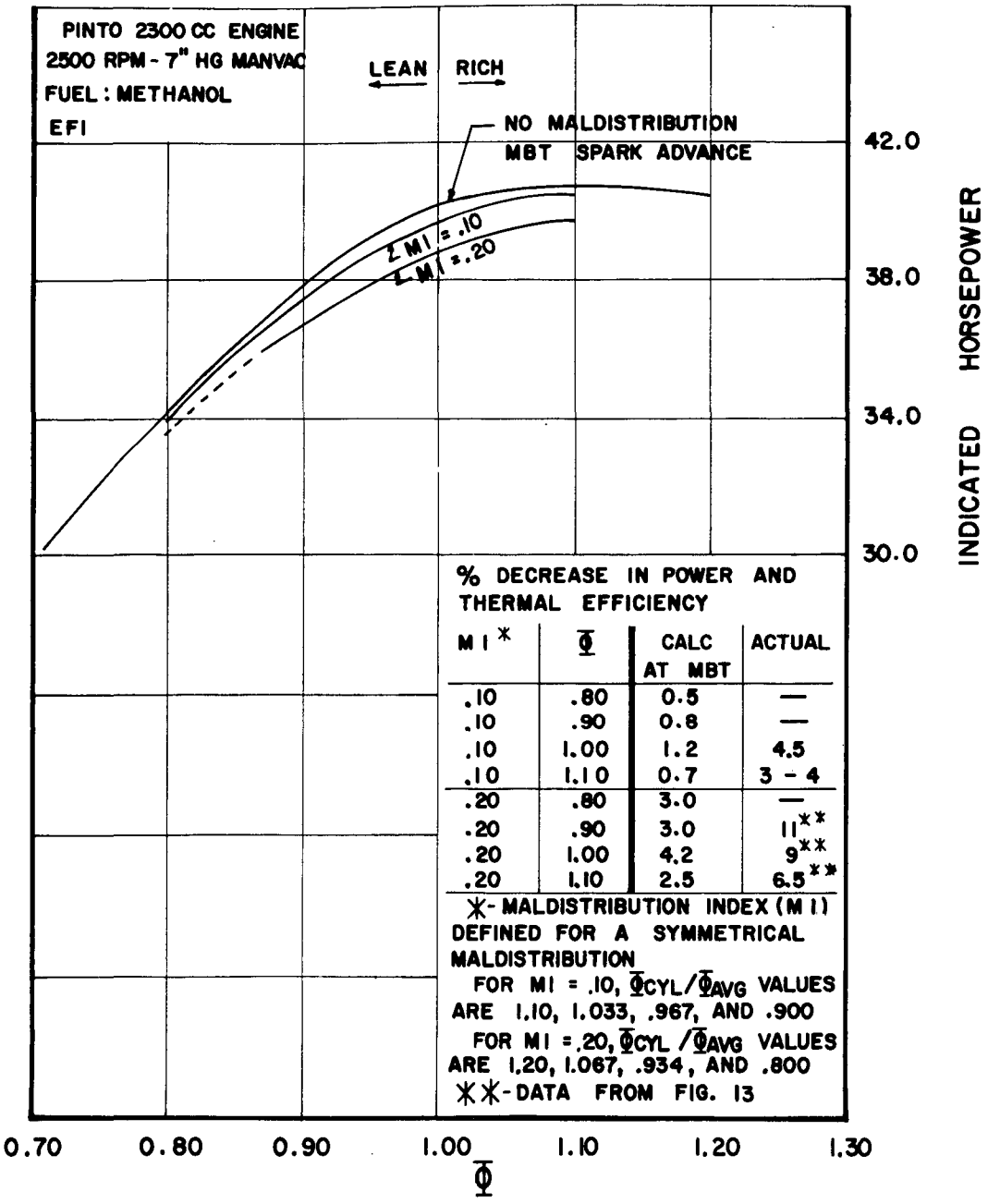

% DECREASE IN POWER AND THERMAL EFFICIENCY

MI *	Φ	CALC AT MBT	ACTUAL
.10	.80	0.5	—
.10	.90	0.8	—
.10	1.00	1.2	4.5
.10	1.10	0.7	3 - 4
.20	.80	3.0	—
.20	.90	3.0	11**
.20	1.00	4.2	9**
.20	1.10	2.5	6.5**

*- MALDISTRIBUTION INDEX (MI) DEFINED FOR A SYMMETRICAL MALDISTRIBUTION

FOR MI = .10, Φ_{CYL}/Φ_{AVG} VALUES ARE 1.10, 1.033, .967, AND .900

FOR MI = .20, Φ_{CYL}/Φ_{AVG} VALUES ARE 1.20, 1.067, .934, AND .800

**- DATA FROM FIG. 13

FIGURE IV-15: EFFECTS OF MALDISTRIBUTION ON POWER - CALCULATED VS ACTUAL

maldistribution alone. Other maldistribution variations can be assumed and superimposed on the graph; however, the symmetric case presented here appears to closely approximate the actual maldistribution seen with the OEM-Indolene, OEM-methanol, and Dresserator systems. Thus, the table in Figure IV.15 is used in this report to estimate the expected gains in fuel economy if maldistribution is eliminated in the OEM (Indolene and methanol) and Dresserator systems. For average Φ values leaner than 0.8 no estimate of expected improvement in thermal efficiency is attempted since the leanest cylinder is usually undergoing intermittent misfire.

Effect on Exhaust Emission: The maldistribution index as defined appears from a qualitative standpoint to be somewhat unsatisfactory in explaining trends in average exhaust emission level. The following discussion is somewhat academic, since measurements from the individual cylinders were utilized in displaying emission characteristics; nevertheless, the discussion is important in trying to interpret the simulation of the FTP (Section IV.3.) relative to actual exhaust emissions measured in the FTP. The importance lies in the fact that FTP emissions are based on the mixed or average levels of emissions which are collected at the exhaust tailpipe (i.e. the effects of maldistribution are included). CO and UBF trends with maldistribution can be explained through calculations similar to those utilized to generate the power curve (Figure IV.15.). The two figures below illustrate in a qualitative way the expected effects.

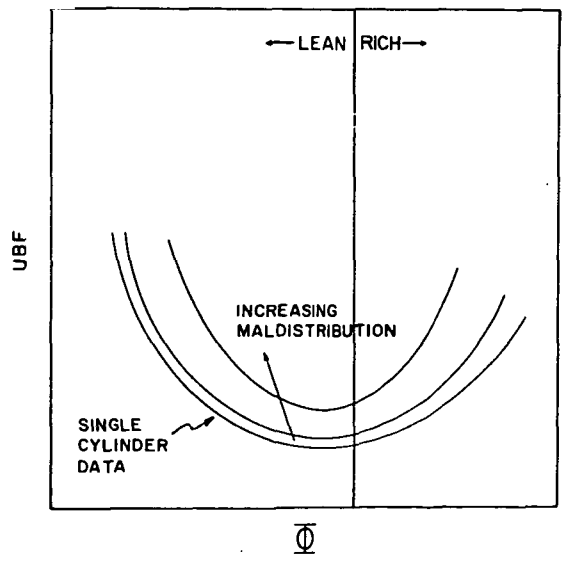

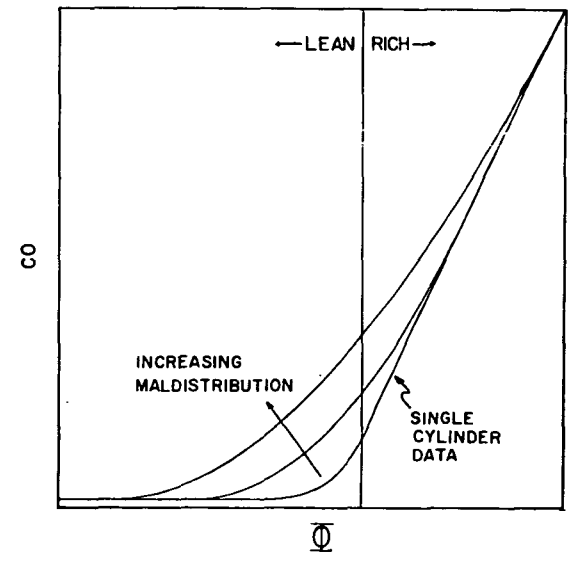

The NO_x emissions have a highly non-linear character when plotted against the cylinder Φ as is indicated in Figure IV. 8 and IV. 9. Average values of NO_x when maldistribution is present produces results such as seen in Figure IV. 16. Here is an illustration of actual test data based on the measurement of the average (a composite) NO_x for methanol and indolene at 2000 RPM and WOT. The peak of Figure IV. 8 for the OEM-Indolene now has two maxima due to the maldistribution. The OEM-methanol data which had a mean MI value almost double that of the indolene shows a more divergent character of the two maxima. The fact that smooth curves could be drawn for the two cases indicates that the maldistribution symmetry remained fairly constant for the range of Φ investigated. Figure IV. 17 predicts the methanol results of Figure IV. 16. based on calculated mean values of NO_x for an assumed constant maldistribution which is indicated. This maldistribution approximates the WOT methanol maldistribution at 2000 RPM (see Figure IV. 13.). Any number of maldistribution combinations could be plotted and thus the random nature of a four cylinder average NO_x plot versus Φ can be anticipated.

Summary: Maldistribution of the fuel-air mixture among the cylinders of this four cylinder engine appears to effect power and thermal efficiency in a predictable manner except at very lean operating conditions. The maldistribution index (MI) provides a means to quantify the effect for average $\Phi \geq 0.8$ while operating on methanol. The exhaust emissions can't be accurately predicted for the simple definition of maldistribution used; however, by assuming a constant maldistribution symmetry average exhaust emission curves can be generated from the single cylinder measurements made.

The variations in exhaust emissions (especially NO_x) that can be seen with varying degrees of maldistribution provides the rationale for using MI = 0.0 emission results for predicting emissions in the simulated FTP and HFETP driving cycles (see Section IV.3.). Though few automotive engines operate at steady state conditions with no maldistribution, calculations on the basis of MI = 0.0 provide the boundary conditions which real engines may approach. Through design of fuel-air metering systems which yield virtually no maldistribution (such as the WHB system)

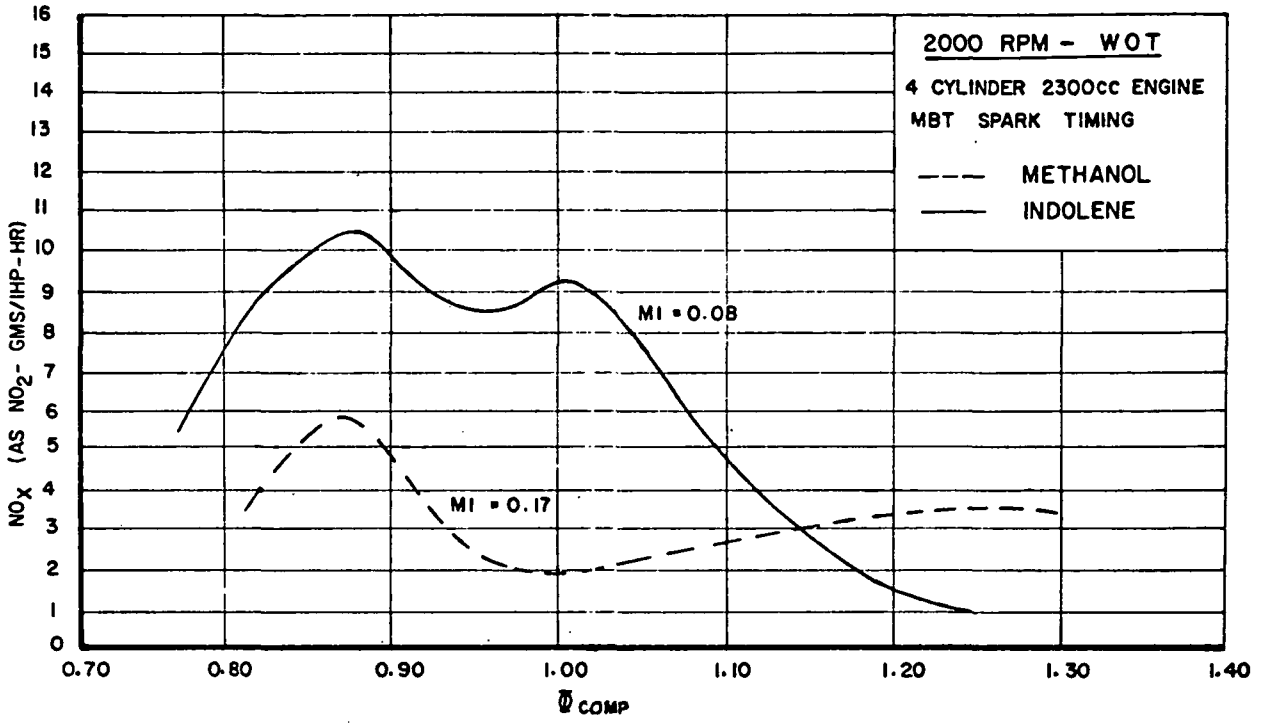

FIGURE IV. 16: EFFECT OF MALDISTRIBUTION ON NO_X – EXPERIMENTAL DATA

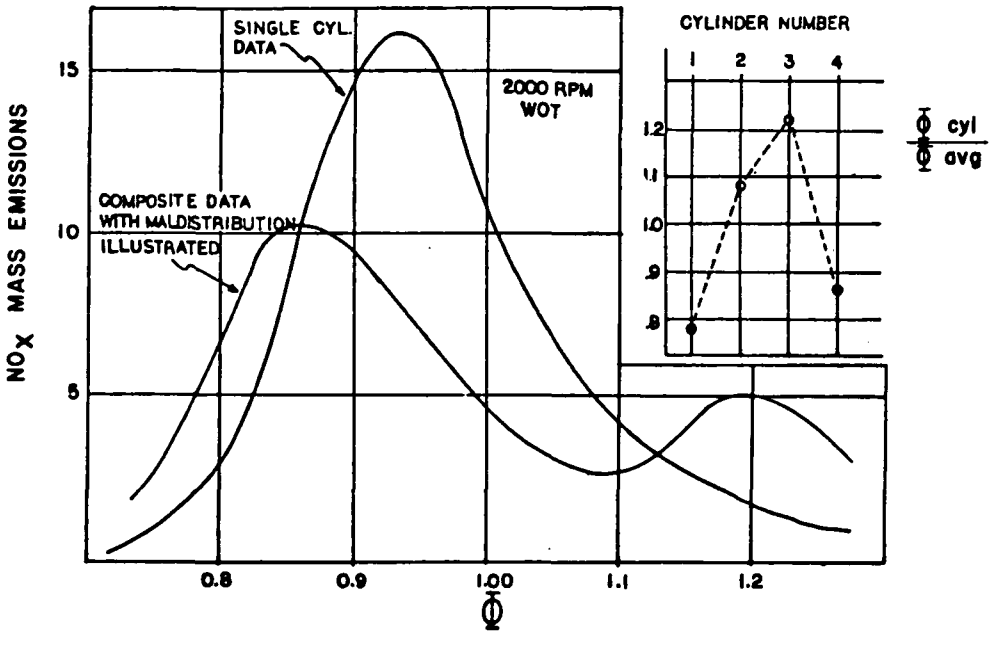

FIGURE IV.17 CALCULATED MALDISTRIBUTION EFFECT ON NO_X FOR A CONSTANT MALDISTRIBUTION SYMMETRY

these predicted emission levels may be attained eventually.

IV.2. Alternative Fuel Induction Systems: From the investigations with the modified OEM carburetor several areas of improvement are needed to design the optimum fuel-air induction system for methanol operation. One of the most significant of these areas is the maldistribution of air and fuel among the cylinders. The consequences are loss of performance and excessive pollutant emissions because the spark advance and air fuel ratio cannot be simultaneously optimized for all cylinders for given speed and load conditions. Evidence of such problems has been presented in Section IV.1.

In the investigation of alternative air-fuel induction systems, one must incorporate gains in thermal efficiency and reduced exhaust emissions with the realities of the production automobile. These factors include economics as well as an ability of the system to adapt to present day emission controls such as PCV and EGR. The best air fuel induction system, thus, must be economic as well as having precise control of air-fuel ratio through better metering, nebulization and mixing.

IV.2.1. WHB System: The basic hardware consists of an intake duct coupled directly to each intake port through a mounting plate which carries a sliding throttle mechanism, a metering orifice in the wall of the intake duct, and a floatless fuel supply system which utilizes a fuel return line for maintenance of liquid level.

When the intake valve opens and the piston begins its downstroke, expansion waves propagate outward through the intake duct, initiating air flow into the duct and fuel flow through the metering orifice. The expansion waves are reflected from the open end of the duct as compression waves delayed by the round trip travel time in the duct, so that the resultant pressure difference at the metering orifice closely approximates the time derivative of the air mass flow rate in the duct. Since suitable fuels are 600-700 times as dense as air, the resultant fuel mass flow rate can be made proportional to the air mass flow rate on an instantaneous basis by proper selection of metering orifice dimensions.

Subsequent wave reflections are prevented by viscous acoustical resistance in the form of a narrow slot through the wall of the duct, providing critical damping for an otherwise resonant acoustical system.

Wave motion in the duct generates a substantial non-turbulent pressure gradient near the wall; the metering orifice outlet is positioned to maximize the effectiveness of this pressure gradient in atomizing the fuel issuing from the orifice. Visual examination indicates mean fuel droplet diameters of the order of 10 microns were produced by a CFR engine at 900 RPM at wide open throttle in a 33 mm diameter duct.

Because an intake duct is coupled directly to each port, the mixture transit time from metering orifice to intake valve can be reduced by an order of magnitude compared to a conventional system with a distributing manifold, so the fuel droplets have much less time to fall out of the air stream. They will not recombine into larger droplets or be deposited on the walls of the intake manifold as in a conventional system because no significant changes in mixture flow direction occur along the path.

WHB System Performance: Due to the relative simplicity of the system and its ability to essentially remove maldistribution among the cylinders, the WHB induction system shows promise as a superior fuel-air inductor for methanol operations. Even though the WHB system requires an inductor for each cylinder, its simplicity places it economically competitive with the OEM system.

In order to obtain low emissions and lean operation, close control of air-fuel ratio is required. In Figure IV.18, the variation of Φ with percentage throttle opening is shown with engine speed as a parameter. Cylinder maldistribution at 2000 and 3500 RPM are also shown. It is clear that there is negligible influence of speed on the equivalance ratio. Hence this fuel preparation system has acheived the design objective of holding a balanced air-fuel ratio among the cylinders over the desired speed range. However, the excurisions in air-fuel ratio from 0.8 to 1.3 with throttle opening are excessive for good performance and emissions control.

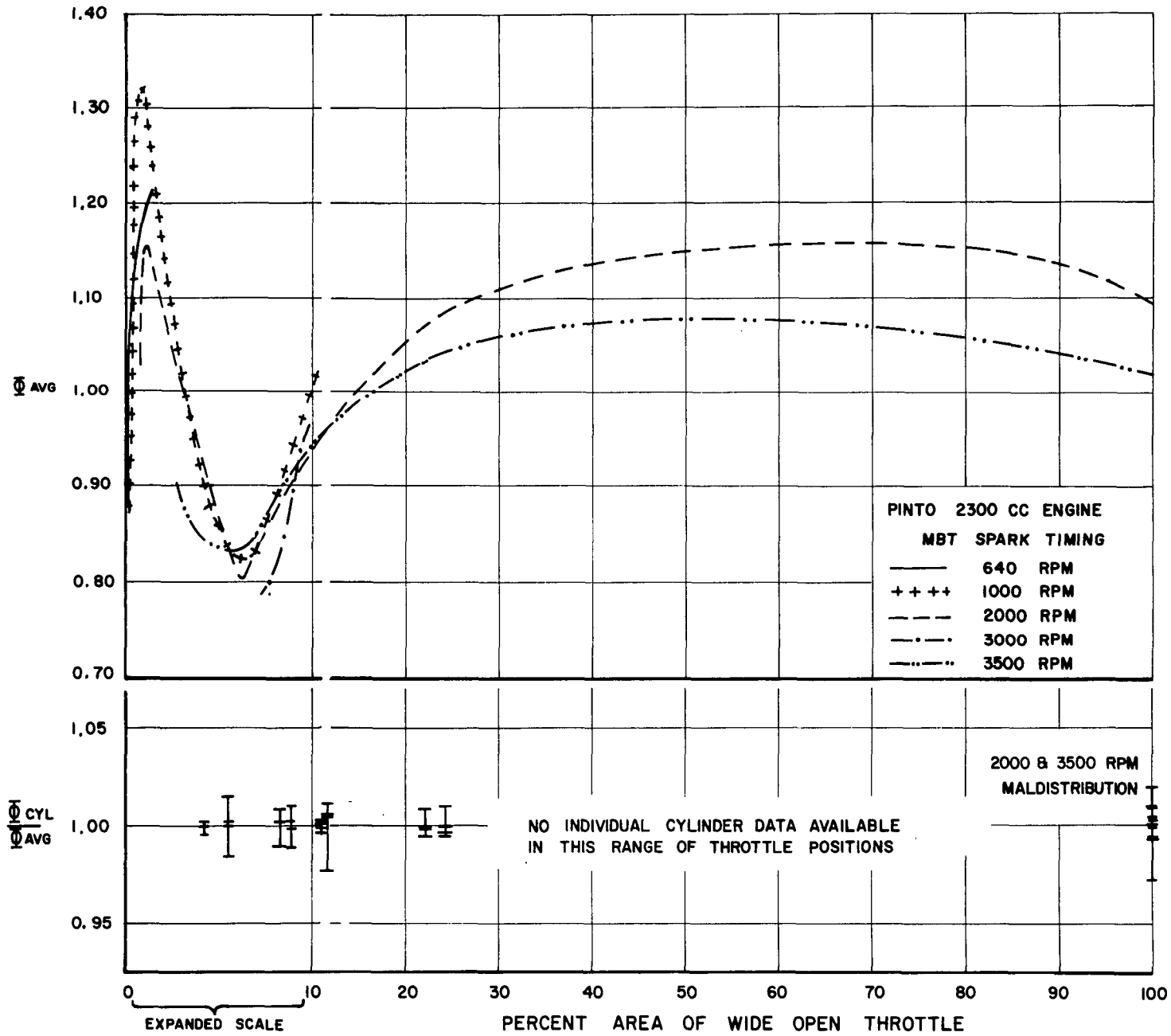

FIGURE IV.18: EQUIVALENCE RATIO VS PERCENT OF WIDE OPEN THROTTLE - WHB INDUCTION SYSTEM

Due to the reduction of flow resistance of the WHB system compared to the OEM carburetor manifold system, coupled with the excessive inlet valve duration (276°), excessive air flow reversal was encountered. Figure IV. 19 shows the mass flow of air inducted versus percentage of throttle port opening. Note that the maximum amount of air inducted occurs at the 70% point for 2000 RPM. In the region between 70% and WOT (100%), the amount of inducted air declines. This is due to the excessive open duration of the intake valve which allows time for reversed flow to occur. This reversed air flow carries some fuel past the carburetor inlet resulting in significant sputter. Evidence like Figure IV.19 generated at higher engine speeds shows that the OEM camshaft was designed for high speed operation. Consequently, a new camshaft is being designed with less intake valve open time for better operation at urban driving speeds. Testing of the WHB system will resume with the fuel circuit modifications and the new camshaft.

IV.2.2. Electronic Fuel Injection (EFI) System: The electronic fuel injection system employed for these tests is shown in Figure IV.20. Basically it consists of Bosch electronic fuel injectors and an analog control unit designed by personnel at the ERDA Lawrence Livermore Laboratory.

Referring to Figure IV.20, there is one injector per cylinder, mounted to spray fuel approximately at the backside of the inlet valve. The injectors are supplied with fuel from a continuous return, pressure regulated system. The fuel pressure regulator is referenced to manifold pressure so that a constant pressure differential of 28 psi is maintained across the injectors regardless of the manifold pressure.

The injectors operate either fully open or closed. The opening and closing times of the injectors have been minimized by the design of the electronic circuit driving them. The controller determines how long the injectors are to remain open based on inputs from a manifold pressure transducer, rpm signal and inlet air temperature.

The metering circuitry can be adjusted to yield a wide variation of equivalence ratios. The injection pulse width is typically four to fifteen milliseconds in going from idle to WOT at 3000 rpm. It is

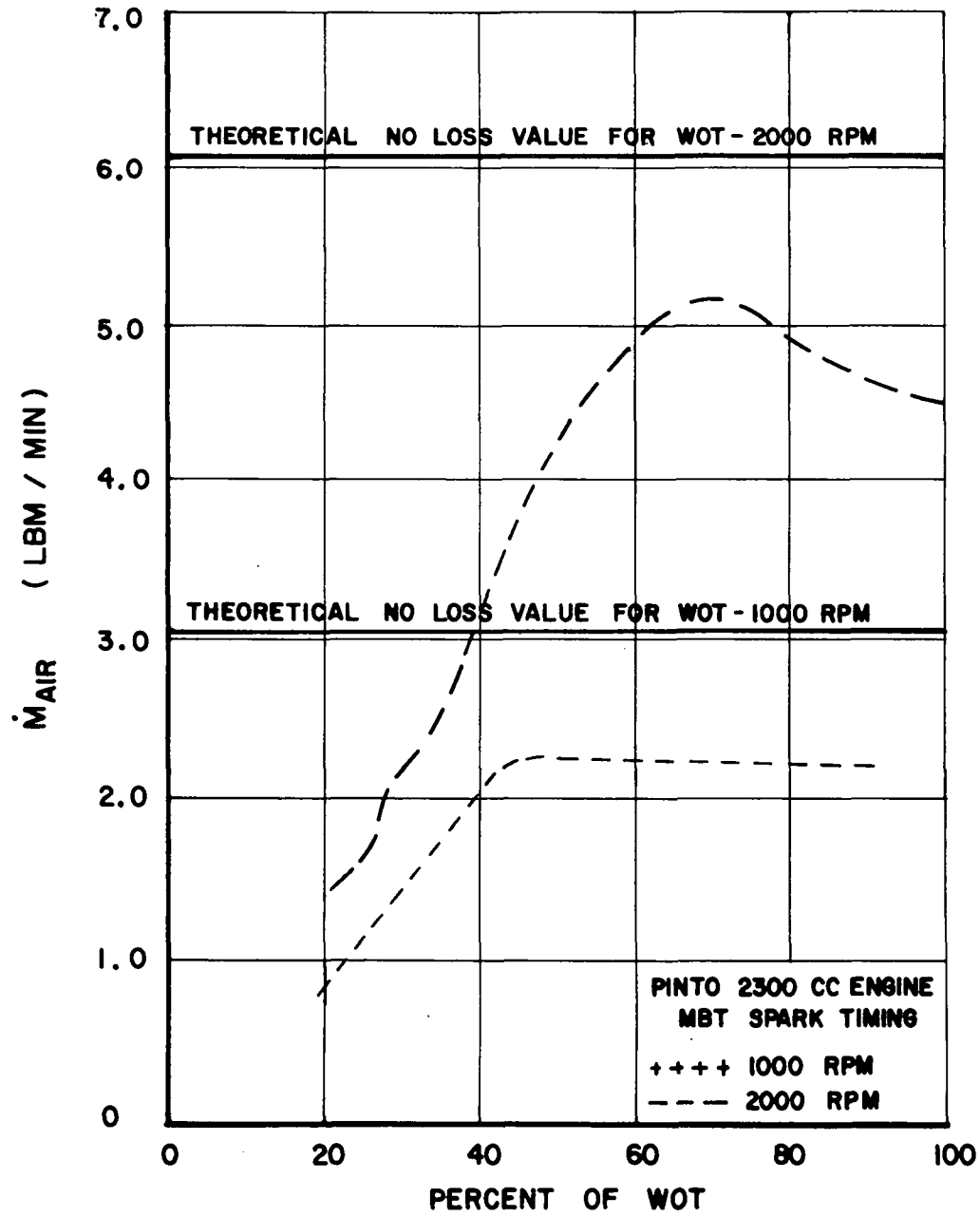

FIGURE IV.19 : AIR FLOW RATE VERSUS PERCENT OF WIDE OPEN THROTTLE - WHB INDUCTION SYSTEM

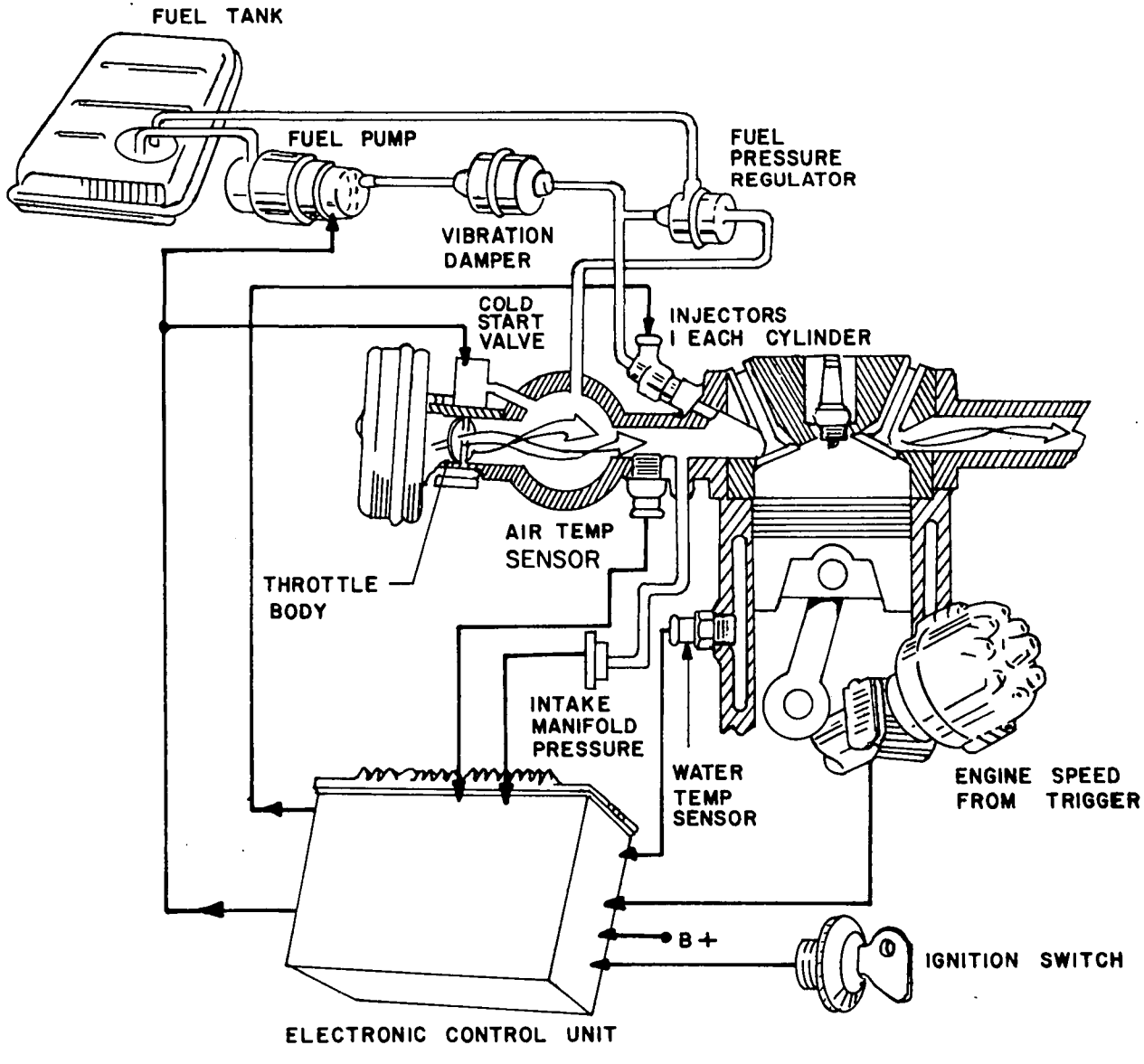

FIG IV.20 ELECTRONIC FUEL INJECTION SYSTEM

possible to manually adjust the starting point of the injection pulse, and the individual cylinder pulse widths. The manifold for the EFI system was designed and built in our laboratory. The primary considerations in design were to achieve uniform air flow among the cylinders and to locate the injectors close to and pointed at the backside of the inlet valves in order to minimize wall wetting.

It was felt that four equal length runners connected to a common plenum would provide uniform air flow to each cylinder. The runners were approximately nine inches long. The location of the injectors became problematic in that intake port entry angle for the inboard and outboard cylinders is different and the injectors are not equally directed at the valves. The EFI test program encountered several problems. Ignition noise from both the secondary and primary circuits was a persistent source of intermittent trouble. Effective safeguards against the noise were only found near the end of the reporting period.

Although measures were taken to provide uniform distribution of air and fuel in the manifold design, it was found necessary to adjust the individual cylinder injection times to balance the equivalance ratio in all cylinders. Due to the sensitivity of the trim potentiometer, time delay in the emissions instrumentation and interactions of engine variables, this balancing operation became a serious time sink requiring up to three quarters of an hour to set a given engine condition. Due to these difficulties, the test matrix was limited to mostly 2000 rpm.

The EFI system is unique in that the point of fuel injection can be varied. This provides differing cases of fuel preparation, i.e., percent of fuel vaporized and/or fuel-air stratification.

Figure IV.21. demonstrates the effect of the starting point of injection on the levels of unburned fuel, CO, and formaldehyde. Point of injection is measured as crankshaft degrees before top dead center of the induction stroke. Note the intake valve effective opening is at 23°BTDC. Exhaust equivalence ratio is stated on the graph and is seen to vary slightly. Power and indicated thermal efficiency remain nearly constant. Clearly, the effect on emissions is due to mixture preparation.

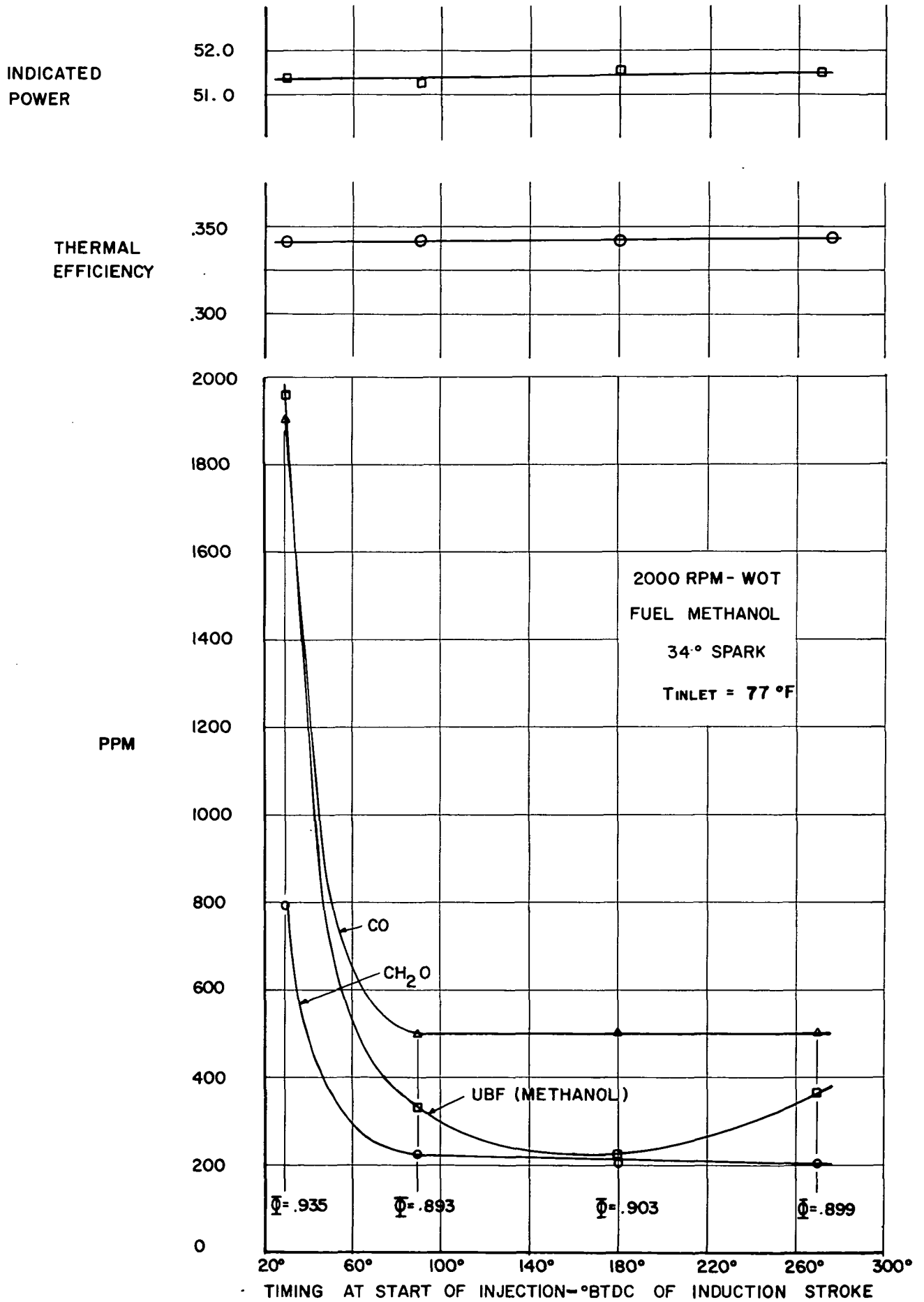

FIGURE IV.21: EFFECTS OF INJECTION TIMING ON POWER, THERMAL EFFICIENCY & EMISSIONS

Matthes and McGill (Ref. 6) and others have suggested that non-homogeneity in the cylinder can shift the knee of the CO curve. The nonuniform charge will shift the CO versus equivalance ratio curve toward the lean side. The CO emissions may be explained by this mechanism. Injecting fuel into the manifold before the valve is open allows time for vaporization and a more homogeneous charge to be inducted. On the other hand, injection at or near the time of valve opening leads to a stratified charge of liquid droplets. Impingment of the drops against the cylinder wall would lead to an excessively rich quench zone resulting in the high unburned fuel and formaldehyde emissions which were observed.

Based on these observations, the majority of EFI data was acquired with the injection point set @ 90° BTDC of the induction stroke. Although this system is tedious to operate, it has produced some informative data as discussed in Section IV.1. It is planned that data will continue to be generated with this system in subsequent phases of the program.

IV.2.3. Dresserator Inductor: The Dresserator Type III prototype is a third generation experimental carburetor built by Dresser Industries. It uses a sliding venturi to maintain sonic conditions at the throat of the carburetor for a wide range of manifold vacuums. The fuel is delivered from a slotted bar which is mounted directly above the venturi and spans the entire length of the carburetor's cross-sectional area. The choked condition created at the throat of the carburetor and the subsequent shock wave are used to finely atomize the fuel spray into a non-wettable fog, allowing a more homogeneous mixture of fuel and air to enter the engine cylinder. This well atomized mixture reduces cycle to cycle variations in peak cylinder pressures as well as reducing the droplet fallout as the mixture passes through the intake manifold.

Another objective of the Dresserator is to maintain a constant air-fuel ratio. This is accomplished by maintaining choked conditions in the throat of the carburetor through the reduction in throat area. Thus the use of the sliding venturi to maintain sonic conditions at the throat of the carburetor not only aids in fuel atomization but is also intended to hold the air and fuel flow conditions constant. Although the model tested did not totally fulfill this objective, it could be adjusted for the desired values of Φ.

The Dresserator carburetor is shown in Figure IV.22a. It should be noted that the prototype model tested is experimental and has been designed to operate only at steady state. It therefore contains no acceleration enrichment circuit found on conventional carburetors.

Adaptation to the Test Engine: In order to best adapt this carburetor system to the Ford Pinto 2300 cc 4 cylinder engine, a special sliding intake manifold adapter was built. This allowed relative movement of the carburetor in a direction normal to the centerline of the engine between the lower portion called the base and the upper portion called the slider. A descriptive drawing of this adaptor is shown in Fibure IV.22b.

Tests were run at a variety of engine speeds and loads at seven different slider positions (0-6cm) to determine the best carburetor position for minimum cylinder to cylinder maldistribution. The effects of two different carburetor fuel distribution bars, the 8 slot and the 4 slot methanol fuel bars, were also examined to determine the optimum carburetor position and fuel bar combination for steady state methanol operation. As a result of these tests, the 8 slot fuel bar with the carburetor at the 5 cm slider location were chosen due to the superior results indicated on methanol fuel at the 2000 rpm, 1/3 and full brake load conditions. Subsequent tests of the Dresserator system were conducted with this fuel bar-slider position combination.

Dresserator Performance: The most outstanding feature of the Dresserator induction system is the improved thermal efficiency due to reduced fuel flow rate needed for a given speed and load setting. It shows the best fuel economy for the simulated CVS driving cycle of all the air-fuel induction systems tested. (See Section IV.3.). The thermal efficiency curves shown in Figure IV.23. indicate peak thermal efficiencies in the range of $0.78 \leq \Phi \leq 0.85$. After this point, however, the dropoff in thermal efficiency is quite rapid, a characteristic not seen in other air-fuel induction systems. Further investigation is needed to determine if the effect of maldistribution and resulting non-MBT spark setting or mixture preparation is responsible for this phenomenon.

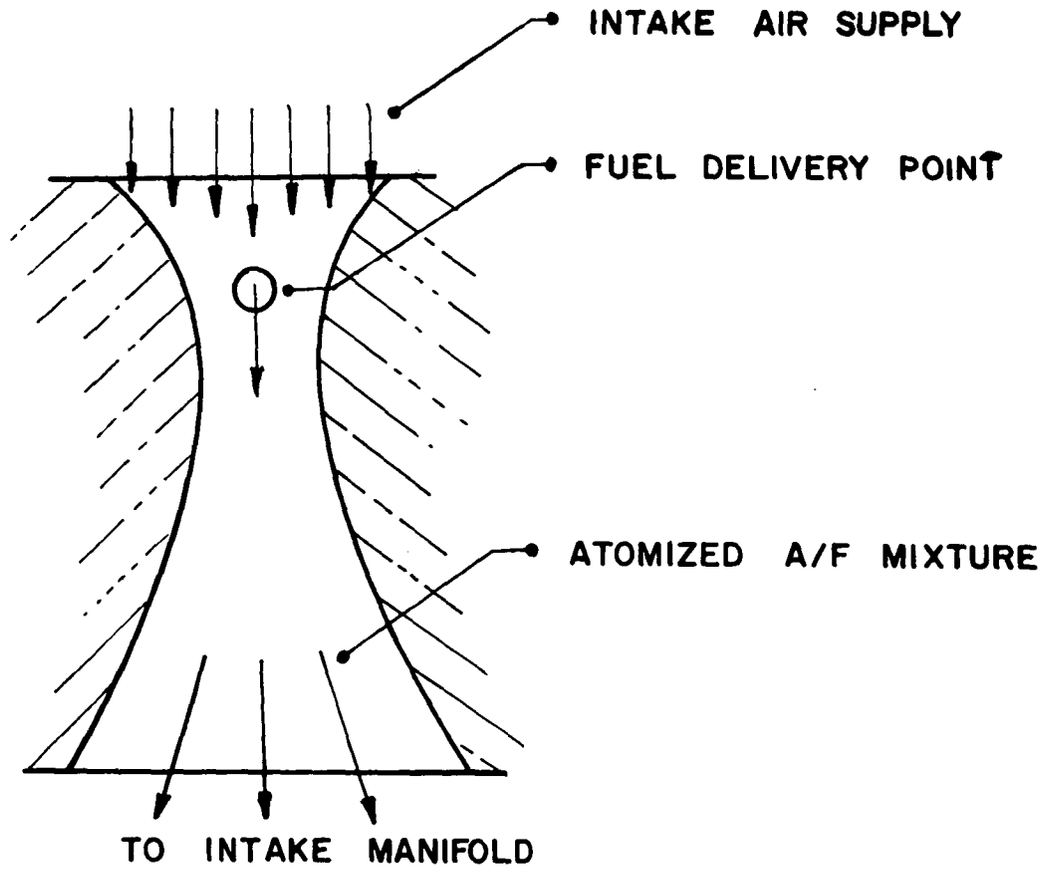

FIGURE IV.22 A: CONCEPTUALIZED DIAGRAM OF THE DRESSERATOR INDUCTION SYSTEM

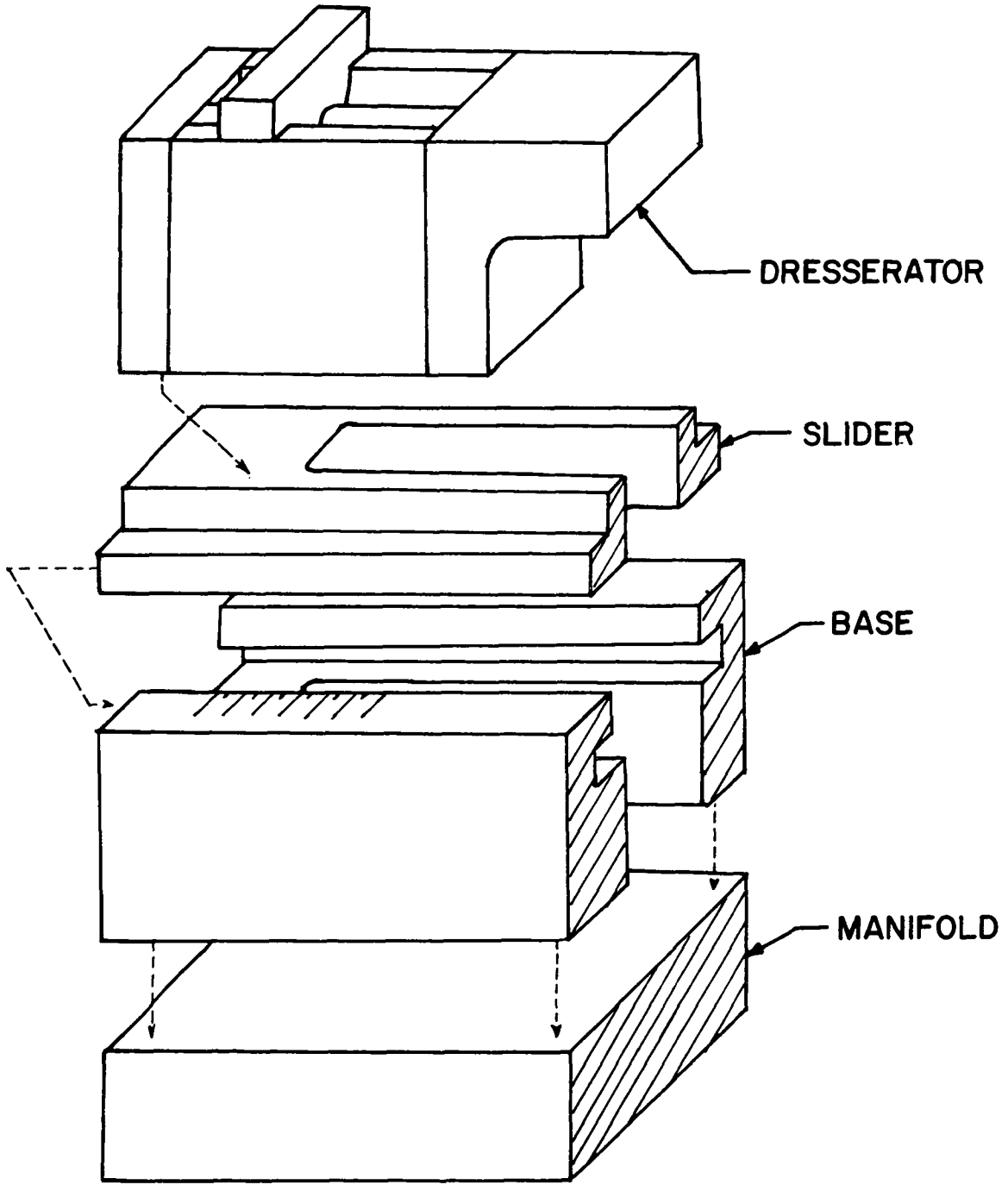

FIGURE IV.22B: MANIFOLD ADAPTER BRACKET

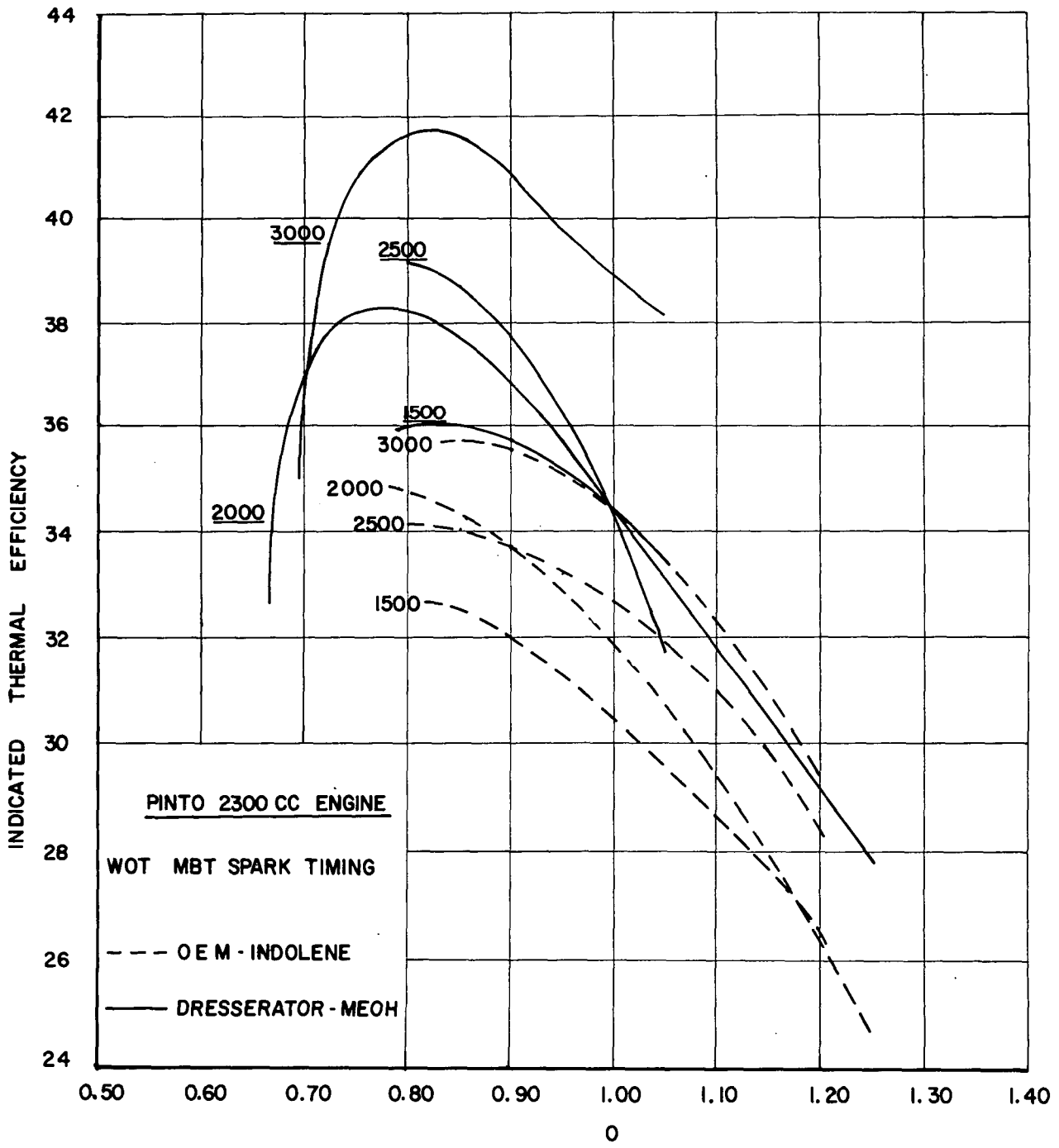

FIGURE IV.23: COMPARATIVE THERMAL EFFICIENCY ACROSS THE SPEED RANGE AT WIDE OPEN THROTTLE – INDOLENE VS METHANOL (MEOH)

At WOT operation particularly at lower speeds, severe standoff of fuel droplets was experienced. This was caused by excessive intake valve open time causing reversed flow in the induction system at manifold vacuums of less than 3 inches Hg. By advancing the camshaft 5° and installing exhaust headers, this standoff problem was reduced. Redesign of the camshaft would tend to minimize this problem and this is under way.

While the Dresserator was not optimally designed for operation on methanol, it did show thermal efficiency increases over the other systems tested. With some necessary redesign of the intake manifold, camshaft and fuel delivery bar, the Dresserator shows promise for good operation in a methanol fueled automobile.

IV.3. Methanol versus Indolene - A Comparison Based on Simulation of the Federal Emission Test Procedure and the Federal Highway Fuel Economy Test Procedure

IV.3.1. Introduction: Predictions of fuel economy and exhaust emissions for transient engine behavior using steady state engine maps of fuel economy and emissions trends have been made possible in recent years through the use of computer simulation programs. The Federal Emission Test Procedure (FTP) and Federal Highway Fuel Economy Test Procedure (HFETP) are prescribed urban and highway driving cycles which can be simulated with the computer. The versatility of these programs is found in their ability to predict fuel economy, emissions and performance for a wide range of engine operating variables and vehicle hardware variables.

In the simulation presented in this section, use was made of a program developed by the Jet Propulsion Laboratory for the prediction of fuel economy and emissions from the steady state engine maps of performance and emissions. Results for a Ford Pinto utilizing the OEM system on Indolene, the modified OEM system on methanol, and the alternate systems (with the exception of EFI) on methanol are presented.

IV.3.2. Simulation Results: Table IV.3. indicates the simulation cases of the FTP and HFETP that were run. Each of the fuel air induction systems was run for a number of fixed equivalence ratios with the exception of the WHB system. (This latter system had a varying equivalence ratio.) Since

the input data for their simulations was based on fully warmed up steady state engine data, the results represent a hot start for the 1972 FTP.

Table IV.3. - Simulation Cases

Run#	Fuel	Equivalence Ratio (Φ)	Carburetion-Fuel/Remarks*
1	Indolene	1.0	OEM Baseline (gasoline)
2	"	0.9	" "
3	"	0.8	" "
4	Methanol	1.0	Modified OEM Baseline (Methanol)
5	"	0.9	" " " "
6	"	0.8	" " " "
7	"	0.7	" " " "very lean operation
8	"	1.0	Dresserator Inductor (Methanol)
9	"	0.9	" " "
10	"	0.8	" " "
11	"	0.7	" " "very lean operation
12	"	variable	WHB induction system (Methanol)640 rpm
13	"	"	" " " 900 rpm

*No EGR throughout

Runs 1 through 7 provide comparative results for the OEM-Indolene and OEM-methanol configurations. Of the alternate fuel-air induction systems chosen for investigation, only the Dresserator and WHB systems appear. There was insufficient steady state data for the EFI to permit a simulation.

Fuel Economy: Figure IV.24. displays the fuel economy on an energy basis (miles traveled per million BTU's of fuel consumed) for the FTP or urban driving cycle as a function of Φ. All 13 simulations are displayed with their characteristic time averaged maldistribution indices. The WHB maldistribution was virtually zero. Table IV.4 summarizes the fuel economy as percentage gains over Indolene on an energy basis. Three general points, which are characteristic of methanol and SI engines become clearly evident from the figure and table:

1. All fuel preparation systems operating on methanol show marked combustion efficiency improvements in comparison to Indolene.

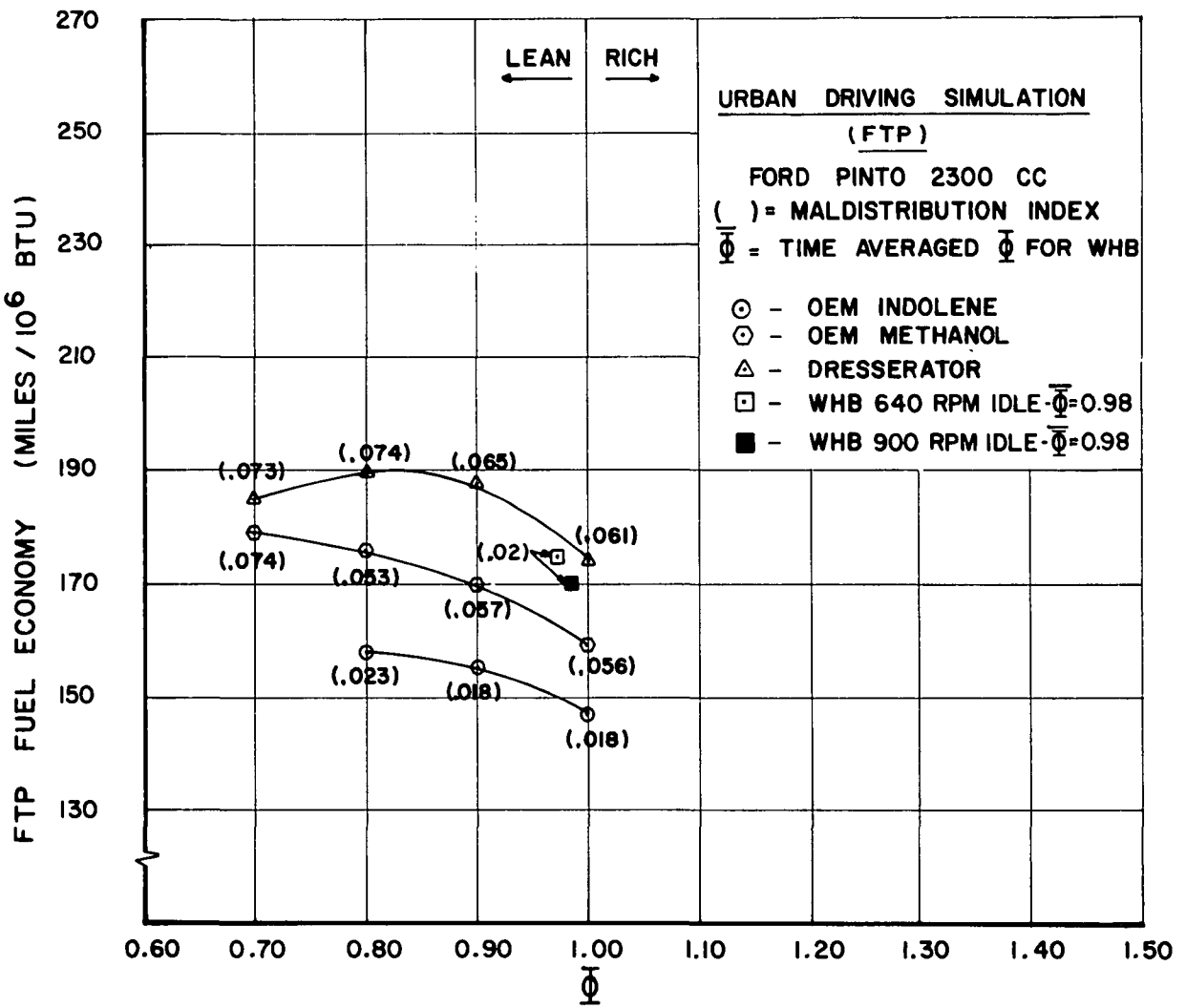

FIGURE IV.24: FUEL ECONOMY VS EQUIVALENCE RATIO FOR ALTERNATE FUEL-AIR INDUCTION SYSTEMS ON METHANOL WITH THE INDOLENE AND METHANOL OEM RESULTS - URBAN DRIVING

2. All systems including the OEM-Indolene show improved combustion efficiency as the fuel-air mixture is leaned.
3. Significant additional gains in thermal efficiency are possible if maldistribution is eliminated.

Table IV.4. Simulated FTP Results

Equivalence Ratio Φ	% Increase in Fuel Economy Relative to OEM-Indolene*		
	OEM-Methanol	Dresserator	WHB**
0.7	22	26	-
0.8	20 (23)***	29 (33)	-
0.9	16 (19)	28 (32)	-
1.0	8 (11)	18 (22)	19

*OEM-Indolene results at Φ = 1.0

**time averaged Φ for WHB was 0.98 (640 RPM idle case)

***numbers in parenthesis indicate expected improvements if maldistribution of Φ among cylinders was eliminated.

The Dresserator shows the highest gain (29% @ Φ = 0.80) when compared with the OEM-Indolene results at Φ = 1.0 (the estimated operating Φ of an actual 1975 "California" Ford Pinto). Even in comparison to the best Indolene results (at Φ = 0.80) the Dresserator still shows a 20% advantage in fuel economy. If maldistribution is eliminated, than an additional gain in fuel economy of from 5 to 7 mi/10^6 BTU can be expected. (The basis for these estimates can be found in Section IV. 1.3.). The estimated percentage improvements for the various systems are the quantities in parenthesis in Table IV.4. Expected improvements at Φ = 0.7 are not displayed for want of sufficient data to provide the estimates. The 33% estimated improvement for the Dresserator emphasizes the influence of maldistribution.

The WHB system displayed no maldistribution. Hence, no gains are expected in this sense. However, its ability to support a lower idle speed is clearly beneficial. In cases 12 versus 13, the reduced idle speed provided a 40% savings in idle fuel consumption and a corresponding increase of 5 mi/10^6 BTU in FTP fuel economy, Figure IV.4. Results for

highway driving (HFETP) in Figure IV.25. show similar trends to the FTP results. A summary of these results is presented in Table IV.5.

Table IV.5. Simulated HFETP Results

Equivalence Ratio Φ	% Increase in Fuel Economy Relative to OEM-Indolene*		
	OEM-Methanol	Dresserator	WHB**
0.7	22	25	-
0.8	19 (23)***	28 (35)	-
0.9	16 (20)	25 (30)	20
1.0	10 (10)	18 (22)	-

*OEM-Indolene results at Φ = 1.0

**time averaged Φ for WHB was 0.87

***estimate for no maldistribution

Improvements up to 28% are seen over the OEM-Indolene results. At Φ = 0.9 the WHB system shows a 20% improvement. The values in parentheses are estimated values of improvement in fuel economy if maldistribution is eliminated from the OEM-methanol and Dresserator systems. At Φ = 0.80 for the Dresserator we could expect to see an additional improvement of 5% or a value of 238 mi/10^6 BTU. This is a 35% improvement over the OEM-Indolene results at Φ = 1.0 or a 25% improvement for the OEM-Indolene at its effective lean operating limit.

Figures IV.24. and IV.25. indicate, with the exception of the Dresserator data, that the peak fuel economy appears at the leanest equivalence ratio. This does not seem consistent with the steady state source data some of which is shown in Figures IV.4. and IV.5. However, increasingly lean operation requires lower manifold vacuums for the same speeds and loads that are dictated by the FTP. With the exception of the Dresserator, the increased efficiency due to lower manifold vacuums more than offsets the decrease in efficiency due to leaning the mixture as anticipated from Figures IV.4 and IV.5.

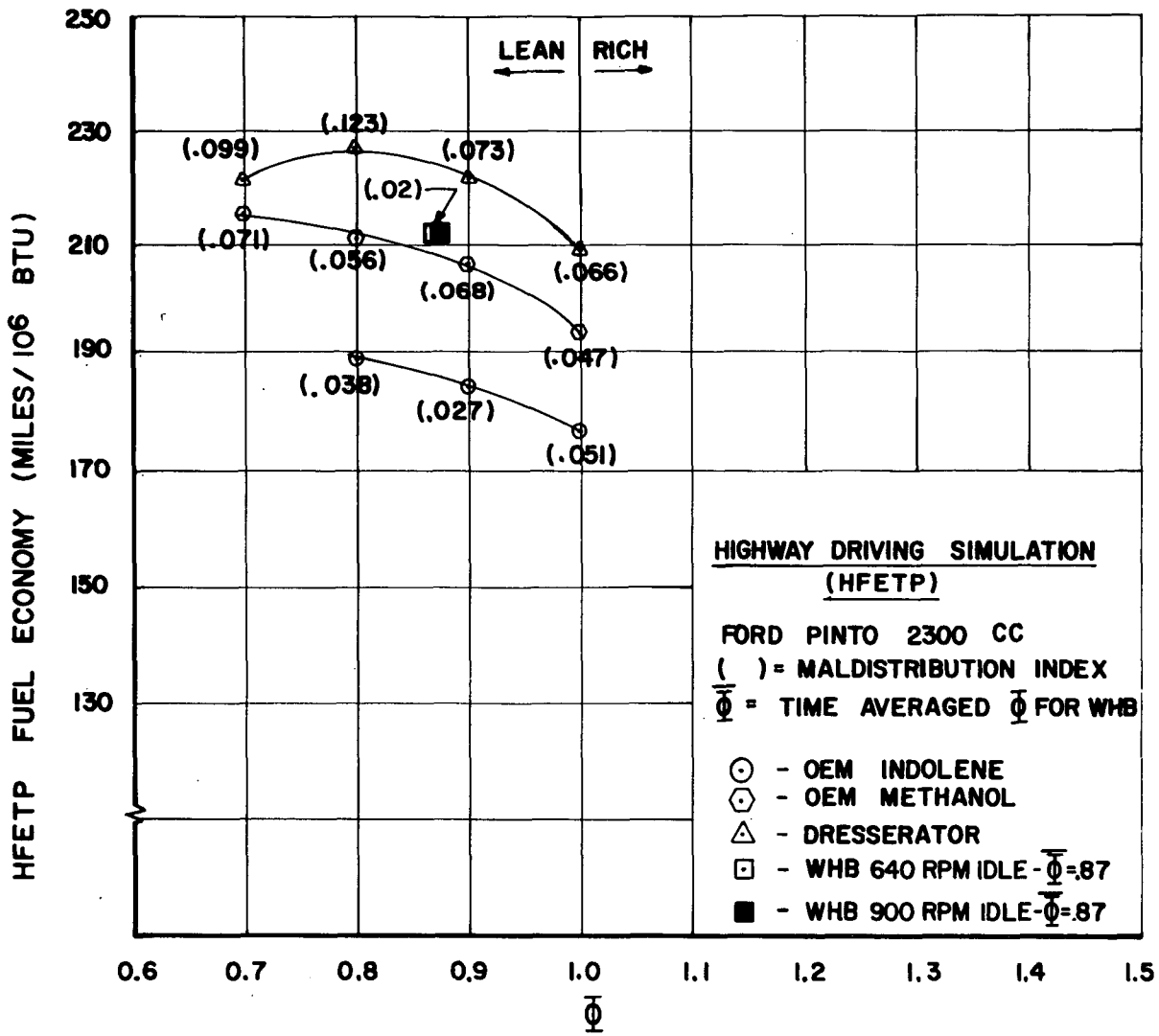

FIGURE IV.25: FUEL ECONOMY VS EQUIVALENCE RATIO FOR ALTERNATE FUEL-AIR INDUCTION SYSTEMS ON METHANOL WITH THE INDOLENE AND METHANOL OEM RESULTS - HIGHWAY DRIVING

In summary, both FTP and HFETP simulation results predict fuel economies for Indolene that are within the range of actual Pinto vehicle performance. Methanol yields increased fuel economy on an energy basis over Indolene. The alternate fuel-air induction systems operating on methanol (Dresserator and WHB) yield additional gains. Lean operation is not only possible but desirable from a fuel economy viewpoint. Elimination of maldistribution will simultaneously further the lean operating equivalence ratio for both methanol and gasoline and raise the fuel economy. Because methanol has a lean burn advantage and a higher energy conversion efficiency than gasoline, these effects can significantly help offset the fact that it only has about half the energy per unit volume as gasoline.

Driveability in the FTP: Driveability or the lack of it is an all important factor in operating any automobile in the lean region. Actual vehicle driveability quality is difficult to reproduce from computer simulation of the Federal Test Procedure. Poor driveability can be caused in part by erratic air-fuel mixture preparation and auto ignition. It can also be caused by inadequate power. These conditions are usually encountered at very lean operation. Our computer simulation assumes a very accurate control on mixture which in turn allows MBT spark setting for all speeds and loads. This eliminates auto ignition and misfire as a driveability constraint. However, the computer simulation does recognize inadequate power. In all the simulated cases power requirements were met, with the exception of a short time interval for $\Phi = 0.7$.

Exhaust Emission Comparisons: Figure IV.26 shows the comparative emissions evidence for all the simulation cases in urban driving (the FTP). The results indicate that by changing fuels, the modified OEM system on methanol yields improvements in all three Federally regulated exhaust emission species. The most significant result displayed is that the statutory NO_x standard of .40 gms/mi can be met by operating near $\Phi = 0.7$. The alternative systems operating on methanol yield results similar to the modified OEM equipment with a few exceptions which are discussed in the following paragraphs.

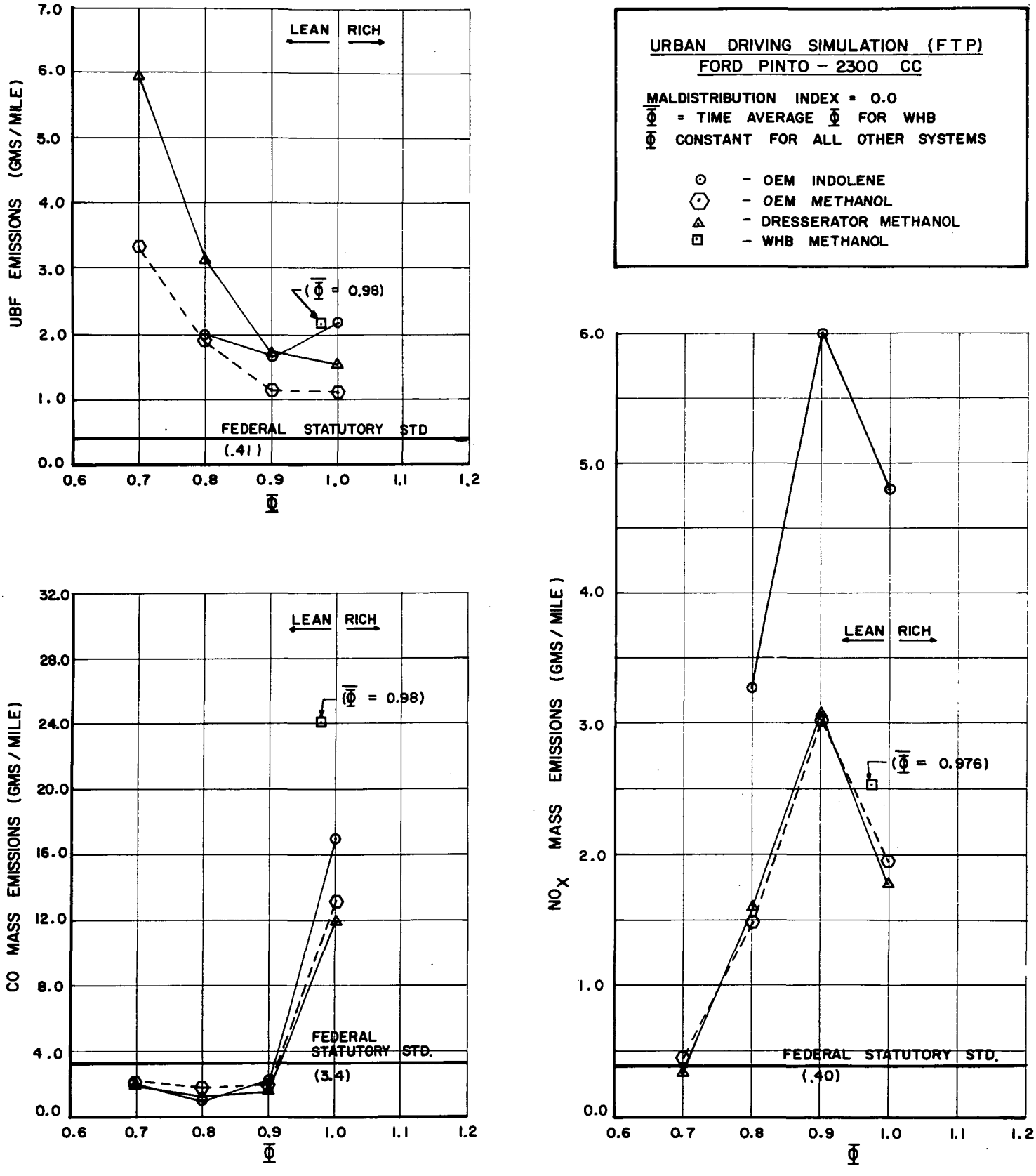

FIGURE IV.26: EXHAUST EMISSIONS VS EQUIVALENCE RATIO FOR OEM AND ALTERNATE FUEL-AIR INDUCTION SYSTEMS FOR THE HOT 1972 FTP SIMULATION

NO_x results show that at similar equivalence ratios methanol yields roughly half the gms/mi that Indolene yields. The urban cycle, time averaged, value of $\Phi = 0.98$ for the WHB system represents a range of values from 0.82 at idle to 1.26 at higher speed and load conditions.

The meeting of the statutory NO_x standard near $\Phi = 0.7$ exploits methanol's lean operation ability and offers an alternative to the state of the art NO_x control strategies of EGR which penalizes fuel economy or, a reducing catalyst which requires operating near stoichimetric Φ also penalizing fuel economy.

Unburned fuel and carbon monoxide results show comparable behavior for both Indolene and methanol (with or without an alternative fuel-air induction system). CO emissions show that the statutory standard is met by operating at $\Phi = 0.9$ or leaner equivalence ratios on either Indolene or methanol. The CO results for WHB at $\Phi = .98$ are predictable since much of the time the engine is operating at rich Φ. All the systems show similar UBF trends, that is, increasing values as Φ approaches the lean limit. The Dresserator shows the highest UBF of all the systems at the lean limit, and all the systems are showing emissions greater than the Federal statutory standard of 0.41 gms/mi. It should be kept in mind, however, that the results presented here are based on exhaust samples taken near the exhaust valve, and thus oxidation of the UBF in the exhaust manifold has not been taken into account. On the basis of measurements downstream of the exhaust manifold, the steady state data would indicate that values of UBF would be lower by a factor of two at the tailpipe.

Even though aldehydes were not calculated in this simulation, they are expected to follow the general behavior of the steady state data just as CO, NO_x and UBF did. We should expect to see higher values of exhaust aldehydes on methanol, and these should increase as leaner Φ values are approached. But, again, the levels are relatively small in comparison to the other pollutant emissions.

Summary: Methanol shows superior performance to Indolene in terms of fuel economy across the Φ range investigated in these simulations of urban and highway driving. There is additional benefit from utilizing alternate air-fuel induction systems. The Dresserator and WHB system show the best results, and the Dresserator may perform even better if the maldistribution associated with it can be eliminated.

The simulation program is a convenient tool for calculating comparative evidence for the FTP and HFETP. It is known that the match up of simulated and actual emissions is generally poor, but the approach used here in the simulation provides the limiting cases in emission behavior. That is, if Φ were maintained constant in the engine, and maldistribution was eliminated, then these results would be attained. Cold starting effects need to be incorporated into future simulations to adequately simulate CO and UBF behavior; however, the NO_x simulation results are representative of both hot and cold starts. This implies that, upon elimination of maldistribution, the NO_x standard of 0.4 gm/mi will be met in an FTP cold-start simulation of lean engine operational on methanol. This interesting possible alternative to EGR or reduction catalyst control of NO_x is appealing because it exploits methanol's superior combustion properties relative to gasoline.

Further study of this computer generated evidence is contemplated. It will include EGR influence and lean operation using a Pinto vehicle powered by methanol and operating on the FTP cycle as well as steady state operation of dynamometer mounted engines. The intent is to find the best combination of fuel preparation system and equivalence ratios for methanol fuel vehicles.

IV.4. Thermochemical Engine Process Modeling: Thermochemical modeling of SI engine processes is important to help provide an explanation and hence indicate methods of improvement in engine performance and reduction in pollutant emissions produced by the experimental Pinto test engine and found in the literature. This modeling is being accomplished by the use of thermodynamic and chemical kinetic computer simulation which has been described in a previous report.[3]

IV.4.1. Prediction of NO_x vs. C.R.: One such trend that has been the subject of much controversy over the last two years has been the compression ratio effect on NO_x emissions for methanol fueled SI engines. This controversy came about over engine experiments conducted by W. E. Bernhardt[7] of Volkswagen. In these tests, he found that the volumetric NO_x emissions decreased with higher compression ratios in methanol fueled SI engines. F. Pischinger[8] subsequently reported similar results. These results differed from the normal logic in which compression ratio increases cause peak cylinder temperature increases and thus increases in the production of NO_x. Neither, however, offered an explanation for their deviation. It was obviously an interesting question which directly related to our computer studies of compression ratio effects and was incorporated in these studies.

In order to match the computer simulation to actual engine data, cylinder pressure-time traces were obtained from the Pinto test engine. Cylinder number one of this engine was instrumented with a model 601B Kistler pressure transducer mounted in a model 640 spark plug adaptor and connected to a model 504E charge amplifier and a Tektronix model 5011 storage oscilliscope.

Even with the forced air cooling of the 601B pressure transducer, temperature instabilities resulted in signal drift and, therefore, made it impossible to store more than one cycle on the oscilliscope

screen. This problem was overcome by using the AC coupling mode on the oscilliscope; however, this led to distortion of the signal trace as discussed by Lancaster et al.[9] In order to retrieve the original data from the distorted trace, an inverse Laplace transform was used.

The AC coupling mode on the oscilliscope can be described as a high pass filter with a corner frequency (fc) of 1.6 hertz. The Laplace transform describing a high pass filter is as follows:

$$P'(t) = L\ (p(t))$$

where $p(t)$ is the actual pressure trace

$P'(t)$ is the resulting AC coupled trace

and $L(s) = \frac{s}{s+a}$

where

$$a = 1/\tau = 2\pi fc = 10\ \text{sec}^{-1}$$

The inverse transform is thus

$$p(t) = L^{-1}\ (P'(t))$$

where

$$L^{-1}(s) = \frac{s+a}{s} = 1 + \frac{a}{s}$$

thus $p(t) = p'(t) + a\int_{\infty}^{t} p'(u)du$

The AC coupled trace which was the average of 100 engine cycles, was then numerically integrated to give the original trace. The AC coupled and the integrated traces are shown in Figure IV.27.

The corrected pressure trace obtained from the Pinto 2300 cc, 4-cylinder engine was then used to determine coefficients for both flame speed and heat transfer equations. As shown by comparing pressure-time traces in Figure IV.28., the combustion rate was well matched during most of the combustion process. However, the peak pressure values computed by the model are higher than those shown in the actual pressure trace.

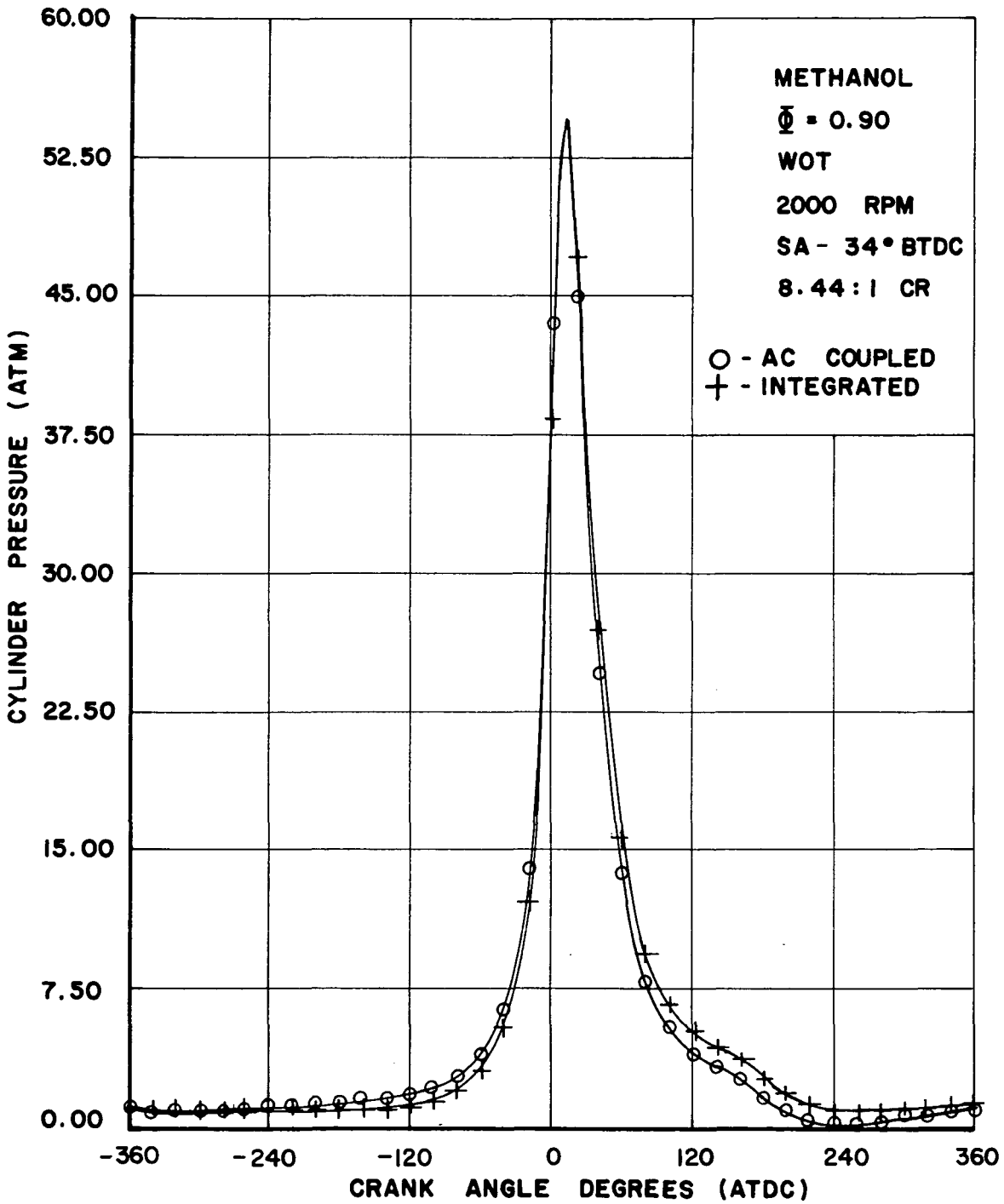

FIGURE IV.27: COMPARISON OF AC COUPLED DATA AND INTEGRATED DATA

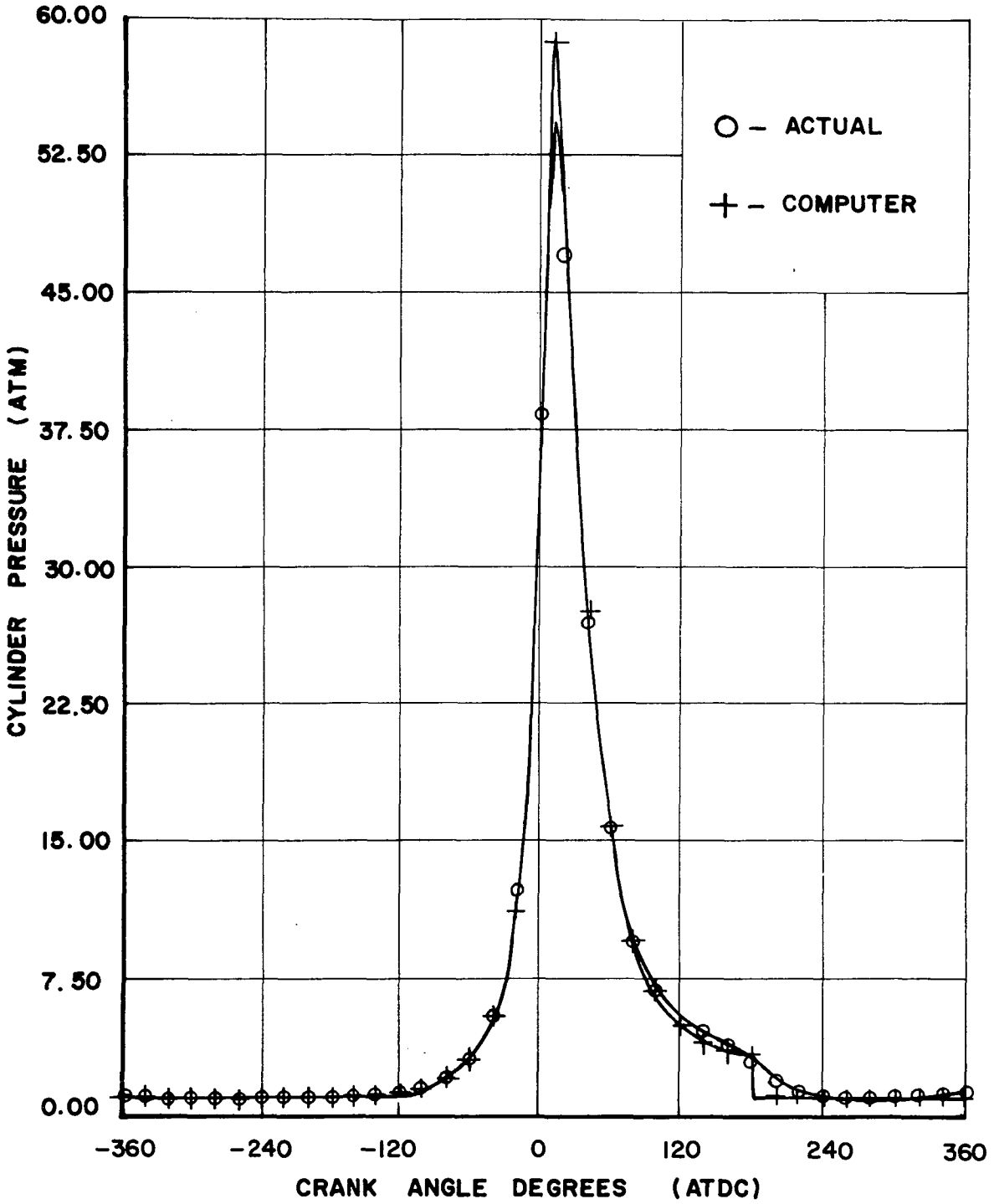

FIGURE IV.28: MATCH OF COMPUTER PREDICTED RESULTS TO ACTUAL PRESSURE TRACES

This discrepancy results from the fact that the model describes a flat combustion chamber and the Pinto engine actually has a squish chamber.

Comparisons between the actual test point and the model's matching predictions of performance and emissions are shown in Table IV.6. Since no quench zone modeling is included in the program, the Otto cycle model shows practically no unburned hydrocarbons in the bulk charge. An interesting point to note is that the program also shows practically no formaldehyde (CH_2O) in the bulk gases, thereby showing it as a quench phenomenon. This can be verified by noting that formaldehyde is an intermediate step in the combustion reactions and therefore would only exist in the quench layer.

This squish-type combustion chamber of the actual engine tends to increase turbulence during the beginning of the combustion process which has been modeled well by the computer simulation. However, as the piston passes TDC, decreased turbulence and increased heat transfer occur, causing drastic changes in flame speed and unburned mixture temperature which are not accounted for in the computer model. This effect not only reduces the peak cylinder pressure but also causes the predicted maximum brake torque (MBT) spark advance curves to be offset or retarded relative to the actual MBT spark advance curve for the Pinto engine as shown in Figure IV.29. While this spark advance distortion causes the computer model to predict higher power and thermal efficiency at MBT spark timing than actual values, the computer model variations with equivalence ratio are consistant with actual trends. Dry exhaust emission comparisons (Figure IV.30) show that while predicted CO_2 and O_2 values match experimental values, predicted CO is much lower than the experimental CO. This indicates too fast a reaction rate constant for the CO oxidation reaction.

$$CO + OH \rightarrow CO_2 + H$$

The rate used here is a slower rate than was used in the gas turbine studies. Yet, the predicted CO values are still too low. This issue

TABLE IV.6

PERFORMANCE AND EMISSIONS COMPARISON

AT MATCH POINT (WOT & 2000 RPM)

	Engine Data	Computer Model
Performance		
Φ	0.90	0.900
SA	34°BTDC	34°BTDC
POWER(KW)	16.7	17.4380
CHARGE WGT (GMS)	0.684	0.68416
ηTH (%)	34.8	36.26
ISFC (g/KWH)	519	498.07
EXH TEMP (K)	916	924.5
Emissions		
UBF (PPM)	429	2.3×10^{-5}
CH_2O (PPM)	177	4
CO (%)	0.07	0.02
CO_2 (%)	13.2	13.411
O_2 (%)	2.26	2.161
H_2 (%)	0.04	0.045
MO (PPM)	2410	2516
NO_x (PPM)	2530	2522
NO (g/KWH)	11	11.560
NO_x (g/KWH)	18	17.769

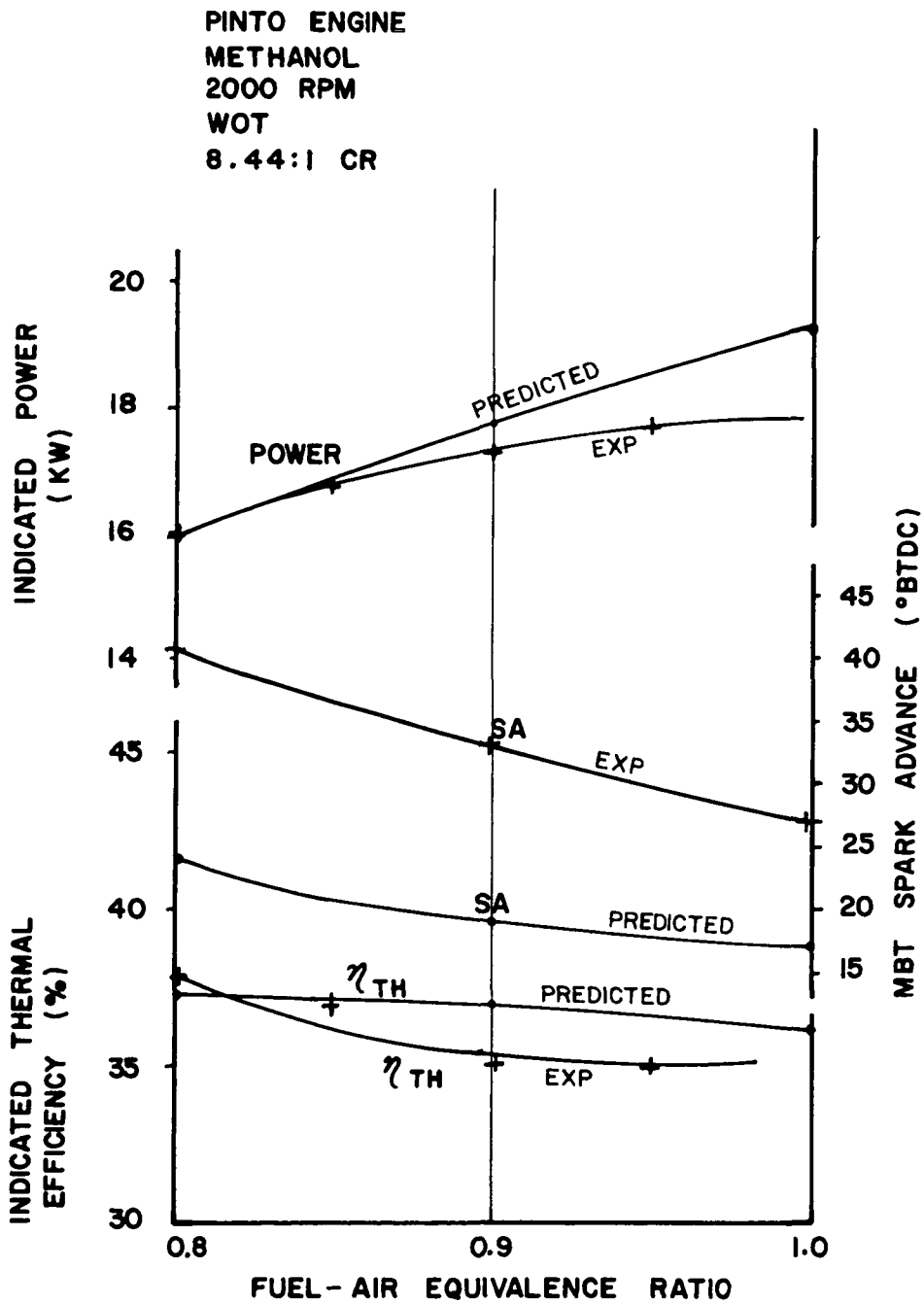

FIGURE IV.29: COMPARISON OF ACTUAL VS PREDICTED PERFORMANCE DATA

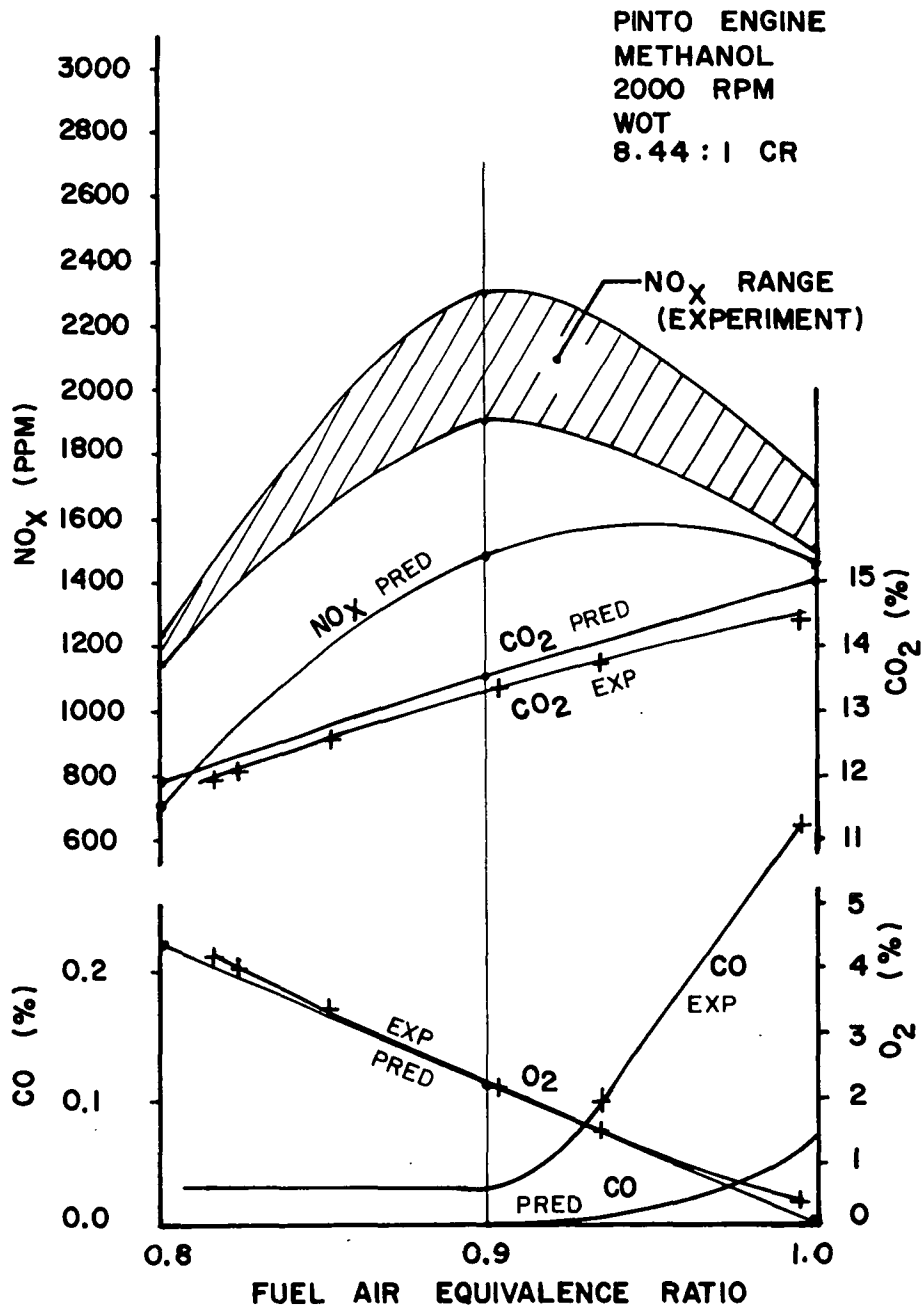

FIGURE IV.30: COMPARISONS BETWEEN EXPERIMENTAL AND PREDICTED DRY EXHAUST EMISSIONS

requires further study. Predicted MBT NO_x emissions, as expected due to the spark advance offset, are also lower than actual values. However, trends with equivalence ratio match experimental data reasonably.

The next test of the model was to predict performance and emission parameters for the test engine at 4000 rpm. Predicted performance data for 2000 rpm and 4000 rpm are compared in Figure IV. 31. As expected IMEP and thermal efficiency increase with engine speed. Predicted dry emission comparisons (see Figure IV. 32) show that NO_x and CO emissions decrease with increasing engine speed while O_2 and CO_2 emissions show no change relative to engine speed. Limited experimental data at 4000 rpm support these findings.

With the model showing reasonable trends as functions of equivalence ratio and engine speed, it was then used to predict the performance and emission trends with increasing compression ratio. As shown in Figure IV. 33, the power and thermal efficiency increased 14% when the compression ratio was raised from 8.44:1 to 14:1, while NO_x emissions increased 18% on a volumetric basis. It is interesting to note that these factors combine over the range of compression ratios mentioned, to give a net increase of indicated specific NO_x ($ISNO_x$) of only 2.7%. This information is contrary to that reported from experimentation which indicated a drop in volumetric NO_x in going from a compression ratio of 9.7:1 to 14:1. A possible explanation for this experimental trend may be that preignition or knock reactions have caused the experimentalists to retard the spark from the MBT value. To support this argument, the predicted spark retard performance and exhaust emissions are shown in Figure IV. 34. With a 3° spark retard from MBT, the volumetric NO_x at 14:1 compression ratio is equal to that at 8.44:1 with MBT spark timing. This still shows a 13.7% increase in thermal efficiency and power with a 12.4% reduction in $ISNO_x$. Consequently, the experimental results reported by Bernhardt and by Pischinger can be obtained with a slight spark retard. Since only a 3° retard was necessary to duplicate the NO_x trend and with a power reduction of only 0.4%, the reported experimental conclusions could also have resulted from a missetting of MBT spark advance.

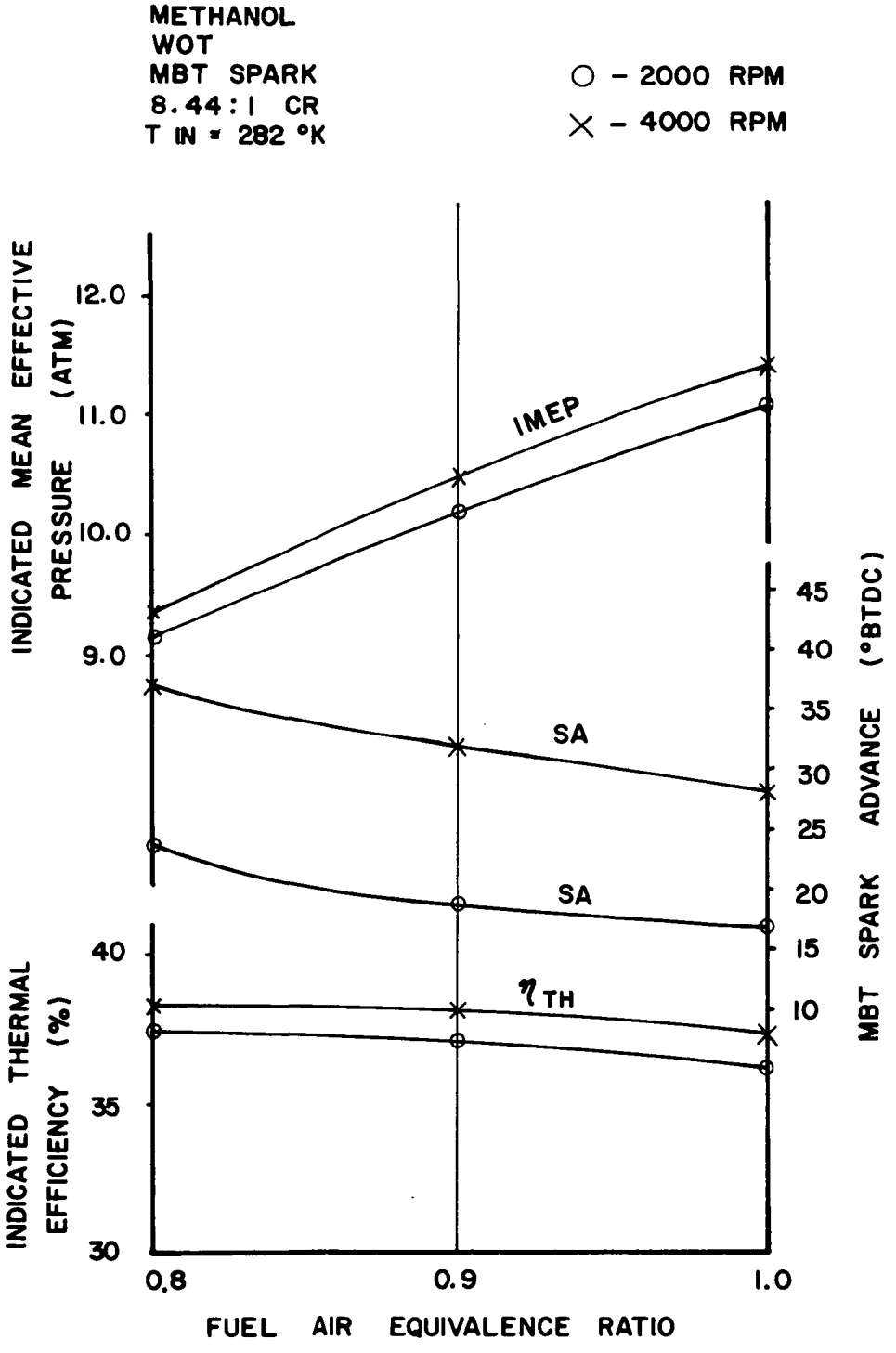

FIGURE IV.31 : COMPUTER PREDICTED PERFORMANCE FOR 2000 RPM AND 4000 RPM

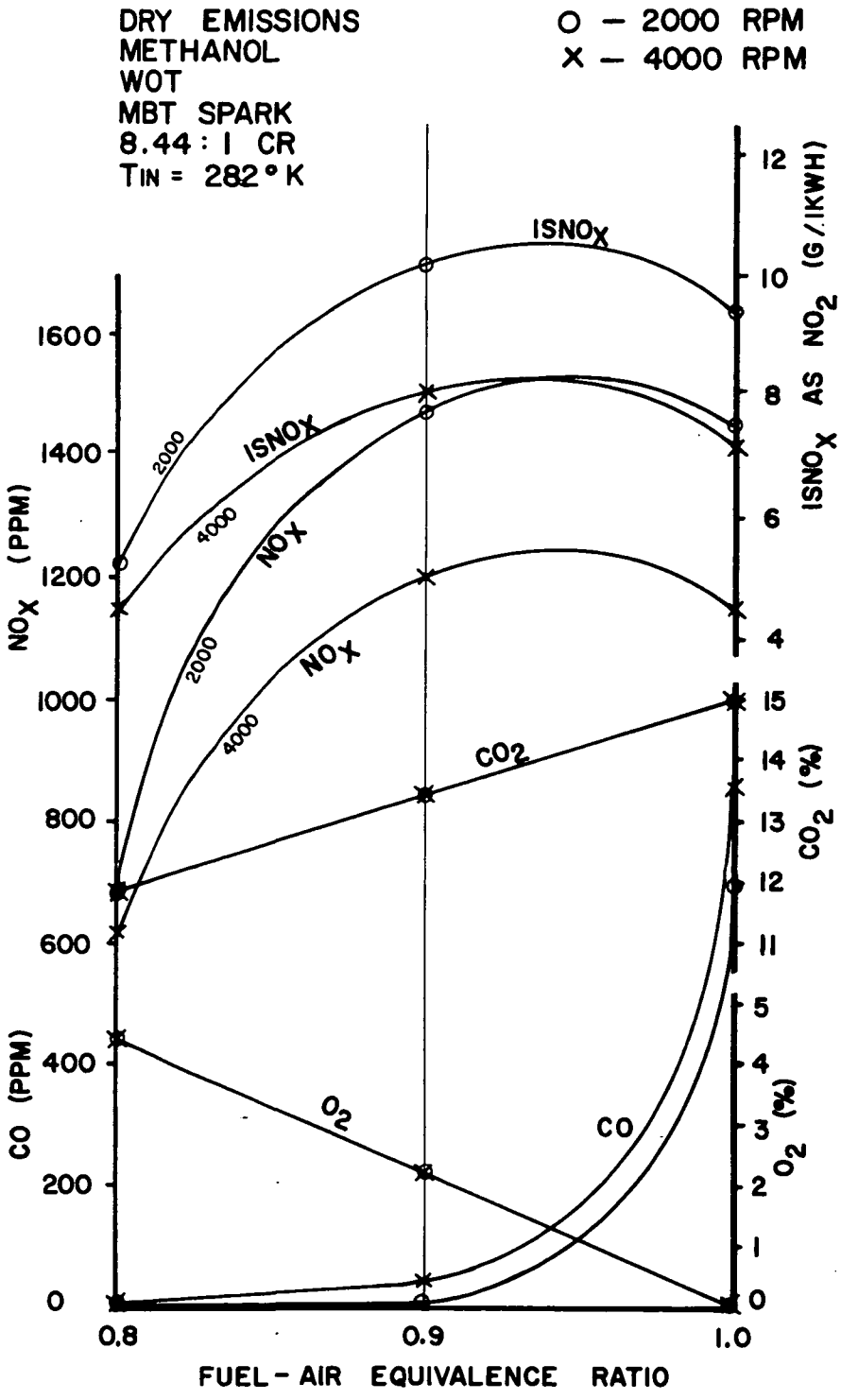

FIGURE IV.32 : COMPUTER PREDICTED DRY EMISSIONS FOR 2000 RPM AND 4000 RPM

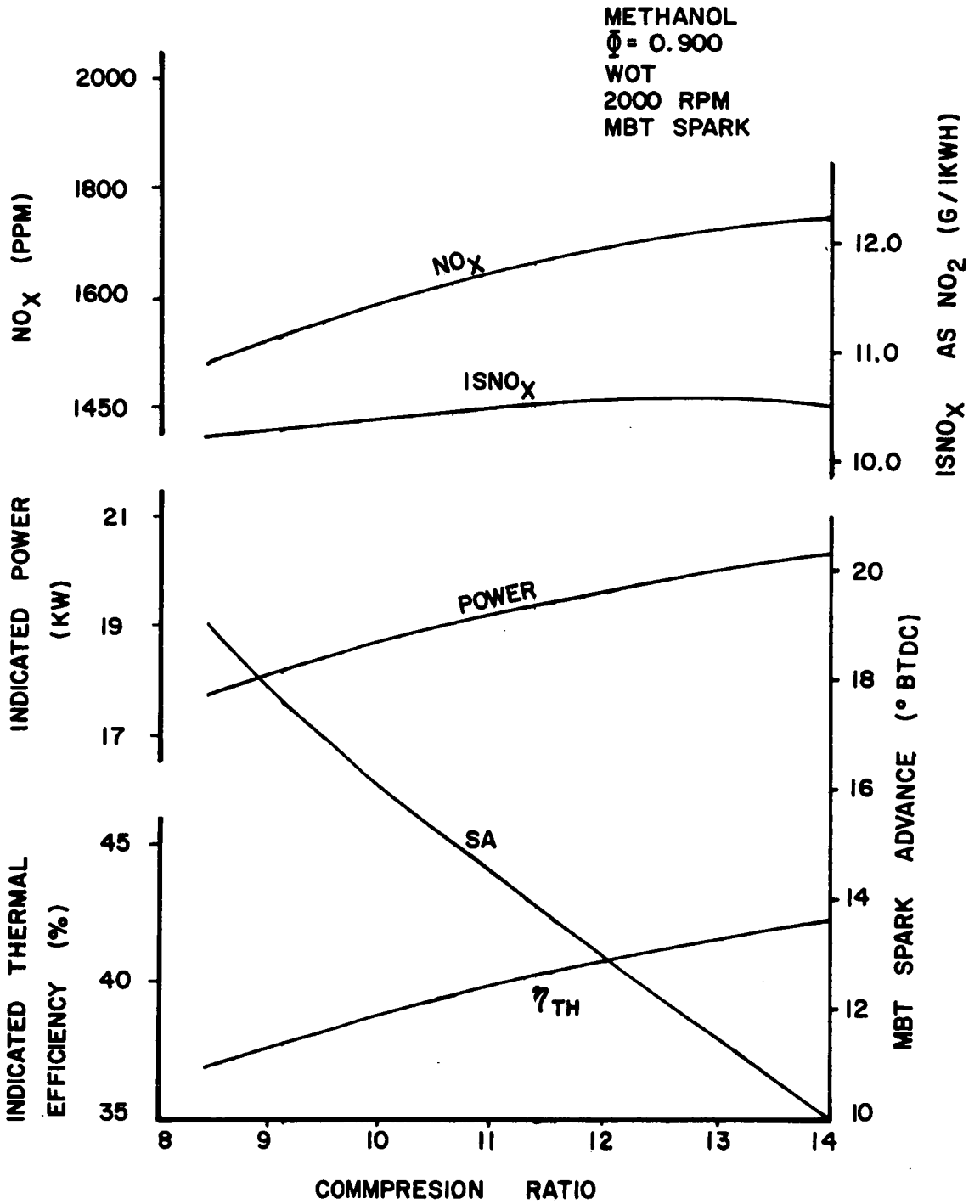

FIGURE IV.33: COMPUTER PREDICTED MBT COMPRESSION RATIO EFFECT

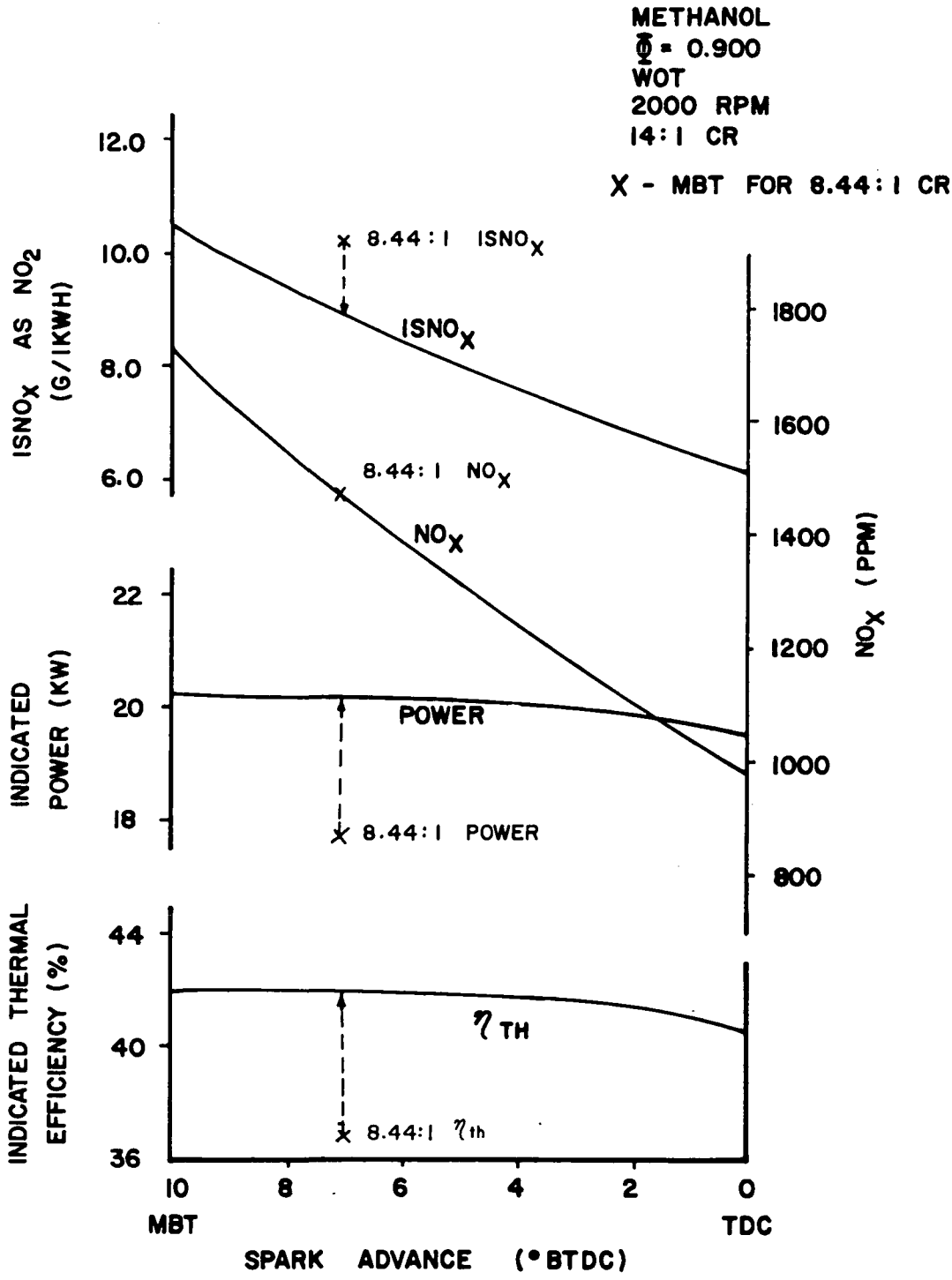

FIGURE IV.34: COMPUTER PREDICTED SPARK RETARD EFFECTS

We have concluded that our thermokinetic computer model of a specific SI engine does correctly predict trends in performance and emissions as functions of equivalence ratio and speed when compared with actual data. However, the absolute values of the predicted parameters are not in as good agreement. This is believed due to oversimplified modeling of the combustion chamber.

The computer model predicts an increase in volumetric NOx emissions with CR at MBT spark timing, which is contrary to reported experimental results. However, the computer model reveals that the volumetric NOx emissions at a CR of 14:1 can be reduced to those of a CR of 8.44:1 and MBT spark timing by retarding the spark 3° from MBT spark setting at 14:1 CR. There remains a 13.7% increase in power and efficiency at this retarded spark setting. Assuming the TDC surface to volume ratio is held constant, it is expected that the cylinder hydrocarbon and aldehyde emissions will not be significantly affected by increasing the compression ratio. The high CR will also enhance cold starting. Hence, the very important conclusion is reached that the CR of a methanol fueled engine should be as high as possible without introducing autoignition.

IV.4.2 Continuation of Modeling Study: One of the least studied areas of methanol combustion is the quench zone which is believed to be the source of most of the hydrocarbon and aldehyde emissions. Therefore, we plan to use the model to look at the quench phenomenon in methanol fueled SI engines. Another area which holds much interest in the use of methanol in automotive engines is the cold start problem. This is another area we plan to investigate with the computer model. Other areas which should also be included in our future plans are better modeling of the squish type combustion chamber, droplet combustion, use of charge stratification and the spark initiation phenomenoa.

IV.5 COLD STARTING AND LEAN BURNING

IV.5 Cold Starting and Lean Burning: Like gasoline, methanol fueled engines become progressively more difficult to start in winter temperatures. However, the onset of this difficulty occurs at a higher ambient temperature for methanol (30 to 40° F) than for gasoline (0 to 20°F). Gasoline will permit startup at these lower temperatures because of its volatile components. Volatile components such as butane can also be blended with methanol for cold starting enhancement. However, this is not considered satisfactory as it weakens the safety of methanol from explosive ignition associated with spills and tank leakage. In pure form, methanol is much less hazardous than gasoline in this regard.

To date, cold starting of methanol fueled automotive engines has usually been accomplished by use of an auxiliary gaseous fuel. For example, the vehicle operated by the City of Santa Clara, which is now entering its sixth year of operation, has always used propane for cold weather starts. These auxiliary fuels present no special problems to the experienced operator. However, they are seen as a source of consumer complaint if they are to be incorporated in vehicles operated by the public.

Our early research efforts[1] showed that methanol in dissociated form ($CO+2H_2$) could be mixed with methanol in any percentage and used successfully as an automotive fuel. Because of the wide flammability limits of H_2 and the fact that dissociated methanol is a gaseous fuel, it has appeal for cold starting providing it can be generated under cold start conditions from the liquid methanol stored in the vehicle's fuel tank using the vehicle's battery power. It is toward this goal that our research efforts over the past year have been principally directed.

IV.5.1 Battery Power Generation of Dissociated Methanol: Equilibrium studies from our computer, which do not consider activation energies, show that methanol can be considered thermodynamically unstable even at room temperature, and, if all possible products are considered, it

decomposes to a variety of compounds at low temperatures, eventually ending with only carbon monoxide and hydrogen at the higher temperatures. It is of further interest that once started, decomposition at lower temperatures can provide an energy output. While the latter is a potentially intriguing method of sustaining a decomposition reaction, our initial approach was based on higher temperature decomposition in which the reaction is endothermic and energy must be supplied. This simple thermal approach was also considered more practical since it appeared likely to be accomplished without the need for catalysts.

Following the decision to use a thermal decomposition approach, other basic questions arose. How much methanol must be decomposed and how much energy is required? Based on typical engine cranking speeds, it was estimated that a fuel flow rate of 0.6 grams/sec would occur. Since this represents the total fuel rate at cranking speed, must all or only a fraction of this methanol be dissociated? Initially it was assumed that all should be dissociated if possible.

The present test setup for exploring the practicality of the thermal dissociation concept is shown schematically in Figure IV.35. The apparatus has undergone a series of changes since inception but basically all variations involved a means to pump, meter and initiate methanol flow. Similar means were required for air or nitrogen which was often injected simultaneously with the methanol as it was found to enhance dissociation. Also required was a means to initiate battery input and measure its electrical current.

The present apparatus is described as follows. Compressed nitrogen is used to pressurize the methanol storage tank, using a null-type gas regulator to maintain constant pressure. The liquid is forced from the bottom of the tank first through a rotometer where flow is measured and then to an electrically operated solenoid valve, located slightly downstream of the methanol pressure gauge. The solenoid valve leads directly to a hypodermic-needle-sized tube that

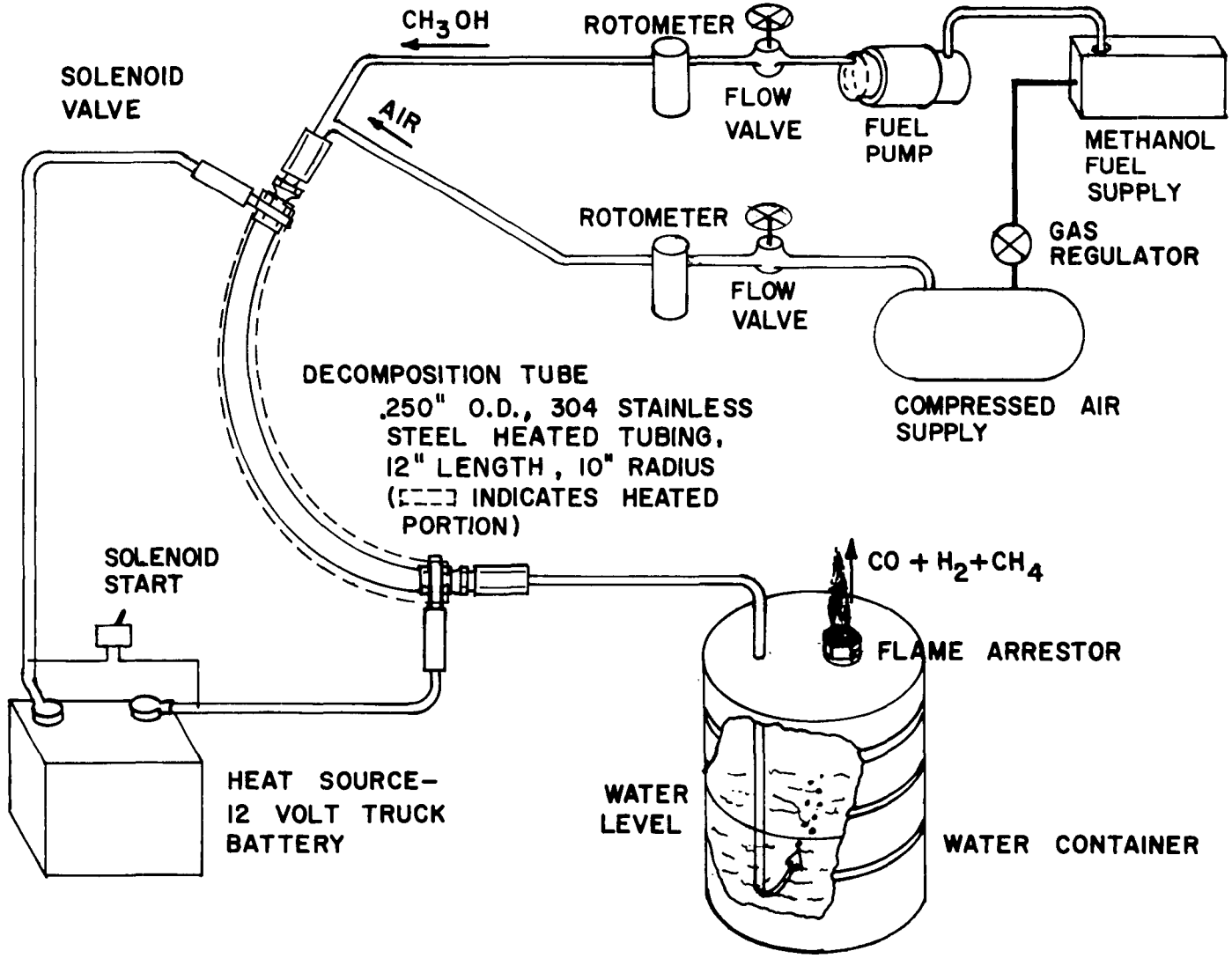

FIGURE IV.35: PROTOTYPE METHANOL COLD START SYSTEM

injects the liquid into the decomposition tube. Often air or nitrogen is injected into the latter tube and it flows from the compressed gas injector leading directly into the decomposition tube. The tube itself is heated as a shunt to the truck battery through the contacts shown. Battery current is initiated via a starter-solenoid and then passes through an ammeter with a calibrated shunt for measuring current flow. The run interval and time of initiation of the battery, methanol and gas inputs are controlled with an interval timer, and the methanol flow, especially, is timed during the run (and also during calibration) with an electric stop watch. In most of the tests, the effluent from the decomposition tube was passed directly into a wash water bath that dissolves the water soluble components, and then the insoluble gases exit the container to a tube where they are ignited by an electric spark generator. In these tests, the degree of decomposition is estimated by weighing the contaminated wash water, and some qualitative information is ascertained by observing the extent of the flame and further traces of insoluble non-gaseous products. In a few later tests, the effluent from the decomposition tube was passed into the top of an enclosed container that was completely filled with water. The insoluble gases displace the water into a separate container, and the amount carried over is taken as a measure of the extent decomposed. Samples of gases are also removed from the top of the enclosed container and analysed on a gas chromatograph.

Tests were performed using various tube configurations. Because of problems in attaining reproducibility in flow rates of methanol, it is now realized that the early test results are not satisfactory. The problem stemmed from the formation of air bubbles in the methanol line at points where restrictions occurred, and these bubbles affected the methanol flow rates. It is presently believed that the bubbles were a consequence of degassing of dissolved gases on passage through a point of low pressure. Their effect on flow rates has been largely eliminated by the scheme indicated in Figure IV.35 in which the flow is controlled by a tiny orifice placed within the decomposition tube. As a consequence,

air bubbles which may be evolved do so downstream of the injector where they have no effect on flow rate.

The procedure of heating the decomposition tube by shunting it directly across the battery appears to have certain simplicities which are desirable for an automobile application. However, it also results in restricting tube dimensions to those with acceptible electrical resistances. We have found, both experimentally and from calculations, that dimensions that represent a tube of 1/4" O.D., .01" wall and length of 12 to 14" is satisfactory. Our first reliable experiements indicate that simply injecting the methanol into such a tube, along with an air flow between 1 and 6 ft^3/hr., with an electrical input from about 220 to 300 amps, and at methanol flows of about 0.5 grams/sec. for about 3.8 secs., results in about 10% decomposition of the methanol to water insoluble gases. Despite many diverse inter-relations of the tube dimensions and flow rates, we did not succeed in improving this value. It was, moreover, quite apparent that minor changes in dimensions of the tube, generally resulted in a lower electrical input or decreased temperature rise of the tube, could easily lower this value. It was often decreased to negligible amounts by fairly small changes in geometry. Our thermocouple measurements of tube temperatures during the more successful runs ranged from 600 to 800°C. The effluent from the wash water container burned with a clear blue flame. After we adopted stainless steel tubes in our lines from the decomposition tube to the wash container, there was rarely more than negligible insoluble non-gaseous residue produced, and we never found more than a trace of formaldehyde in the wash water.

In continuing experiments, we sought to improve decomposition by thermally insulating the tube. Radiation tubes, in which the decomposition tube was surrounded by a larger one of reflective materials, produced very small increases. However, thermally insulating by wrapping with glass cloth effectively increased the yield to a range of 15 to 20%, compared to 10% for the non-insulated tubes. Experiments were therefore performed in which the fuel was more assurredly heated. They comprised locating the 1/4" tube within a 1/2" tube, with methanol injected into the smaller tube and then passing via holes into the annulus between the tubes before

being led to the wash water. The concentric tubes were electrically heated for lengths of time required to attain selected temperatures, prior to injection of the methanol. Under these circumstances, decomposition of about 10% was achieved at only 500°C, and well over 25% at 900°C. While this experimental device does not qualify for use on an automobile and it requires a much greater electrical input than normally available, it indicated that great improvements in decomposition can be achieved by heating methanol to moderate temperatures for sufficiently long stay-times.

Based on the above, a decomposition device was constructed of similar design but with characteristics that might be satisfactory for use on an automobile. For reasons already discussed, these seem to be limited to dimensions corresponding to 1/4" diameter by .01 wall by 12", and we chose to simulate the latter with two concentric tubes, 3/16" and 1/16" O.D. In essence, the methanol is injected into the smaller of the tubes, passes via orifices at the end of the tube into the annulus between it and the larger tube, and then exits near the point of injection. This apparatus resulted in decompositions between 50 and 60%, which represents very attractive progress.

In addition to tests with the above device in which the effluent was passed directly into water and the water-solubles determined by weighing, the effluent was passed into the closed water container indicated in the bottom right of Figure IV.35. The displaced water indicated decomposition of over 40%. Analysis of the collected gas showed about 17% CO, 41% H_2, and 2-1/2% methane. The CO and H_2 concentrations appear, within experimental error, of the 1:2 ratio required of complete dissociation of methanol; but the total gas concentration found is less than 100%, which may indicate the presence of other gases.

This vein of exploration has demonstrated that methanol may be thermally decomposed in an apparatus of practical dimension for use in an automobile.

However, the electrical energy input is too high to meet cold starting requirements. Studies will continue with emphasis on ways to decrease this energy requirement.

IV.5.2 Cold Start and Lean Burn Experiments: Initially it was assumed that all the methanol flowing at cranking speeds must be dissociated to achieve ignition and burning under cold start conditions. But is this the case? Is it possible that a pilot amount of gaseous fuel can sustain a flame in the very lean air-methanol vapor mixture encountered with cold start conditions? Two avenues of exploration of this issue are available.

Experiments have been performed by others using a hollow electrode spark plug to create a stratified charge in the cylinder with the rich zone in the proximity of the spark plug.[10] It is the intent of our experiments to attempt to inject and hold a gaseous mixture of dissociated methanol ($CO + 2H_2$) in the proximity of the hollow electrode spark plug for supporting combustion of methanol under cold-start, lean-burn conditions. Percentage of the fuel injected through this electrode will be varied to determine the least percentage necessary as a function of ambient temperature down to -10°F or -23°C.

Chemical chains and reaction rate data already exists in our computer for the combustion of dissociated methanol. By incorporation of a stratified charge configuration for the simulated gases in the combustion chamber, it may be possible to study the cold-start, lean-burn problem with the computer. If so, limited experimental testing could be used to verify the computer predictions and the computer data would, at relatively low cost, provide the bulk of the information relative to the percentage of dissociated methanol required as pilot fuel for cold starting.

Lean burning of a homogenous mixture under normal engine operation will continue to be explored experimentally in our dynamometer tests and computer modeling studies. If the use of the hollow electrode spark plug proves satisfactory in the cold start studies, it will then also be incorporated in our lean burn studies for normal operation. This is an important issue for our early studies[1] have shown that engine operation on equivalence ratios as low as 0.4 are possible using dissociated methanol.

IV.6. Engine Wear Rate and Crank Case Blow By: Investigators have reported a variety of evidence relative to the influence of methanol fuel on engine wear rates. The summation of this evidence is inconclusive.[11, 12, 13]

One very favorable piece of evidence, that there is no significant difference between methanol and gasoline, relates to our methanol fueled vehicles. The 1970 model American Motors Gremlin is now in its seventh year of operation on pure methanol with no detectable engine wear problems. Indeed there have been no failures in either engine components or major fuel system components. A 1972 Plymouth Valiant is now in its 6th year of operation on pure methanol. During its entire life, it has been operated in stop-go driving by the meter-readers for the City of Santa Clara. This is a very severe wear mode of operation. Yet, there have been no failures in either engine components or major fuel system components.

Other evidence in the literature suggests that methanol may be incompatible with some of the materials presently used in the internal combustion engine. It is known that methanol will attack the terne plate coating on the fuel tank. Other workers[14, 15] have reported wear or the lack of it while using methanol and methanol-gasoline blends, but their results are cloudy as engine wear has not been studied in a controlled test until recently.[3, 16]

Our present engine tests utilizing methanol fuel include an engine wear rate test designed to analyze the change in engine wear rate due to the use of methanol fuel in comparison with unleaded gasoline fuel. In this context engine wear rate is defined as the rate of accumulation of copper, lead, iron and chromium metals in the lubricating oil of the engine due to the loss of these metals from the engine.

The choice of these metals is based on their significance in the engine parts. In the early phases of the tests, aluminum and tin were also measured but showed negligible evidence of wear and so were dropped from the tests.

In order to monitor metal loss from the engine, a warm oil sample (approximately 200 grams) was removed from the lubricating system approximately every ten engine hours and tested for metals level. The oil samples were diluted in xylene, and analyzed by atomic absorption spectroscopy for lead, copper, chromium and iron concentration. Atomic absorption spectroscopy is a common technique for oil analysis used by industry. [17, 18, 19]

During the course of the test, the engine load and speed were varied in a regular pattern as explained elsewhere in this report. The engine was started and stopped frequently. Fuels were also used for various lengths of time. Thus, the effects of engine start-up, load and speed are approximately the same for the methanol and gasoline runs.

The accumulated wear metals in the oil as functions of engine hours and fuel type are plotted on a semilogrithmic graph, Figure IV.36. Atomic absorption data corrected for oil dilution (due to oil addition) and oil concentration (due to oil losses) is the basis for this evidence. Events that may have influenced this data are keyed to Figure IV.36. by event numbers listed in Table IV. 7.

The only wear rate contrast that may be significant from tests is the possible increase in the wear rate of copper due to the use of methanol fuel. The slope of the accumulated copper curve has distinct transitions at 260, 330, 415, 510 and 550 engine hours where the fuel was changed.

Though the wear rate of both iron and chromium varied during the test, there is no consistent correlation between fuel and wear rate of either the iron or chromium.

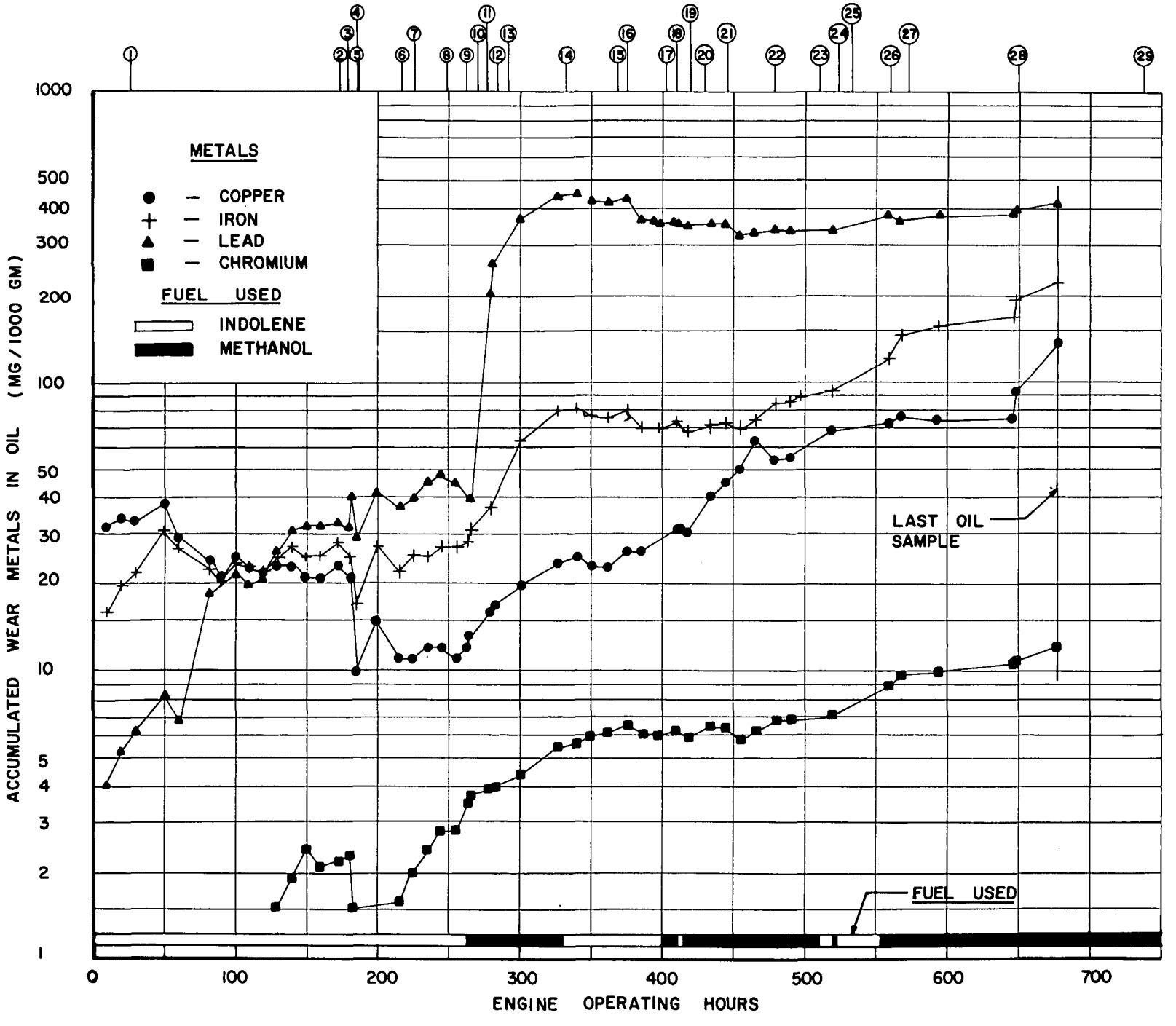

FIGURE IV. 36: EFFECT OF FUEL TYPE ON ENGINE WEAR

TABLE IV.7 HISTORY OF ENGINE EVENTS

NO.	ENGINE HOURS	EVENTS
0	000	Indolene Fuel
1	030	Oil Leaks
2	171-180	Oil Leaks
3	180	Oil Pressure Drop
4	182	Filter Change
5	185	Oil Change
6	216-225	Oil Leaks
7	225-236	Extensive Oil Leak
8	246-257	Oil Leak
9	263	Oil Change--New Filter
10	265	Methanol Fuel
11	265-278	Oil Leaks
12	278-282	Oil Circuit Failure-total pressure loss
13	282	Oil Changed
14	329	Chevron Unleaded Fuel
15	362-376	Oil Leak
16	365	Filter Change
17	401	Methanol Fuel
18	409	Chevron Unleaded
19	414	Methanol Fuel
20	418-434	Oil Leak
21	444	Oil Leak
22	466-498	Oil Leak
23	510	Chevron Unleaded
24	519	Methanol Fuel
25	524	Chevron Unleaded
26	558	Methanol Fuel
27	567	Oil Leaks
28	648	Oil Change, Filter Change
29	732	Oil Change

The wear rate of lead rapidly increased after the oil pressure failure (event 12) but eventually becomes negligible. It is concluded that the wear rate of the lead bearings is unaffected by the fuel.

The calculated results using this evaluation technique are very sensitive to the engine oil volume. During the course of the study, the amount of oil in the engine at any given time was only known within ± 204 grams and the oil losses which were assumed to occur at a constant rate were uncertain within ±102 grams. These uncertainty errors decreased as the test went on due to refinement of sampling techniques so that the uncertainty due to losses was reduced to 50 grams and the uncertainty of the amount of oil in the engine was reduced to 100 grams. It is estimated by error analysis that uncertainties in the final accumulated wear concentrations do not exceed ± 5%.

In order to strengthen the validity of this particular wear analysis, oil filters were removed and analyzed for wear metal content. It was found that the oil filter removes between 25 and 50 percent of the wear metals from the oil and does so at a constant rate of removal except when extremely high metal concentrations are present (i.e., during the oil pressure loss). Thus, the presence of the oil filter in the oil line affects the magnitude of the actual metals lost but it does not alter the relative wear rate evidence.

Atomic absorption analysis was also conducted on the large particles (>.45 microns) for several oil samples (#51, 54, 55). The metals level of the large particles of chromium, iron and lead represented only 18-27% of the total metals content in the oil. However, the large copper particles were up to 80% of the level of copper in the oil for these samples. These samples were only taken when methanol was used as fuel. This evidence casts significant uncertainty on the conclusion of increased copper wear from methanol.

Analysis of engine wear rates as functions of fuel yields the following conclusions:

a. The wear of copper parts may be affected by methanol fuel.
b. The wear rate of iron, chromium and lead parts does not change due to the use of methanol fuel.
c. Engine wear studies should investigate large (>.45 micron) particles as well as small particles to evaluate wear.
d. The presence of oil filters in the oil system does not significantly effect wear rate data.

It is not presently known if the lost copper is from the bearings or oil pump. This will be investigated when the test engine is disassembled. Further wear studies using the same technique of oil analysis will continue to be conducted for the test engines and future test cars in order to broaden our data base and provide more accurate evidence.

V. CONCLUSIONS

The past year's work has provided further evidence of methanol's advantages over gasoline. Some of the conclusions which follow from this work reinforce previous observations and some appear for the first time.

1. Methanol is generally superior to gasoline in power, thermal efficiency, and reduced emissions with the exception of aldehydes.
2. Maldistribution of the air-fuel mixtures among the cylinders of a multicylinder engine and variation of the mixture with speed and load must be reduced for good performance and emissions control for both gasoline and methanol fueled engines.
3. Prototype hardware (WHB system) has been used in our experiments that solves the maldistribution problem and allows a 20-30% reduction in idle speed. However, it does not as yet control the air-fuel ratio as function of speed and load to a satisfactory degree.
4. Three different fuel metering systems (WHB, Dresserator, and EFI) were found to provide superior steady state performance on methanol when compared with the OEM carburetor system with enlarged fuel jets.
5. Computer simulation of the engine's thermokinetic combustion events shows reasonable predictive trends in power, thermal efficiency and NOx emissions due to changes in equivalence ratio, speed, and compression ratio. It does not as yet satisfactorily deal with "squish" type combustion chamber effects nor with quench zone effects. However, the evidence from the study clearly suggests use of higher compression ratios with methanol.
6. Computer simulation of the Federal emissions test procedure using steady state data from our experimental engines has produced evidence that lean-burning, methanol-fueled vehicles

may meet statutory limits of emissions if tight control is maintained on the equivalence ratio.

7. There do not appear to be any major wear contrasts with the possible exception of copper for engines using methanol or gasoline.
8. There does not appear to be any significant difficulty in converting small gas turbines to run on methanol with equal power at lower turbine inlet temperatures and with marked reduction in NO_x.
9. Preliminary studies relative to marine spills indicates that methanol is naturally present in that environment. Other than localized and short term damage it may not cause harm to the ecosystem in the event of a major coastal spill.

IV. REFERENCES

1. R. E. Fitch and J. D. Kilgroe, "Investigation of a Substitute Fuel to Control Automotive Air Pollution," Final Report, CETEC Corp. NAPCA Contract No. CPA 22-69-10, Mountain View, Ca., 1970.

2. R. K. Pefley, et. al., "Study of Decomposed Methanol as a Low Emission Fuel," Final Report, Santa Clara Univ., EPA, Contract No. EHS 70-08, Santa Clara, Ca., 1971.

3. R. K. Pefley, A. E. Bayce, L. H. Browning, M. C. McCormack, and M. A. Sweeney, "Characterization and Research Investigation of Methanol and Methyl Fuels in Automobile Engines," Report ME-76-2, Santa Clara Univ., EPA Grant No. R. 803548-01, Santa Clara, Ca., 1976.

4. R. K. Pefley, et. al., "Methanol-Gasoline Blends--University View Point," Engineering Foundation Conference, Henniker, New Hampshire, 1974.

5. H. G. Adelman, L. H. Browning, and R. K. Pefley, "Predicted Exhaust Emissions from a Methanol and Jet Fueled Gas Turbine Combustor," AIAA Journal, Vol. 14, No. 6, June, 1976, pp. 793-798.

6. W. R. Matthes, R. N. McGill, "Effects of the Degree of Fuel Atomization on Single-Cylinder Engine Performance," Society of Automotive Engineers, # 760117, Feb. 23-27, 1976.

7. W. E. Bernhardt, "Engine Performance and Exhaust Emission Characteristics from a Methanol-Fueled Automobile," 1975, GMR Symposium, Michigan, 1975.

8. F. Pischinger, "Discussion Contribution," Methanol as an Alternate Fuel Proceedings, Stockholm, Sweden, 1976, pp. 113-116.

9. D. R. Lancaster, R. B. Krieger, and J. H. Lienesch, "Measurement and Analysis of Engine Pressure Data," SAE Paper No. 750026, SAE Transactions, Vol. 84, 1975, pp. 155-172.

10. M. D. Leshner, W. H. Baisley, and E. Leshner, "A Fuel Vapor Injector/Igniter System," Final Report, Fuel Injection Development Corp., ERDA Contract # E (04-3)-1237, Bellmawr, New Jersey, February, 1977.

11. J. C. Ingamells and R. H. Lindquist, "Methanol as a Motor Fuel," preprint, Chevron Research Laboratory Report J 4802, Richmond, Ca., May, 1974.

12. J. D. Rogers, "Ethanol and Methanol as Automotive Fuel," Report No. P813-3, E. I. Du Pont De Nemours and Co., Inc., 1973.

13. R. M. Tillman, Data Presented at the Bureau of Mines Sponsored Technical Meeting, Denver, Colorado, Sept., 1974.

14. R. R. Adt, Jr., R. D. Doepker, and L. E. Poteat, "Methanol-Gasoline Fuels for Automotive Transportation," University of Miami.

15. "On the Trail of New Fuels-Alternative Fuels for Motor Vehicles," Federal Ministry for Research and Technology, Bonn, Germany, 1974.

16. "Engine Lubricants for Use in Methanol Fueled Highway Vehicles," Southwest Research Institute, San Antonio, Texas, October, 1976.

17. E. A. Means and D. Ratcliff, "Determination of Wear Metals in Lubricating Oils by Atomic Absorbtion Spectroscopy," Atomic Absorbtion Newsletter, Vol. 4, No. 1, January, 1965.

18. "Testing Used Engine Oils-the Why and How," Chevron Research Bulletin, Chevron Research Laboratory, Richmond, Ca., 1973.

19. "Scheduled Oil Sampling as a Maintenance Tool," Paper No. 720372, presented at Earthmoving Industry Conference, Society of Automotive Engineers, April 1972.

TECHNICAL REPORT DATA
(Please read Instructions on the reverse before completing)

1. REPORT NO. M.E. 77-1	2.	3. RECIPIENT'S ACCESSION NO.
4. TITLE AND SUBTITLE Characterization and Research Investigation of Methanol and Methyl Fuel: Final Report		5. REPORT DATE August 1977
		6. PERFORMING ORGANIZATION CODE
7. AUTHOR(S) R. K. Pefley, L. H. Browning, M. C. McCormack, M. L. Hornberger, W. E. Likos, B. Pullman		8. PERFORMING ORGANIZATION REPORT NO.
9. PERFORMING ORGANIZATION NAME AND ADDRESS University of Santa Clara Department of Mechanical Engineering Santa Clara, California 95053		10. PROGRAM ELEMENT NO.
		11. CONTRACT/GRANT NO. R803548-01
12. SPONSORING AGENCY NAME AND ADDRESS Environmental Protection Agency Motor Vehicle Emission Laboratory 2565 Plymouth Rd. Ann Arbor, MI 48105		13. TYPE OF REPORT AND PERIOD COVERED
		14. SPONSORING AGENCY CODE

15. SUPPLEMENTARY NOTES

16. ABSTRACT

An automotive engine mounted on a dynamometer is used to generate power, efficiency and emissions maps which compare methanol with gasoline. This data is also used in conjunction with a computer program to predict vehicle performance and emissions. Methanol is found to offer advantages over gasoline. Two alternates to the stock fuel preparation system are also evaluated. They show improvements over the stock system.

Computer modeling of the thermokinetic events in the test engine using methanol has allowed predictions of power, efficiency and emissions as functions of compression ratio, spark advance, air-fuel ratio and speed. High compression ratios appear beneficial.

The report also considers engine wear, cold start aspects of methanol. It also presents some gas turbine evidence which favors methanol over commercial turbine fuel.

17. KEY WORDS AND DOCUMENT ANALYSIS

a. DESCRIPTORS	b. IDENTIFIERS/OPEN ENDED TERMS	c. COSATI Field/Group
Methanols Methyl Alcohol Exhaust Emissions		

18. DISTRIBUTION STATEMENT Not Restricted	19. SECURITY CLASS *(This Report)* Unclassified	21. NO. OF PAGES 108
	20. SECURITY CLASS *(This page)* Unclassified	22. PRICE

EPA Form 2220-1 (9-73)